Doctoral dissertation

Biological activity of *Bifidobacterium animalis* ssp. *animalis* CCDM 218 and *Bifidobacterium adolescentis* CCDM 368 surface antigens in complex interactions with the host organism - prevention/treatment of allergy diseases

MSc Katarzyna Pacyga-Prus

Supervisor

PhD Sabina Górska, Associate Professor at HIIET PAS

Prepared in a Laboratory of Microbiome Immunobiology

at the Institute of Immunology and Experimental Therapy

of the Polish Academy of Sciences

Wrocław 2024

Praca doktorska

Aktywność biologiczna antygenów powierzchniowych *Bifidobacterium animalis* ssp. *animalis* CCDM 218 i *Bifidobacterium adolescentis* CCDM 368 w złożonych interakcjach z organizmem gospodarza - profilaktyka/leczenie chorób alergicznych

Mgr Katarzyna Pacyga-Prus

Promotor

Dr hab. Sabina Górska, prof. IITD PAN

Przygotowana w Laboratorium Immunobiologii Mikrobiomu

w Instytucie Immunologii i Terapii Doświadczalnej

Polskiej Akademii Nauk

Wrocław 2024

Funding

Research presented in this work was carried out and financed by:

The National Science Centre of Poland grant (SONATA BIS 7, UMO-2017/26/E/NZ7/01202) "The structure and biological role of *Bifidobacterium* components in allergy disease development"

and

The Polish National Agency for Academic Exchange grant (MOBILITY, PPN/BIL/2018/1/00005) „New strategy for alleviating allergic response: Effect of the surface bacterial antigens in the prevention and treatment of allergic inflammation in mouse model"

Acknowledgements / Podziękowania

I would like to express my gratitute towards / Chciałabym złożyć serdeczne podziękowania

Dr hab. Sabinie Górskiej *za wprowadzenie mnie w fascynujący świat probiotyków i alergii oraz za zarażenie mnie miłością do nauki. Dziękuję za wszystkie naukowe i nienaukowe rozmowy, cierpliwość, wsparcie i wiarę w moje umiejętności.*

Naszej wspaniałej ekipie z ***Laboratorium Immunobiologii Mikrobiomu*** *za nieocenioną pomoc w realizacji projektów, za inspirujące rozmowy przy kawie na wszystkie możliwe tematy (nie zawsze te związane z pracą) oraz wspólne laboratoryjne wyjścia.*

Moim kochanym ***dziewczynom z pokoju 254*** *za nieustające wsparcie i wiarę we mnie w momentach, gdy mi jej brakowało. Pomimo tego, że nasze drogi się rozeszły, to wiem, że zawsze mogę na Was liczyć. Dzięki Wam ta droga do obrony była jedną z najwspanialszych przygód na jakie się zdecydowałam.*

Colleagues from the Laboratory of Gnotobiology *for successful collaboration and warm welcome in Novy Hradek. Thank you for all your help, for sharing your facilities, knowledge, and skills… and for teaching me a little bit of the Czech language!*

Prof. Corine Sandström *for introducing me to the world of NMR and for such a warm welcome in Uppsala. Even though COVID tried to disrupt our first meeting, it started a successful collaboration.*

Moim wspaniałym rodzicom *za wiarę we mnie od samego początku. Za Wasze nieocenione wsparcie w każdej decyzji, którą podjęłam. To dzięki Wam zaszłam tak daleko!*

Mojemu kochanemu mężowi *za wytrwanie ze mną podczas wszystkich wzlotów i upadków. Dziękuję Ci za bycie najlepszym stażystą i recenzentem. Za Twoją wyrozumiałość i cierpliwość za moją pracę do późna. Za pilnowanie, żebym nie zapominała o jedzeniu i piciu, kiedy byłam zbyt pochłonięta doktoratem. Tę pracę dedykuję przede wszystkim Tobie!*

Contents

Tables and Figures

Abbreviations

Bad368	*Bifidobacterium adolescentis* CCDM 368
BAL	Bronchoalveolar lavage
BALF	BAL fluid
Ban218	*Bifidobacterium animalis* ssp. *animalis* CCDM 218
BMDCs	Bone Marrow Dendritic Cells
CCL	Chemokine (C-C motif) ligand
CSDB	Carbohydrate Structure Database
DCs	Dendritic cells
DOSY	Diffusion-Ordered Spectroscopy
EAACI	European Academy of Allergy and Clinical Immunology
FPLC	Fast protein liquid chromatography
GF	Germ-free
GLC-MS	Gas-liquid chromatography-mass spectrometry
HDM	House dust mites
HEK	Human embryonic kidney cells
IFN-γ	Interferon gamma
Ig	Immunoglobulin
IL	Interleukin
ISAPP	International Scientific Association for Probiotics and Prebiotics
LPS	Lipopolysaccharide
LTA	Lipoteichoic acid
NMR	Nuclear Magnetic Resonance
OVA	Ovalbumin
PG	Peptidoglycan

PRR	Pattern recognition receptor
PS	Polysaccharide
Th	T helper cell
TLR	Toll-like receptor
TNF-α	Tumor necrosis factor α

Streszczenie

Alergia oddechowa to schorzenie objawiające się nadwrażliwością organizmu na nieszkodliwe cząsteczki zwane alergenami. Choroba ta należy do najczęstszych problemów zdrowotnych w krajach rozwiniętych. Wpływa nie tylko na jakość życia pacjentów, ale także na gospodarkę, zwiększając koszty opieki zdrowotnej i obniżając produktywność osób cierpiących na alergię. Chcąc skutecznie stawić czoła rosnącemu problemowi alergii oddechowej, konieczne jest poszukiwanie nowych, alternatywnych metod leczenia. Dostępne terapie są często niewystarczające i mogą powodować liczne efekty uboczne. Najnowsze badania wykazują związek między mikrobiotą a ryzykiem wystąpienia alergii. Opisują również znaczenie szczepów *Bifidobacterium* w łagodzeniu objawów astmy. Okazuje się, że nie tylko żywe i proliferujące bakterie mogą korzystnie wpływać na zdrowie gospodarza. Cząsteczki efektorowe, metabolity produkowane przez bakterie, czy też jej fragmenty, znane jako postbiotyki, mogą wykazywać podobne lub lepsze właściwości niż mikroorganizm z którego pochodzą. Dzięki możliwości określenia ich struktury chemicznej, cząsteczki te są idealnymi kandydatami do szczegółowych badań funkcjonalnych. Co więcej, w przeciwieństwie do żywych organizmów, nie mogą przenosić genów oporności na antybiotyki ani wywoływać bakteriemii, co zwiększa bezpieczeństwo ich stosowania.

W niniejszej rozprawie doktorskiej zbadano potencjał antygenów powierzchniowych produkowanych przez *Bifidobacterium animalis* ssp. *animalis* CCDM 218 (Ban218) oraz *Bifidobacterium adolescentis* CCDM 368 (Bad368). W pierwszej kolejności wyizolowano i oczyszczono antygeny powierzchniowe, do których należały peptydoglikan (PG, jeden na szczep), kwasy lipotejchojowe (LTA, jeden na szczep) oraz polisacharydy (PS) (B.PAT, PS 2, PS 3 dla Ban218 oraz BAP1, PS 2, PS 3 dla Bad368). Badanie wpływu antygenów na aktywność splenocytów wyizolowanych z myszy uwrażliwionych owoalbuminą (OVA) wykazało, że BAP1 ma największy potencjał w przywracaniu równowagi między limfocytami T pomocniczymi typu 1 (Th1) i 2 (Th2). Z tego powodu BAP1 poddano dalszym, szczegółowym analizom. Wykazały one efektywny transfer PS między komórkami nabłonkowymi a komórkami układu odpornościowego. Dokładna analiza chemiczna BAP1 pozwoliła określić nieopisaną wcześniej strukturę heksasacharydu, składającego się z reszt ramnozy, glukozy i galaktozy, tworzących PS o masie cząsteczkowej około 9.99×10^6. Następnie, BAP1 testowano na myszach wolnych od drobnoustrojów (GF). Okazało się, że mimo ogólnego neutralnego wpływu PS na naiwny układ odpornościowy, był on w stanie zmniejszyć poziom ligandu chemokiny 2 (CCL2) i eotaksyny, jednocześnie zwiększając ekspresję *Rorc* w płucach. Co ciekawe, donosowe podanie BAP1 myszom uczulonym na OVA wywołało zarówno ogólnoustrojową, jak i lokalną odpowiedź organizmu. Przede wszystkim zmniejszyło ono

poziom specyficznej dla OVA immunoglobuliny (Ig) E w surowicy, jak i produkcję cytokin Th2 oraz IL-10 w splenocytach. W płucach, BAP1 zredukował zapalenie poprzez zahamowanie napływu eozynofilów i makrofagów oraz ograniczenie produkcji cytokin IL-5, IL-13, IL-4 i IL-10. Analiza ekspresji genów powieliła wyniki uzyskane na myszach GF dotyczące wpływu BAP1 na ekspresję *Rorc*, choć wynik ten był statystycznie nieistotny. Potwierdziła również rolę testowanego PS w hamowaniu produkcji cytokiny IL-10, poprzez zmniejszenie ekspresji odpowiedzialnego za jej produkcję genu.

Spośród antygenów powierzchniowych Ban218, B.PAT okazał się najbardziej interesujący z powodu występowania w jego strukturze fosforu. Chcąc sprawdzić, czy określone modyfikacje PS mogą poprawić jego funkcję, B.PAT poddano defosforylacji. Wyniki pokazały, że zabieg ten zmienił strukturę przestrzenną PS, a co ważniejsze, zwiększył jego właściwości immunomodulujące, jak wykazano na badaniach z wykorzystaniem komórek dendrytycznych szpiku kostnego (BMDCs). Ponadto, defosforylacja skutkowała wzmocnieniem właściwości przeciwzapalnych B.PAT w modelu stanu zapalnego wywołanego interleukiną(IL)-1β.

Podsumowując, za najważniejsze osiągnięcie przedstawione w tej rozprawie doktorskiej należy wskazać opisanie ogromnego potencjał BAP1 w łagodzeniu alergii dróg oddechowych. Jednakże, w przyszłości konieczne będą dalsze eksperymenty mające na celu dokładne zrozumienie jego mechanizmu działania. Niezbędne będą również badania kliniczne na ludziach, aby zweryfikować wyniki uzyskane w modelach mysich.

Abstract

Airway allergy is defined as a disorder manifested by a hypersensitive reaction of an organism to a harmless molecule called an allergen. This disease is one of the most common healthcare issues in developed countries. It affects not only patients' quality of life but also the world's economy through high healthcare costs and lower performance of allergic patients. Alternative treatments are indispensable to overcome the emerging problem of airway allergy since available therapies are insufficient in some patients and cause numerous side effects. Recent studies connected healthy microbiota with lower allergy risk. The importance of *Bifidobacterium* strains' presence in reducing asthma outcomes was described. However, not only life and proliferating bacteria can beneficially impact a host's health. Effector molecules, metabolites produced by bacteria or their compounds, so-called postbiotics, can show the same or enhanced properties of their bacteria of origin. Due to their easy-to-determine structure, these molecules are perfect candidates for detailed functional studies. Moreover, due to their inanimate state, they cannot transfer antibiotic-resistance genes or cause bacteremia, which increases the safety of their use.

In this doctoral dissertation, the biological potential of the effector molecules produced by *Bifidobacterium animalis* ssp. *animalis* CCDM 218 (Ban218) and *Bifidobacterium adolescentis* CCDM 368 (Bad368) was investigated. First, surface antigens were isolated and purified including peptidoglycan (PG, one per strain), lipoteichoic acids (LTA, one per strain), and polysaccharides (PS) (B.PAT, PS 2, PS 3 for Ban218, and BAP1, PS 2, PS 3 for Bad368). Investigation of the antigen's impact on the splenocytes isolated from OVA-induced mice showed the biggest potential of BAP1 to restore the balance between T helper cells type 1 (Th1) and 2 (Th2). For this reason, it was BAP1 that was subjected to further detailed analysis. The investigation showed efficient transfer of the selected PS between epithelial and immune cells. A comprehensive investigation of the BAP1 structure allowed the determination of a unique hexasaccharide repeating unit consisting of rhamnose, glucose, and galactose residues creating a PS of molecular mass approximately 9.99 x 10^6. Next, the impact of BAP1 was tested in germ-free (GF) mice. It turned out that despite the general neutral effect of this PS on the naïve immune system, it was able to decrease allergy-related chemokine (C-C motif) ligand 2 (CCL2) and eotaxin levels and increase *Rorc* expression in the lungs. Intriguingly, intranasal administration of BAP1 to OVA-allergy mice induced both systemic and local responses. It decreased OVA-specific immunoglobulin (Ig) E in sera as well as IL-10, and Th2-related cytokine production in splenocytes. In the lungs, it reduced inflammation by inhibiting eosinophils and macrophage infiltration together with IL-5, IL-13, IL-4, and IL-10 cytokine production by lung cells. Finally, gene expression analysis recalled the results obtained in GF mice regarding BAP1's impact on the *Rorc* expression, however, the result was insignificant.

Also, it confirmed the role of the tested PS in the inhibition of IL-10 cytokine production since it led to a decrease in *Il10* gene expression.

Among Ban218 surface antigens it was B.PAT which appeared to be the most interesting due to the presence of phosphorus substitution. To investigate whether the introduction of certain modifications to a PS may improve its function, in this work, the B.PAT underwent dephosphorylation. Results showed that this treatment changed the spatial structure of B.PAT, and importantly, it increased PS's immunomodulatory functions in bone marrow dendritic cells (BMDCs). In addition, dephosphorylation enhanced the anti-inflammatory properties of B.PAT in the model of interleukin(IL)-1β inflammation.

Overall, the results presented in this doctoral dissertation positively confirm the great potential of BAP1 to alleviate airway allergies. In the future, extensive research on the BAP1 is needed to fully understand its mechanism of action. Furthermore, clinical studies on humans are necessary to validate results obtained in mice models.

1. Introduction

The European Academy of Allergy and Clinical Immunology (EAACI) defines an allergy as "a disorder caused by an abnormal reaction to a harmless substance called an allergen" [1]. Allergy occurrence was observed centuries ago, however, in recent years, the number of cases has increased dramatically [2,3].

With an increased allergy prevalence, few hypotheses occurred to explain this state of affairs. Strachan (1989) formed one of the oldest so-called "hygiene hypothesis" [4]. It claims that decreased exposure to microbes and lower infection rates contribute to a higher risk of allergy and autoimmune diseases. This definition was transformed in the early 2000s by Graham A. W. Rook into the "old friends hypothesis". It indicates that not all microorganisms but those that co-evolved with mammals are responsible for the proper development of the immune system and reduced allergy occurrence [5,6]. Another hypothesis relates to the importance of epithelial barrier integrity in the prevention of inappropriate immune responses. It suggests that urbanization and industrialization, associated with modern life, are responsible for the production of epithelial-damaging molecules, contributing to the development of allergies [7]. Moreover, it highlights the role of healthy microbiota in maintaining proper epithelial barrier functions. Interestingly, studies performed on germ-free (GF) mice showed that the presence of microbes is essential for the development of allergy symptoms indicating the vital role of microorganisms in the modulation of immune responses [8]. In addition, the use of GF mice allows the study of the impact of molecules on the naïve immune response, the observation of molecule-specific effects, and easier functional studies [9].

1.1 Airway allergies

Airway allergies are a major healthcare problem with allergy rhinitis affecting even 50 % of the population in some countries and asthma occurrence in almost 350 million people worldwide [10–12]. It impacts not only patients' quality of life but also world economics, including healthcare expenses and costs related to lower productivity and absence of employees at work [13]. Current allergy treatments are focused on allergen avoidance, drug treatment (e.g. antihistamines, glucocorticoids), or allergen-specific immunotherapy. Unfortunately, those therapies are inefficient in some patients or cause numerous side effects including excessive sleepiness [14]. Moreover, in the majority of cases, they focus on symptom relief rather than an allergy mechanism of action (Fig. 1).

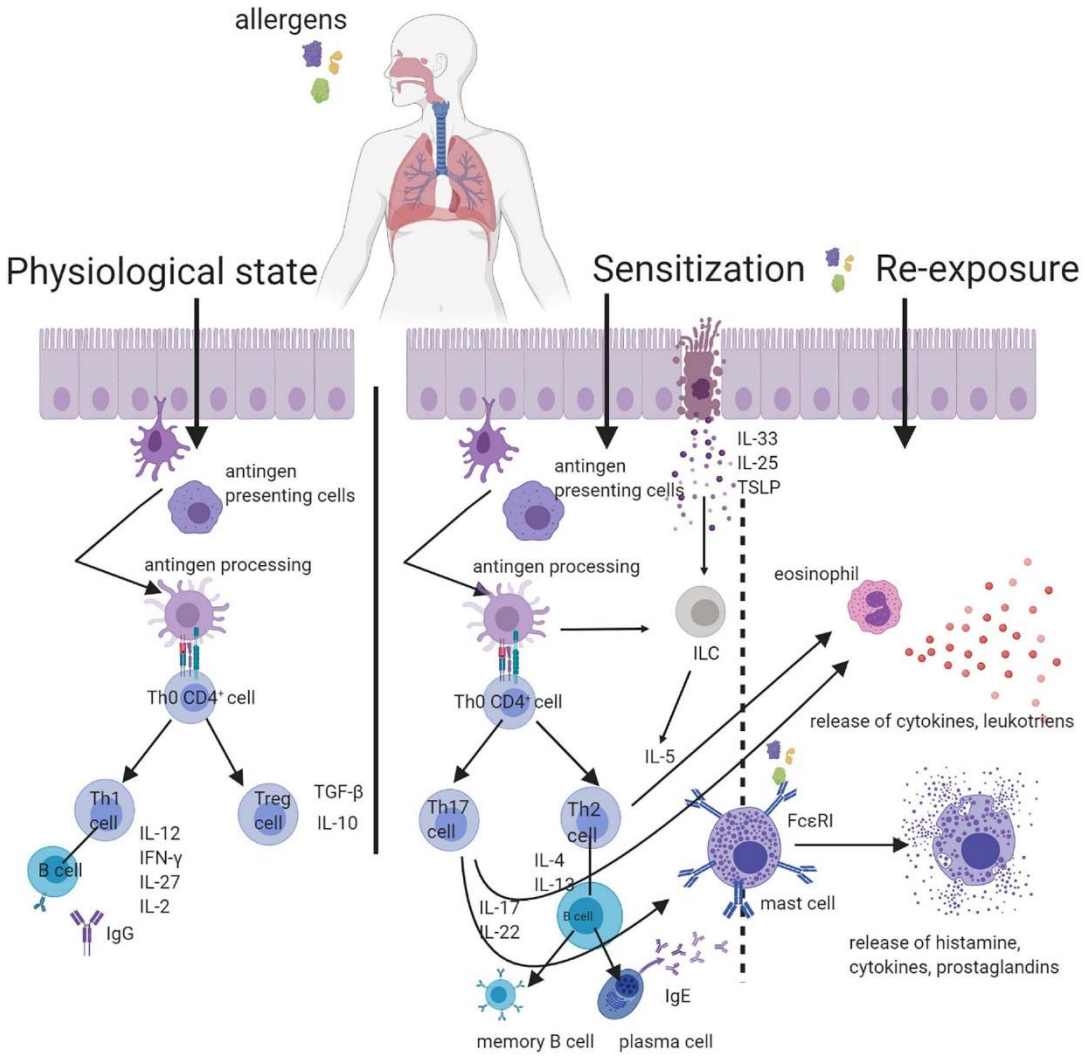

Fig. 1. Mechanism of airway allergy (adapted from Jakubczyk and Górska, 2021)[12].

In a physiological state, a well-functioning epithelial barrier protects the organism against the penetration of foreign particles. Moreover, the balance between T helper cells (Th1 and Th2) is maintained. Loss of tight connections in the epithelium results in further allergen penetration, and a switch of naïve T cells into a Th2 subpopulation[12].

The loss of epithelial barrier integrity may be caused by an allergen through direct and indirect mechanisms. For instance, house dust mites (HDM) is an allergen consisting of different antigens that include components of bacterial and fungal origin. Those molecules can activate different pattern recognition receptors (PRRs), e.g. lipopolysaccharides (LPS) of gram-negative bacteria can be recognized by toll-like receptor (TLR) 4 or β-glucans by TLR2 or Dectin-1. Those can indirectly increase the inflammation process and the disruption of the epithelial barrier permeability. On the other hand, remaining HDM molecules, which include proteases, can directly demolish epithelium integrity allowing allergen entrance to the organism. In the next step, dendritic cells

(DCs) process the allergen and present it to T-cells that further differentiate into Th2 cells producing interleukin(IL)-4, IL-5, and IL-13. It leads to the activation of (1) eosinophils and (2) B-cells, which produce immunoglobulin (Ig) E that in the presence of an allergen binds to the IgE-specific receptor and activates the degranulation of mast cells and basophils. The latter, together with eosinophils, produce various molecules that further facilitate the allergic reaction and Th2 responses [15]. Thus, developing a therapy that could restore the disrupted balance between Th1 and Th2 cells or improve the integrity of the respiratory barrier would be highly desirable.

1.2 Microbiota dysbiosis in allergy

Differences in nasal bacteria composition were observed in newborns with asthma (higher abundance of *Haemophilus* and *Streptococcus* strains) when compared to healthy volunteers, which in turn were characterized by an increased level of *Lactobacillus* [16]. Furthermore, microbiota dysbiosis in the gastrointestinal tract, and recently also in the respiratory tract, has been connected with a higher risk of airway allergies [17–19]. Given that the microbiota of healthy and allergic patients differ noticeably, there is a consensus among scientists that probiotics play a crucial role in inhibiting inappropriate immune responses. According to the definition, probiotics are "live microorganisms that, when administered in adequate amounts, confer a health benefit on the host" [20]. They are known to play vital roles in many physiological and immunological functions. They are essential for the integrity of the epithelial barrier, as well as for the maturation of the immune system, the induction of tolerance, and the development of immune responses [14].

1.3 Bifidobacterium in allergy diseases

Bifidobacterium strains are gram-positive bacteria that live under anaerobic or microaerophilic conditions. They are one of the first colonizers of the human gut and are responsible for the proper growth and development of infants [21]. They are key in modulating the immune system, maintaining the composition of the microbiota, and producing vital molecules such as vitamins [22]. The role of *Bifidobacterium* in the prevention and treatment of allergy diseases was also described in detail [12,17]. For instance, studies performed by Fujimura *et al.* underlined the role of *Bifidobacteria, Akkermansia*, and *Faecalibacterium* in the prevention of asthma outcomes [23]. Liu *et al.* investigated the preventive and therapeutic effect of *Bifidobacterium infantis* CGMCC313-2 in ovalbumin(OVA)-induced airway asthma mice. The obtained results were consistent for both strains and showed the ability of the bacteria to reduce OVA-specific IgE and IgG1 in sera and lung cell infiltration in bronchoalveolar lavage fluid (BALF), as well as to inhibit IL-13 and IL-4 production both in sera and BALF [24].

1.4. Postbiotics in allergies

Further studies of probiotics revealed that not only live and proliferating bacteria can exhibit beneficial effects on humans (Fig. 2). In 2019, the International Scientific Association for Probiotics and Prebiotics (ISAPP) proposed a new term "postbiotics" and defined it as a "preparation of inanimate microorganisms and/or their components that confers a health benefit on the host" [25]. Postbiotics are associated with crucial advantages over probiotics:

A. easy-to-define structure and function,
B. opportunity for structure-function studies,
C. inability to reproduce and therefore to cause bacteremia or transfer of antibiotic-resistance genes,
D. high stability [25,26].

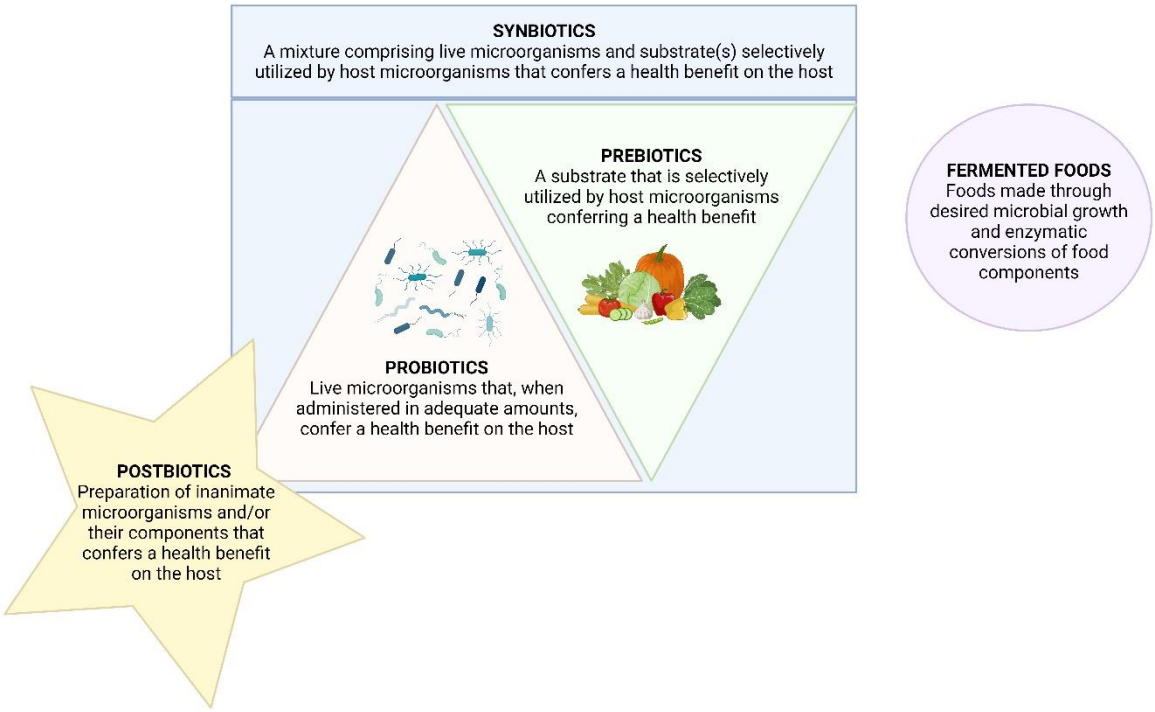

Fig. 2. Types of biotics described by the ISAPP [20,25,27–29].

Postbiotics can include antigens found on the surface of bacteria, including (Fig. 3):

1. Peptidoglycan (PG): a 3-dimensional structure, composed of *N*-acetylglucosamine and *N*-acetylmuramic acid, connected by β-1,4-O-glycosidic bonds and linked by peptide chain. *Bifidobacterium* strains were identified with a type A PG that features a connection

between the amino group of the diamino acid at the third position of the adjacent peptide and the carbonyl group of D-alanine at the 4th position [30,31].

2. Lipoteichoic acids (LTAs): anionic cell surface molecules. Their structure can be divided into two main components: hydrophilic backbone and hydrophobic glycolipid anchor, which affect the LTA amphiphilic nature that allows them to play significant, biological roles [32].
3. Surface proteins: proteins attached to the cell surface of bacteria by covalent or non-covalent bonds [33].
4. Polysaccharides (PS): high molecular weight polymers created by repeating monosaccharide units connected by glycosidic bonds [34]. They may be chemically modified, which can influence their spatial structure, charge, molecular weight, and function [35,36]. In *Bifidobacterium* strains, they consist mostly of glucose and galactose moieties [37–40].

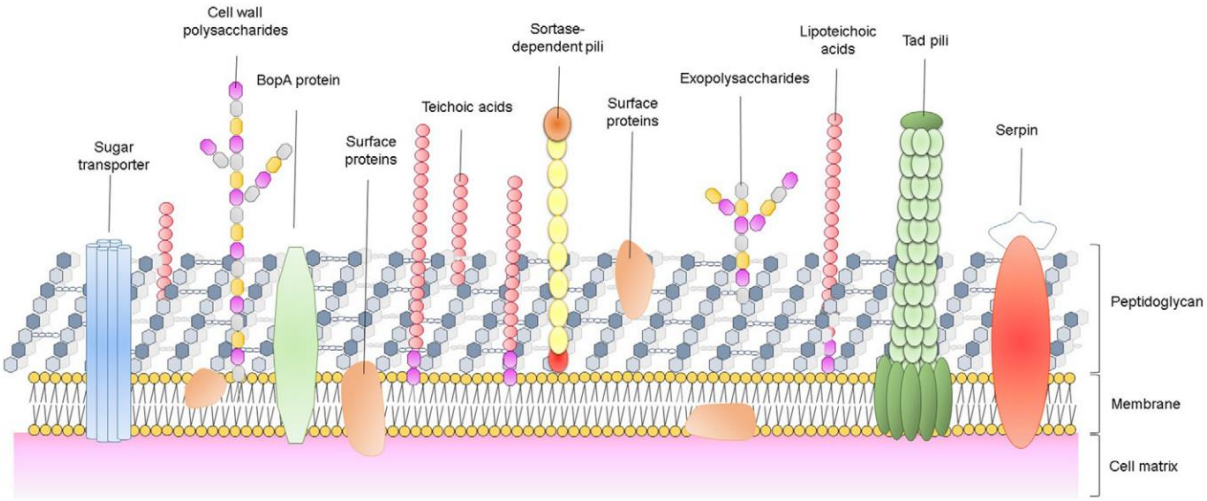

Fig. 3. The surface antigens present on the bifidobacteria cell wall (adapted from Pyclik et al., 2020) [30].

First, to fully understand the role of the tested molecule, it is crucial to determine its structure in detail. This will allow the structure-function relationship studies and introduction of the chemical modifications to improve the initial properties. Next, prior to *in vivo* studies, it is important to consider the delivery mode of postbiotics, as this may affect the final result. Suzuki *et al.* (2022) investigated different administration methods of OVA-pulsed CD-40 silenced DCs in OVA-treated mice. He observed different effects while testing subcutaneous, intraperitoneal, intravenous, and intranasal administration [41]. In the context of allergy treatment, not only systemic response activation, but also the local effect is desirable for the alleviation of lung inflammation. Thus, intranasal administration seems to be the most appropriate for this type of study [42,43]. Although publications regarding the immunomodulatory role of postbiotics started to gain attention in

recent years, there is little information about their impact on airway allergies. Studies performed with heterogeneous PS from *Lonicera japonica* showed reduced symptoms of OVA-induced airway allergy in mice treated with this molecule [44]. Also, *Lacticaseibacillus rhamnosus* LOCK900 PS inhibited the development of allergy inflammation in OVA-treated mice [42]. Overall, research on surface antigens holds great promise and could offer innovative solutions for treating and preventing allergies in the future.

2. Research background and objectives

The results presented in this doctoral dissertation are a natural continuation of the previous studies performed in our laboratory. 10 different *Bifidobacterium* strains were tested for their potential anti-allergic properties and 5 of them were selected for further analysis [22]. Two of them, *Bifidobacterium animalis* ssp. *animalis* CCDM 218 (Ban218) and *Bifidobacterium adolescentis* CCDM 368 (Bad368) are of interest in this study. They were subjected to detailed investigation to determine which of the surface antigens may be responsible for bacteria's ability to alleviate allergy symptoms.

Therefore, the main objective of this study was established as follows:

The determination of the surface antigens responsible for bacteria's ability to alleviate allergy symptoms.

It was achieved by breaking down and accomplishing 4 smaller objectives:

O1. Isolation and purification of *Bifidobacterium* surface antigens and determination of their cytokine profile in OVA-induced mice splenocytes and DCs.

O2. Structure determination of antigens with the most promising abilities to alleviate OVA-induced mouse sensitization.

O3. Analysis of selected surface antigen’s impact on the development of the naïve immune system of GF mice when administered intranasally.

O4: Investigation of the anti-allergic potential of selected surface antigens in the mouse OVA-induced allergy model when administered intranasally.

Therefore, before commencing the research, a hypothesis was proposed:

The surface antigens of *Bifidobacterium animalis* ssp. *animalis* CCDM 218 and *Bifidobacterium adolescentis* CCDM 368 are responsible for the anti-allergic potential of the whole bacteria.

4. 1st manuscript

4.1. Foreword to the 1st manuscript

A. Rationale of research objectives

Over the last decades, allergies have become a worldwide emerging issue. Unfortunately, available allergy treatments have drawbacks and can be less efficient in some patients. Recent studies have linked bacterial dysbiosis with allergic hypersensitivity. The research data underlined the importance of different probiotic strains, including *Bifidobacterium*, in preventing and treating allergy outcomes **(Chapters 1.2 and 1.3)**. The newest attempt focuses on bacterial surface antigens that can surpass the properties of their parent bacteria **(Chapter 1.4)**.

Given the above, *Bifidobacterium adolescentis* CCDM 368 was selected as promising in alleviating allergy diseases. To fulfill objectives **O1** and **O2**, Bad368 surface antigens were isolated, purified, and tested in splenocytes and DCs isolated from OVA-sensitized mice. This allowed the selection of the molecule with a known structure with promising anti-allergic properties, which also was found to be efficiently transferred between epithelial and antigen-presenting cells.

B. Methodology:

- Selection of the Bad368 strain by evaluating the Th2-related cytokine production in OVA-treated splenocytes, isolated from OVA-sensitized mice.
- Cultivation of the Bad368 strain and bacterial mass collection.
- Isolation and purification of Bad368 surface antigens, including PSs, LTAs, and PG.
- Determination of innate immune receptors' activation in human embryonic kidney cells (HEK-Blue™) transfected with TLR2, TLR4, and NOD2 after stimulation with tested antigens.
- Determination of cytokine production by splenocytes and bone marrow dendritic cells (BMDCs) cells isolated from the mice sensitized with OVA after treatment with tested antigens.
- Antigens staining, uptake by epithelial cell line (TC-1), and transfer between mouse epithelial (TC-1) and DCs (JAWS II).
- Structure determination of the BAP1 compound with the use of chemical methods, gas-liquid chromatography-mass spectrometry (GLC-MS), fast protein liquid chromatography (FPLC), and nuclear magnetic resonance (NMR) spectroscopy.

C. Results:

- Bad368 strain's surface contained 3 structurally different PSs (BAP1, Bad368.2, and Bad368.3) and one LTA and PG.
- All antigens except Bad368.2 PS were recognized by TLR2 receptor. TLR4 was activated by BAP1 and Bad368.3, while NOD2 – by PG.
- Splenocytes response:
    - BAP1 tended to decrease IL-13 and significantly reduce IL-5 cytokine levels in splenocytes. Moreover, as the only one, caused a burst in interferon gamma (IFN-γ) production. It was also able to induce regulatory IL-10 cytokine.
    - Bad368.3 significantly decreased IL-5 levels in mice splenocytes, however, did not affect IL-10 cytokine. Compared to BAP1, it caused a notably smaller increase in IFN-γ production.
    - Even though PG induced higher levels of IL-10 and IFN-γ, it did not decrease Th2-related cytokines and even enhanced IL-13 production.
    - Bad368.2 and LTA did not show any interesting changes in cytokines levels.
- BMDCs response:
    - BAP1 induced the strongest cytokine response with a significant increase in IL-6 production.
- Investigation of BAP1 processing showed 99.9 % uptake by epithelial cells (TC-1) and 71.3 %. transfer from epithelial cells to DCs
- NMR and GLC-MS analysis allowed the determination of BAP1 structure, which is a linear, high molecular mass PS of approximately 9.99 x 10^6, containing glucose, galactose, and rhamnose residues, creating a following repeating unit:

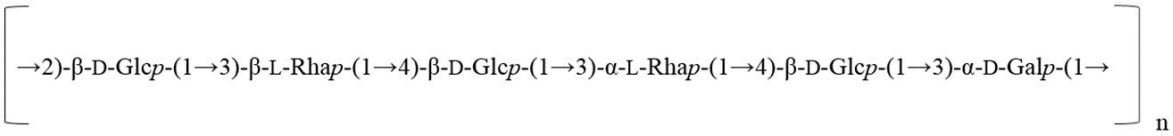

D. Conclusions:

BAP1 isolated from the surface of the Bad368 strain is an antigen of a high molecular mass and unique structure. It exhibits a high potential to alleviate allergy diseases by restoring the balance between Th1 and Th2-related cytokines. Moreover, the efficient uptake and transfer of BAP1 works in favor of inducing immune responses including TLR2-dependent processes.

4.2. Copy of the 1st manuscript

Pacyga-Prus, K., Jakubczyk, D., Sandström, C., Šrůtková, D., Pyclik, M.J., Leszczyńska, K., Ciekot, J., Razim, A., Schwarzer, M., Górska, S. Polysaccharide BAP1 of *Bifidobacterium adolescentis* CCDM 368 is a biologically active molecule with immunomodulatory properties. Carbohydr Polym. 2023 Sep 1;315:120980. doi: 10.1016/j.carbpol.2023.120980.

A. Graphical abstract

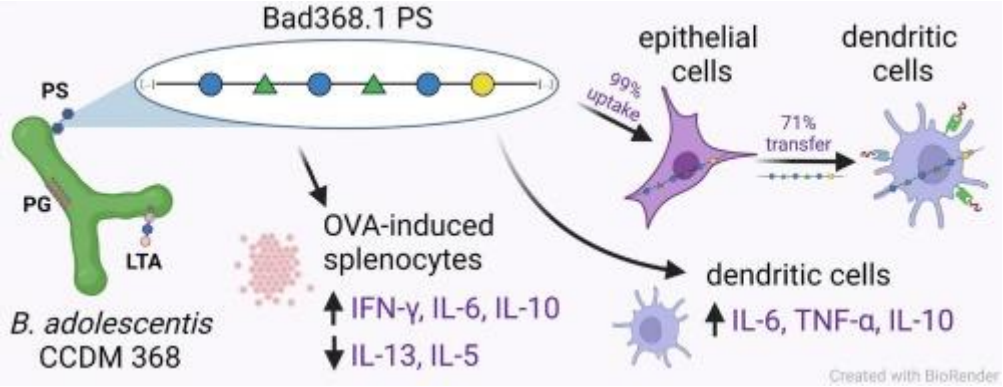

B. Manuscript and supplementary data

Carbohydrate Polymers 315 (2023) 120980

Contents lists available at ScienceDirect

Carbohydrate Polymers

journal homepage: www.elsevier.com/locate/carbpol

Polysaccharide BAP1 of *Bifidobacterium adolescentis* CCDM 368 is a biologically active molecule with immunomodulatory properties

Katarzyna Pacyga-Prus [a,*], Dominika Jakubczyk [a], Corine Sandström [b], Dagmar Šrůtková [c], Marcelina Joanna Pyclik [a], Katarzyna Leszczyńska [a], Jarosław Ciekot [d], Agnieszka Razim [a], Martin Schwarzer [c], Sabina Górska [a,*]

[a] Laboratory of Microbiome Immunobiology, Hirszfeld Institute of Immunology and Experimental Therapy, Polish Academy of Sciences, 53-114 Wroclaw, Poland
[b] Department of Molecular Sciences, Swedish University of Agricultural Sciences, Box 7015, SE-750 07 Uppsala, Sweden
[c] Laboratory of Gnotobiology, Institute of Microbiology, Czech Academy of Sciences, 549 22 Novy Hradek, Czech Republic
[d] Laboratory of Biomedical Chemistry, Hirszfeld Institute of Immunology and Experimental Therapy, Polish Academy of Sciences, 53-114 Wroclaw, Poland

ARTICLE INFO

Keywords:
Allergy
Bifidobacterium
Polysaccharides
Surface antigens
Macromolecules

ABSTRACT

Bifidobacteria are among the most common bacteria used for their probiotic properties and their impact on the maturation and function of the immune system has been well-described. Recently, scientific interest is shifting from live bacteria to defined bacteria-derived biologically active molecules. Their greatest advantage over probiotics is the defined structure and the effect independent of the viability status of the bacteria. Here, we aim to characterize *Bifidobacterium adolescentis* CCDM 368 surface antigens that include polysaccharides (PSs), lipoteichoic acids (LTAs), and peptidoglycan (PG). Among them, Bad368.1 PS was observed to modulate OVA-induced cytokine production in cells isolated from OVA-sensitized mice by increasing the production of Th1-related IFN-γ and inhibition of Th2-related IL-5 and IL-13 cytokines (*in vitro*). Moreover, Bad368.1 PS (BAP1) is efficiently engulfed and transferred between epithelial and dendritic cells. Therefore, we propose that the Bad368.1 PS (BAP1) can be used for the modulation of allergic diseases in humans. Structural studies revealed that Bad368.1 PS has an average molecular mass of approximately 9,99 × 10^6 Da and it consists of glucose, galactose, and rhamnose residues that are creating the following repeating unit:

$[\rightarrow 2)$-β-D-Glc*p*-$(1\rightarrow 3)$-β-L-Rha*p*-$(1\rightarrow 4)$-β-D-Glc*p*-$(1\rightarrow 3)$-α-L-Rha*p*-$(1\rightarrow 4)$-β-D-Glc*p*-$(1\rightarrow 3)$-α-D-Gal*p*-$(1\rightarrow]_n$

1. Introduction

The definition of probiotics associated with bacterial cell viability has been established over 20 years ago and the promise of applied probiotic bacteria for a variety of health purposes is well-described (Kerry et al., 2018). *Bifidobacterium* strains are Gram-positive, anaerobic bacteria that are constituents of the human microbiota. They play a pivotal role in the immune system maturation and modulation of immune cell responses (Ruiz et al., 2017). Administration of live *Bifidobacterium* strains triggers immune responses either in healthy or allergy-sensitized mice through e.g. changes in cytokine production or specific activation of the immune cells subsets (Hiramatsu et al., 2011; Raftis et al., 2018). Nowadays, it becomes clear that not only live and proliferating bacteria are having a beneficial effect but also certain effector molecules produced by them (Schiavi et al., 2016; Speciale et al., 2019; Xu et al., 2017). The exopolysaccharides, (lipo)teichoic acids, glycolipids, peptidoglycans, proteins, and other components of probiotic bacteria are of interest as potentially biologically active structures. Recently, they have been named by the International Scientific Association of Probiotics and Prebiotics as "postbiotics" (Nataraj et al., 2020). Health-promoting effects of these molecules are easy to establish through identifiable structures, thus enabling the analysis of structure-function relationships. However, our understanding of the link between a defined postbiotic structure and its biological effect on the host is still in its infancy. Among the most intensively studied bifidobacterial postbiotic molecules are polysaccharides (PSs), peptidoglycans (PGs), and lipoteichoic acids (LTAs).

Bifidobacterial PSs consist mainly of galactoses and glucoses (Inturri

* Corresponding authors.
E-mail addresses: katarzyna.pacyga-prus@hirszfeld.pl (K. Pacyga-Prus), dominika.jakubczyk@hirszfeld.pl (D. Jakubczyk), corine.sandstrom@slu.se (C. Sandström), srutkova@centrum.cz (D. Šrůtková), marcelina.pyclik@hirszfeld.pl (M.J. Pyclik), katarzyna.leszczynska@hirszfeld.pl (K. Leszczyńska), jaroslaw.ciekot@hirszfeld.pl (J. Ciekot), agnieszka.razim@hirszfeld.pl (A. Razim), schwarzer@centrum.cz (M. Schwarzer), sabina.gorska@hirszfeld.pl (S. Górska).

https://doi.org/10.1016/j.carbpol.2023.120980
Received 2 March 2023; Received in revised form 14 April 2023; Accepted 1 May 2023
Available online 4 May 2023

et al., 2017; Nagaoka et al., 1996; Speciale et al., 2019; Zdorovenko et al., 2009). Differences between PSs are based generally on the α/β isomers composition, linkages between monosaccharides, and the order of the sugar residues in a PS chain unit. Bifidobacterial PSs may also contain relatively abundant rhamnose and less frequent mannose or 6-deoxy-D-talose (Altmann et al., 2016; Kohno et al., 2009; Nagaoka et al., 1988; Shang et al., 2013). The biological function of PSs is still not fully explored, but it appears to be strongly related to their chemical structure. The neutral and/or high molecular weight PSs can act as suppressors of the immune responses, while acidic and/or small molecular weight PSs are associated with immunostimulatory properties (Górska et al., 2017; Pyclik et al., 2020; Zhou et al., 2019). PG of the *Bifidobacterium* genus belongs to type A (divided into 4 subtypes A1-A4) and is characterized by the binding of the D-alanine carbonyl group (at the 4th position) and the diamino acid (at the 3rd position) of the neighboring peptide. The primary role of PG is to scaffold bacterial cell and protect against environmental factors. It is also a potent immunomodulator that regulates homeostasis and triggers immune responses by continuous stimulation of NOD receptors (Clarke et al., 2010; Martinic et al., 2017; Wolf & Underhill, 2018). The bifidobacterial LTAs are composed of a hydrophilic backbone (e.g. glycerol-, ribitol-phosphate) and hydrophobic glycolipid anchor creating together an amphiphilic structure, which plays biologically significant roles. Recently, it has been shown that the LTA from *B. animalis* subsp. *lactis* BPL1 reduces fat deposition through the regulation of the IGF-1 pathway in *the Caenorhabditis elegans* model (Balaguer et al., 2022). Moreover, LTA derived from *Lactobacillus reuteri* exhibited anti-inflammatory activity through MAPK and the NF-κβ pathways in LPS-induced macrophages (Lu et al., 2022).

Allergic diseases remain a major public health problem that impacts patients' quality of life (Palomares et al., 2017). Allergic inflammation is typically driven by type 2 immune responses to environmental allergens manifested by the differentiation of naïve T CD4+ cells towards Th2 effector cells, allergen-specific IgE induction, IL-4, IL-5, and IL-13 production, eosinophilia, and mast cells activation. *Bifidobacterium* strains were shown to restore immunological balance and effectively alleviate allergic responses. Tian et al. showed the potential of *B. animalis* KV9 to alleviate β-globulin induced food allergy in BALB/c mice (Tian et al., 2022). Moreover, we have previously shown that neonatal colonization of germ-free mice with *B. longum* ssp. *longum* CCM 7952 prevented sensitization to major birch pollen allergen Bet v1 (Schwarzer et al., 2013). Of note, intranasal administration of the same bifidobacterial strain exhibited allergy-reducing properties in ovalbumin (OVA)-sensitized mice (Pyclik et al., 2021).

We showed the ability of live as well as heat-killed *Bifidobacterium adolescentis* CCDM 368 (Bad368) to modulate the OVA-stimulated cytokine release from cells isolated from OVA-sensitized mice. Given the functionality of the heat-treated Bad368, we attempted to decipher which of the cell wall-associated postbiotics can actively participate in the Bad368 modulatory properties. Here, we demonstrate that one of the PSs, Bad368.1 with a unique structure, actively participates in the Bad368 immunomodulatory activities and is efficiently engulfed by lung epithelial cells and transferred to dendritic cells. Finally, the comprehensive chemical and NMR spectroscopy analysis allowed us to determine the structure of Bad368.1 PS, which we consider a prerequisite for potential use as a postbiotic in further medical applications.

2. Materials and methods

2.1. Bifidobacterium adolescentis CCDM 368 cultivation

Bifidobacterium adolescentis CCDM 368 (Bad368) from human adult feces was obtained from the Czech Collection of Diary Microorganisms (CCDM, Laktoflora, Milcom, Tábor, Czech Republic). The isolates were cultivated for 72 h in MRS broth (Sigma Aldrich) with 0.05 % L-cysteine (Merck Millipore) at 37 °C in an anaerobic chamber (Oxoid, 80 % N_2, 10 % CO_2, 10 % H_2). Before the start of the experiments, Bad368 was centrifuged (4500 ×*g*, 15 min, 4 °C) and washed with sterile phosphate-buffered saline (PBS). Finally, the bacterial pellet was frozen, freeze-dried and used for further isolations.

2.2. Isolation and purification of antigens

2.2.1. Polysaccharides

The isolation protocol was conducted according to Górska et al. (Górska et al., 2010). Briefly, bacterial mass was sonicated, incubated with shaking in 10 % trichloroacetic acid (2.5 h; room temperature (23 °C), and centrifuged (15,000 ×*g*; 4 °C; 20 min). The supernatant was treated with 5 volumes of ethanol and incubated overnight at −20 °C. On the next day, the suspension was centrifuged (as before) and the obtained pellet was dialyzed to miliQ water for 24 h at 4 °C (MWCO 6–8 kDa, Roth) and freeze-dried. Later, NGS Chromatography System (Bio-Rad) equipped with a UV detector was used to separate the resulting PSs mixture with the use of ion exchange chromatography (DEAE-Sephadex A-25 column; 1.6 × 20 cm (Pharmacia); buffer A: 20 mM Tris-HCl, buffer B: 2 M NaCl; linear-gradient (0 % B – 100 % B); 23 °C) and size exclusion chromatography (TSK HQ-55S column; 1.6 × 100 cm (Amersham Pharmacia Biotech); eluted with 0.1 M ammonium acetate; 23 °C). The phenol-sulfuric acid method was used to measure carbohydrate content in fractions collected after column separations (DuBois et al., 1956). Finally, obtained polysaccharide samples were analyzed using classical chemical methods and NMR spectroscopy (Górska et al., 2014).

2.2.2. Lipoteichoic acids

The LTA isolation procedure was conducted according to the modified protocol of Morath et al. (Morath et al., 2001). Briefly, bacterial mass was incubated with shaking in miliQ water and n-butanol mixture (1:1 v/v; 30 min; 23 °C). Next, the suspension was centrifuged (13,000 ×*g*; 20 min; 4 °C) and the pellet was re-extracted in the same manner (3 to 4 times). Finally, the water phase was collected, frozen, and freeze-dried. To purify and separate the obtained structures, crude LTA underwent ion exchange chromatography (DEAE-Sephadex A-25 column; 1.6 × 20 cm (Pharmacia); buffer A: 0.1 M sodium acetate (pH = 4.7), buffer B: 2 M NaCl; linear-gradient (0 % B – 100 % B); 23 °C) and hydrophobic interaction chromatography (Octyl Sepharose CL-4B; 1.6 × 60 cm (GE Healthcare); buffer A: 15 % n-propanol in 0.1 M sodium acetate (pH = 4.7), buffer B: 60 % n-propanol in 0.1 M sodium acetate (pH = 4.7); linear-gradient (0 % B – 100 % B); 23 °C) on the NGS Chromatography System equipped with UV detector. Finally, LTA fractions were determined with the use of the phenol-sulfuric acid method and underwent NMR spectroscopy analysis.

2.2.3. Peptidoglycan

The PG isolation was conducted according to the modified method of Schaub and Dillard (Schaub & Dillard, 2017). Briefly, bacterial mass was suspended in 25 mM phosphate buffer (100 ml, pH = 6) and added drop by drop to a boiling 8 % sodium dodecyl sulfate (100 ml, SDS). Then, the suspension was boiled (30 min; 100 °C), cooled, and ultra-centrifuged (200,000 ×*g*; 15 °C; 30 min). The obtained pellet was re-extracted, washed (4 to 6 times) with phosphate buffer, and freeze-dried. To receive a pure PG, 5 mg of the freeze-dried mass was dissolved in 2 ml of 50 mM Tris-HCl with 10 mM $MgCl_2$ (pH = 7.5) and underwent digestions, first for 6 h at 37 °C with 0.21 mg/ml of DNase and RNase, and next overnight with protease (0.45 mg/ml, 37 °C).

2.3. HEK-Blue™ cells cultivation and stimulation

Transfected human embryonal kidney (HEK) 293 cells were purchased from Invivogen and cultivated according to the manufacturer's instructions. Briefly, cells were cultured (37 °C, 5 % CO_2) in DMEM with 10 % (v/v) fetal bovine serum, 100 U/ml penicillin, 100 mg/ml

streptomycin, and 100 mg/ml Normocin™ (Invivogen) and selective antibiotics: (1) null: 100 μg/ml of Zeocin™ (Invivogen); (2) TLR2 and TLR4: 1 × HEK-Blue™ selection (Invivogen); (3) NOD2: 30 μg/ml of blasticidin (Invivogen) and 100 μg/ml of Zeocin™. After reaching 80 % of confluency, sterile PBS was used to collect the cells.

To determine the recognition pathways of studied antigens, 190 μl of the cells suspension (140,000 cells/ml in HEK-Blue™ Detection (Invivogen)) was added to each well in the 96-well plate. Next 10 μl of analyzed samples (1 μg/ml – 10 μg/ml) was added. Corresponding positive controls were used for tested cell lines: Pam3CSK4 (Pam3CysSerLys4, Invivogen) for TLR2, LPS ultra-pure (lipopolysaccharide, Invivogen) for TLR4 and MDP (muramyl dipeptide, Invivogen) for NOD2 cells. The results were observed as a colorimetric reaction that was developing over time and the level of receptor activation was measured by absorbance read at $\lambda = 630$ and 650 nm. The results were presented as Δ absorbance at $\lambda = 630$ nm between tested samples and negative control (PBS-stimulated cells).

2.4. Stimulation of the splenocytes and dendritic cells isolated from the OVA-sensitized mice

2.4.1. Stimulation of the splenocytes isolated from OVA-sensitized mice

The immunomodulatory potential of Bad368 antigens was investigated *ex vivo* on the splenocytes isolated from OVA-sensitized BALB/c mice according to the method described by Pyclik et al. (Pyclik et al., 2021). Briefly, female mice (8–12 weeks of age) were sensitized by two intraperitoneal injections of 10 μg of OVA (Sigma Aldrich, grade V) mixed with 0.65 mg/100 μl of Alum (Serva) and one boosting injection of 15 μg of OVA mixed with 0.65 mg/100 μl of Alum (Serva) one week later. Seven days after the third sensitization, mice were anesthetized with 3 % isoflurane and euthanized by cervical dislocation. The animal experiment was approved by the committee for the protection and use of experimental animals of the Institute of Microbiology, The Czech Academy of Sciences (no. 91/2019). All procedures were performed in accordance with the EU Directive 2010/63/EU for animal experiments.

Spleens were aseptically removed and cells were isolated and cultured in RPMI 1640 medium (Sigma Aldrich) supplemented with 10 % FBS (Fetal Bovine Serum, Gibco), 100 U/ml of penicillin, 100 μg/ml streptomycin, and 10 mM HEPES (Sigma Aldrich). Cells were counted and seeded on a 96-well plate (5×10^6 cells/ml, 100 μl/well), re-stimulated with OVA (100 μg/well, Purified OAC, Worthington), and treated with studied antigens (PSs 30 μg/ml, PG and LTA 10 μg/ml in PBS) for 72 h (37 °C, 5 % CO_2). The concentration of cytokines was measured in supernatants by the Milliplex Map Mouse Cytokine/Chemokine Panel (IL-4, IL-5, IL-13, IL-10, and IFN-γ) according to the manufacturer's instructions and analyzed with Luminex 2000 System (Bio-Rad Laboratories). Changes in the levels of the Th1/Th2 cytokines were analyzed and presented as a percentage ratio between tested samples and the OVA-positive control (OVA re-stimulated splenocytes only) referred to as 100 %. Unstimulated cells were used as a negative control (medium without OVA).

2.4.2. Isolation and stimulation of the bone marrow-derived dendritic cells

Bone marrow-derived dendritic cells (BM-DCs) were isolated according to the previously described method (Górska et al., 2014). All procedures were performed in accordance with the EU Directive 2010/63/EU for animal experiments. Briefly, cells were rinsed from femurs and tibias of female BALB/c mice, placed in RPMI 1640 medium, centrifuged (215 ×*g*, 5 min), and counted. Next, the cells were put on a Petri dish in a medium supplemented with 10 % FBS, 150 μg/ml gentamycin (Sigma Aldrich), and 20 ng/ml murine granulocyte-macrophage colony-stimulating factor (GM-CSF, Invitrogen), and incubated for 7 days with the addition of the fresh medium on the 3rd and 6th day (37 °C, 5 % CO_2). BM-DCs were detached, counted, and seeded on the 48-well plate (1×10^6 cells/well) and stimulated with studied antigens (PSs 30 μg/ml, PG and LTA 10 μg/ml in PBS) for 20 h (37 °C, 5 % CO_2). Finally, the levels of IL-10, IL-6, IL-12p70, and TNF-α in culture supernatants were determined by ELISA Ready-Set-Go! kits (eBioscience) according to the manufacturer's instructions.

2.5. Antigen uptake and transfer between mouse epithelial cells (TC-1) and dendritic cells (JAWS II)

2.5.1. Antigens staining

The staining protocol for PS, LTA, and PG was adapted from FluoroProbes reagent manuals with some changes. PS, LTA, or PG (1 mg) were suspended in 400 μl 0.1 M sodium acetate (pH = 5.5) and metaperiodate (20 mM) and incubated at 4 °C for 30 min. Then, the solution was mixed with 100 μl 40 mM 1-Pyrenebutyric hydrazide (PBA) (Sigma Aldrich) in DMSO. The mixture was incubated for 3 h (23 °C, in darkness, with agitation) and dialyzed to dH_2O water (4 °C, 18 h) using a dialysis cassette (Slide-A-Lyzer Dialysis Cassette, Thermo Scientific). The PS and LTA content in the dialysate was assessed with DuBois assay (DuBois et al., 1956) by the absorbance measurement at $\lambda = 490$ nm. The PG content was checked by an absorbance read at $\lambda = 206$ nm and 254 nm. All the measurements were performed by Power Wave reader (BioTek) with the Gen5 Software (BioTek).

2.5.2. Antigen uptake by epithelial cell line (TC-1)

TC-1 cells (ATCC CRL-2785) were seeded on a 24-well plate (0.2×10^6 cells/ml) in a complete medium of DMEM + GlutaMax (Gibco), 10 % FBS (Gibco), and 1 % L-glutamine-Penicillin-Streptomycin solution and incubated for 2 h. Next, the stained antigens: 10 μg/ml of LTA, 10 μg/ml of PG, 30 μg/ml of PS were added to the cells and incubated for 4 h (37 °C, 5 % CO_2). To distinct the live population of TC-1 cells, the detached cells were stained with viability dye FV780 (BD Horizon, ref 565388) for 15 min at 23 °C. Next, the cells were washed and suspended in 1 % FBS/PBS before flow cytometry analysis (BD LSR Fortessa, BD Biosciences). The main population was marked based on the forward and side scatter. Debris was excluded by the FCS-H/FSC-A gating. The dead population was excluded from the analysis by the forward scatter vs viability dye. Obtained data were analyzed by FlowJo VX.07 software.

2.5.3. Antigen transfer between mouse epithelial (TC-1) and dendritic cells (JAWS II)

JAWS II cells (ATCC CRL-11904) were cultivated in Alpha MEM medium (Gibco) with 10 % FBS (Gibco), 1 % L-glutamine-Penicillin-Streptomycin solution, 1 mM sodium pyruvate (Sigma Aldrich), and 5 ng/ml GM-CSF in an incubator (37 °C, 5 % CO_2). Before co-culture, JAWS II were stained with red fluorescent dye PKH26 (Sigma Aldrich) according to the manufacturer's procedure, and 0.2×10^6 cells were seeded on a 24-well plate and incubated for 1.5 h. Simultaneously, TC-1 cells were grown and loaded with stained antigens as described in 2.5.2 and added to the stabilized JAWS II culture in an approximate ratio of 1:1 in a complete Alpha MEM medium. Cells were observed under the microscope (Axio Observer, Zeiss) for 24 h (37 °C, 5 % CO_2) or were co-cultured for the same amount of time for the flow cytometry analysis (as described in 5.2). In transfer studies, % of cells that acquired tested antigens was calculated exclusively for JAWS II (cells from quartiles Q1 and Q2, stained with PKH26 = 100 %).

2.6. Structure determination of the Bad368.1 polysaccharide compound

2.6.1. NMR spectroscopy and size determination

The NMR spectra were obtained on a Bruker 600 Hz Avance III spectrometer using a 5 mm QCI $^1H/^{13}C/^{15}N/^{31}P$ probe equipped with a z-gradient. The data were acquired using the TopSpin 3.1pl6 software and processed with TopSpin 4.0.7 and SPARKY (Goddard 2001). PSs (10 μg) were dissolved in deuterium oxide and the one- (^1H, ^{31}P) and two-dimensional NMR experiments (^1H-^1H-COSY, ^1H-^1H TOCSY, ^1H-^1H NOESY, ^1H-^{13}C HSQC, ^1H-^{13}C HMBC, ^1H-^{31}P HSQC, and HSQC-TOSCY)

were carried out at 50 °C using pulses sequences from the Bruker library. The mixing times for TOCSY were 30, 60, and 100 ms, and for NOESY 100 and 300 ms. The delay time in HMBC was 60 ms. The chemical shifts for NMR signals were referenced by using acetone as an internal reference (δ_H 2.225 ppm, δ_C 31.05 ppm). To determine the absolute configuration of monosaccharides moieties present in all Bad368 PSs ^{13}C NMR chemical shifts were compared with the reference data (Shashkov et al., 1988).

The average molecular mass of each PS was determined by GPC (Dionex Ultimate 3000) on an OHpak SB-806 M HQ column (8 × 300 mm, maximum pore size 15,000 Å; Shodex) with dextran standards (MW 12, 25, 50, 80, 150 and 270 kDa). 0.1 M ammonium acetate buffer was used as the eluent. The flow rate was 0.5 ml/min and the run was monitored with a refractive index detector (RI 102; Shodex). The working detector temperature and sensitivity were adjusted to 35 °C and 512×, respectively. System control, data acquisition, and treatments were performed using the Chromeleon software (Dionex) (Górska et al., 2016).

2.6.2. Chemical analysis

Monosaccharide content of the purified PS was determined by sugar analysis as described previously (Sawardeker et al., 1965). Briefly, 0.3 mg of PS was hydrolyzed with 10 M HCl (80 °C, 25 min) and dried under a stream of N_2. Next, samples were reduced to sugar alditols using 10 mg/ml $NaBH_4$ (10 °C; overnight incubation). On the next day, the reduction was stopped by the addition of the 80 % acetic acid and free -OH groups were acetylated with methylimidazole and acetic anhydride. Next, the obtained alditol acetates were extracted 3 times by water: dichloromethane (1:1, v/v) mixture. Finally, the organic phase was collected, dried under a stream of N_2, and kept in the fridge before gas-liquid chromatography–mass spectrometry (GLC-MS) analysis. Samples obtained after sugar analysis were mixed with sugar standards to confirm monosaccharide composition in tested PSs.

To gain information about monosaccharide linkage and substitution positions, methylation analysis was performed. 2 mg of PS was dissolved in DMSO, treated with NaOH, and sonicated. To methylate free -OH groups, samples were incubated with iodomethane. Next, acetic acid was used to neutralize the pH of the samples and the methylated PS was extracted by a mixture of chloroform: water (1:1, v/v) (Ciucanu & Kerek, 1984). The obtained solution was dried under a stream of N_2 and subjected to sugar analysis as described previously, except that 10 mg/ml $NaBD_4$ was used for reduction instead of the $NaBH_4$. Dried samples were dissolved in ethyl acetate and analyzed by GLC-MS on the ITQ 700 Thermo Focus GC system equipped with Zebron ZB-5HT Inferno capillary column (Phenomenex) with a temperature gradient from 150 °C to 270 °C (8 °C/min). All data were obtained and analyzed by the Xcalibur™ software (Thermo Fisher).

2.7. Statistical analysis

All experiments were repeated in at least two technical and two biological repetitions. Data are presented as mean ± SD and differences were analyzed with one-way ANOVA together with Dunnett's multiple comparisons. All statistical analyses and visualizations were prepared with the use of Graph Pad Prism version 9.

3. Results

Both live and heat-inactivated *Bifidobacterium adolescentis* CCDM 368 bacteria show the ability to reduce the Th2-related cytokine production of IL-5, IL-4, and IL-13 in OVA-stimulated cells derived from OVA-sensitized mice (Supplementary Fig. S1). Thus, we decided to define the molecules responsible for the immunomodulatory effect present in inactivated bacterial cells. Bad368 antigens that include PSs, PG, and LTAs were isolated and purified. We found out that Bad368 produce three different PSs which will be referred to as the biological fraction 1, 2, and 3 (Bad368.1, Bad368.2, and Bad368.3, respectively) (Supplementary Fig. S2). On the contrary, the LTA and PG purification revealed the presence of only one fraction of each antigen.

3.1. Bifidobacterium adolescentis CCDM 368 antigens are recognized by innate immune receptors

HEK cells transfected with the innate immune receptors from the TLR and NOD receptor family were used to demonstrate the recognition pathways induced by isolated molecules. Studied antigens were added to the cells and colorimetric reaction was developed. We observed that LTA was recognized by TLR2, whereas PG led to the activation of TLR2 and NOD2. Polysaccharides Bad368.1 and Bad368.3 caused a robust activation of TLR2, they were also able to induce TLR4 response. Interestingly, Bad368.2 wasn't recognized by any of the tested immune receptors. Null cells that lack analyzed receptors were used as a negative control for transfected cell lines (Supplementary Fig. S3).

3.2. Bifidobacterium adolescentis CCDM 368 antigens differently affect the OVA-induced cytokine production by splenocytes

Splenocytes isolated from ovalbumin (OVA)-sensitized female BALB/c mice were used to evaluate the potential of isolated molecules to modulate the OVA-induced cytokine production. We observed different effects for each of the PS fractions: Bad368.1 PS significantly inhibited the production of IL-5 while Bad368.3 significantly decreased the level of both IL-4 and IL-5 when compared to OVA-stimulated cells. All three fractions showed tendency to decrease IL-13 (Fig. 1). Stimulation with PG and LTA did not show any notable changes in the levels of Th2-related cytokines. In the case of regulatory IL-10, PG, and Bad368.1 PS were able to induce high levels of this cytokine. Strikingly, it was Bad368.1 PS that caused a robust production of pro-inflammatory cytokines IFN-γ and IL-6 suggesting the Th1-inducing properties. We also observed the induction of IL-6 cytokine after PG and Bad368.3 stimulation as well as increased production of IFN-γ, however the level of the latter was significantly lower when compared to Bad368.1 PS.

3.3. Bad368.1 polysaccharide induces cytokine production in bone marrow-derived dendritic cells

From the tested Bad368 molecules we selected representative antigens: Bad.368.1 PS, PG, and LTA that exhibited interesting immunomodulatory properties for further studies. First, we decided to analyze cytokine production in BM-DCs treated with the selected antigens. Interestingly, we observed that their response depended on the antigen type. Bad368.1 PS showed a tendency to improve TNF-α and IL-10 levels and as the only one among other antigens caused a significant increase in IL-6 production. Upon exposure to PG, BM-DCs produced a very low level of IL-10, TNF-α, and IL-6, whereas stimulation with LTA slightly increased the level of IL-10 (Fig. 2). None of the tested molecules were able to induce IL-12p70 production in BM-DCs (data not shown).

3.4. The efficiency of Bad368.1 polysaccharide, lipoteichoic acid and peptidoglycan uptake by airway epithelial cells (TC-1) and antigen transfer to dendritic cells (JAWS II) vary depending on the molecule

To confirm the efficient recognition and engulfment of studied antigens, the uptake analysis was performed with labeled Bad368.1 PS, PG, and LTA by flow cytometry. The analysis indicated the engulfment of all antigens, with the highest mean value for Bad368.1 PS (99 %), then for PG (81 %). The lowest mean value was noted for LTA (8 %) (Fig. 3, Supplementary Fig. S4). The obtained results indicated the presence of two populations of epithelial cells: 1) which internalized the labeled antigen (positive population), and 2) which did not (negative population).

Next, we examined the antigen transfer between epithelial cells and

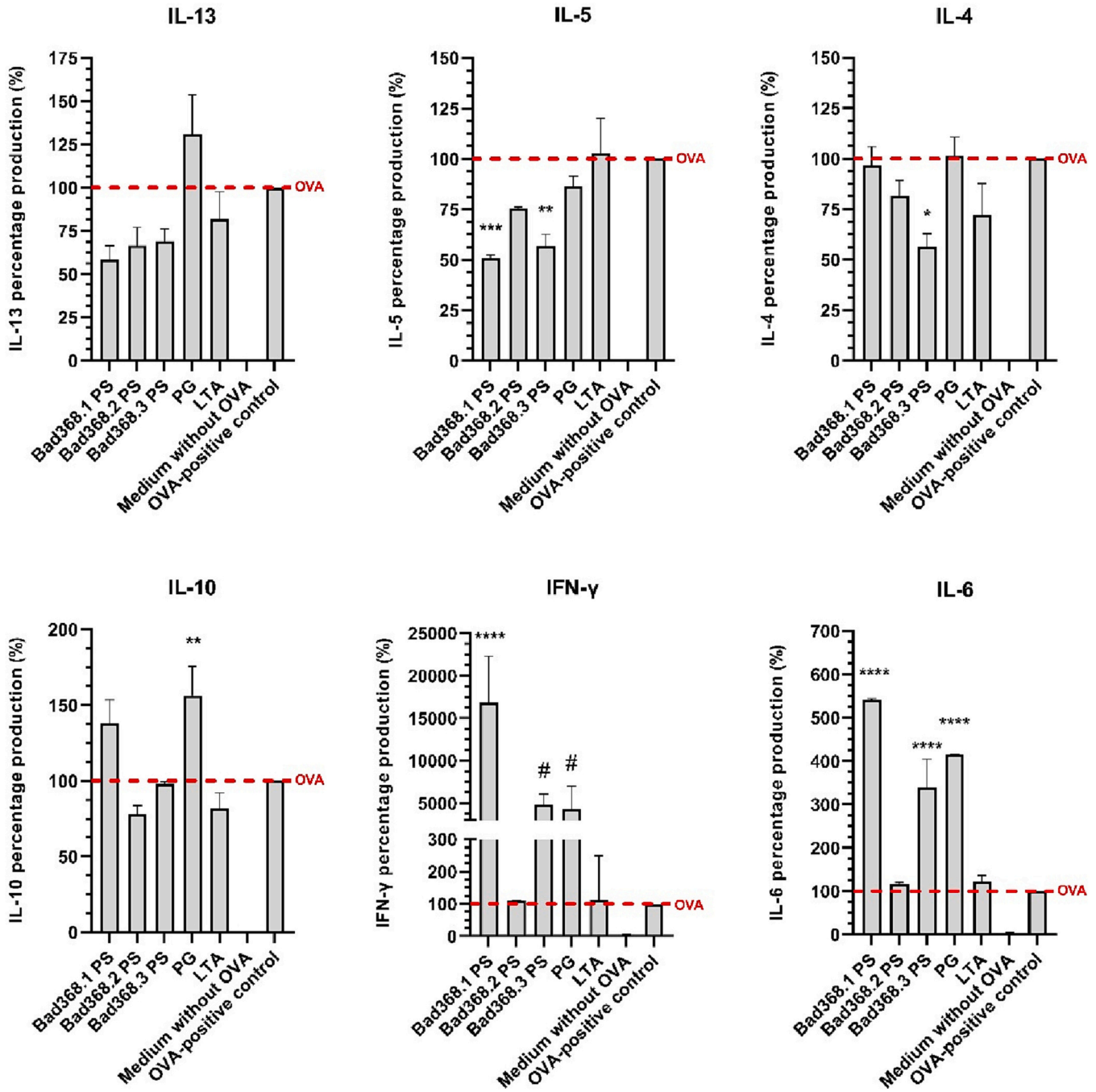

Fig. 1. Cytokine production by OVA-sensitized splenocytes after stimulation with *Bifidobacterium adolescentis* CCDM 368 antigens. Mouse splenocytes were stimulated with OVA (500 μg/ml) together with antigens at a concentration of 10 μg/ml for PG and LTA and 30 μg/ml for PSs (Bad368.1, Bad368.2, Bad368.3) or PBS (OVA-positive control). Unstimulated splenocytes (medium without OVA) served as a negative control. Data are shown as mean ± SD of 2 mice and expressed as a percentage ratio between tested samples and the OVA-positive control. One-way ANOVA with Dunnett's multiple comparison tests were performed and significant differences compared to OVA-control (red dashed line) were calculated (**** $p \leq 0.0001$, *** $p \leq 0.001$, ** $p \leq 0.01$, * $p \leq 0.05$). Additionally, for IFN-γ significant differences between Bad368.1 PS and other PSs (Bad368.2 PS and Bad368.3 PS) were marked with # ($p \leq 0.0001$).

antigen presenting cells (APCs), in which antigen-treated TC-1 cells were incubated in co-culture with JAWS II cells for 18 h. The efficiency of this process was determined by fluorescence microscopy (Fig. 4A) and flow cytometry (Fig. 4B and C). As previously, the ability of the DCs to acquire antigens differed depending on the type of the antigen. In the case of Bad368.1 PS, the uptake by DCs was visible under a microscope. It was also confirmed by flow cytometry analysis, which indicated the presence of labeled Bad368.1 PS in 71.3 % of JAWS II cells (exclusively) (Fig. 4C). Acquisition of LTA by DCs was at the level of approx. 48.8 % as determined by the flow cytometry analysis and confirmed under a microscope, whereas no PG uptake by JAWS II cells was detected.

3.5. Structural analysis of Bad368.1 polysaccharide

Bad368 produces a complex PS blend. The crude PS was subjected to purification by ion-exchange and size exclusion chromatography methods. Analysis of the ^{1}H NMR spectra allowed us to distinguish three structurally different PS fractions that were called Bad368.1 PS, Bad368.2 PS, and Bad368.3 PS (Supplementary Fig. S2).

Further, to investigate monosaccharide composition in each fraction,

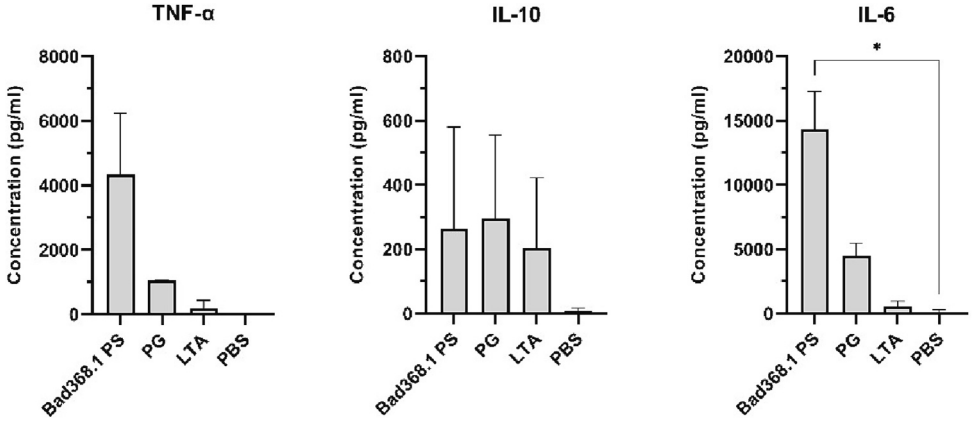

Fig. 2. Bone marrow-derived dendritic cells cytokine production after stimulation with *Bifidobacterium adolescentis* CCDM 368 antigens. Mouse BM-DCs were treated with PBS (negative control) or studied molecules at a concentration of 10 μg/ml for PG and LTA and 30 μg/ml for PSs. Data are shown as mean ± SD of 2 mice and one-way ANOVA and Dunnett's multiple comparison tests were performed and significant differences were calculated (* $p \leq 0.05$).

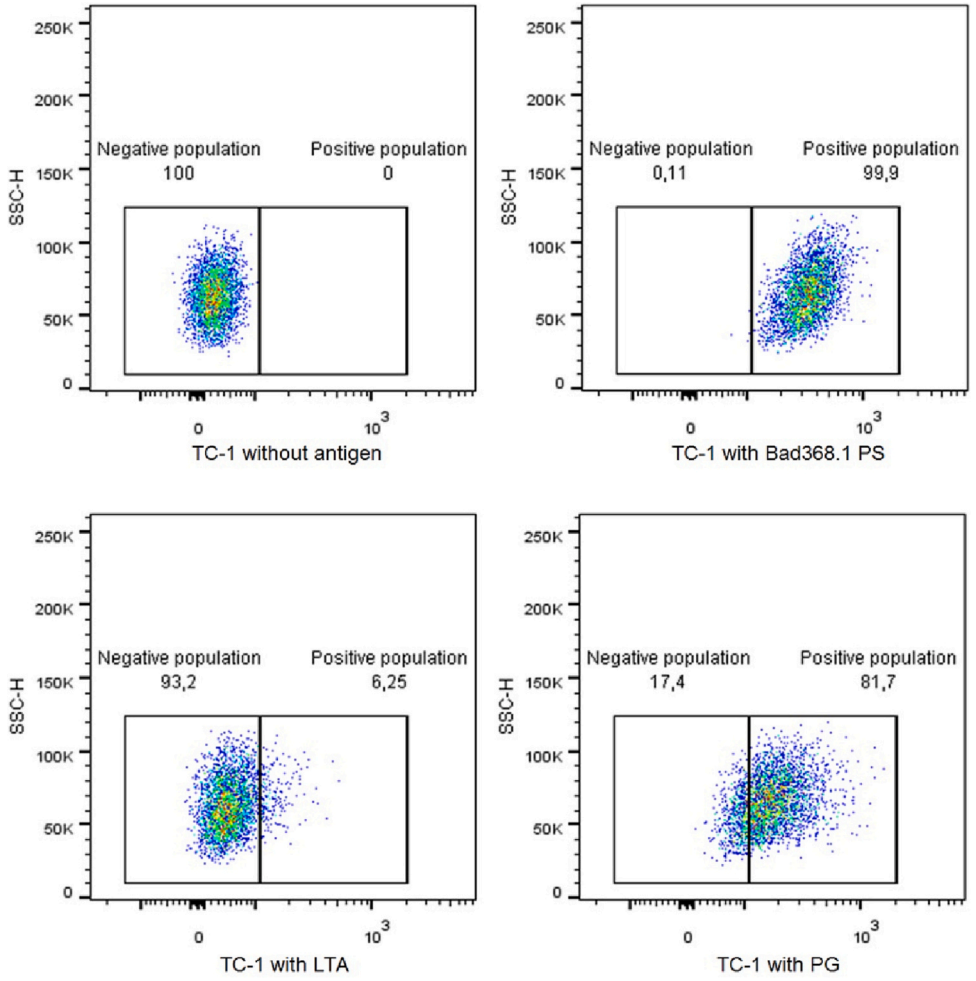

Fig. 3. A dot-plot analysis of the antigen uptake by epithelial cells (TC-1). The cells were stimulated by 30 μg/ml of PS, 10 μg/ml of LTA, and 10 μg/ml of PG for 4 h. The internalization of the antigen was determined as a difference between the population with (positive population) or without (negative population) detectable antigen (Bad368.1 PS, LTA or PG) (SSC-H – side scatter high). Representative dot plots were presented. The experiment was repeated in 2 biological repetitions.

sugar analysis was performed and molecular mass was determined. The GLC-MS sugar analysis revealed that:

a. **Bad368.1 PS** consists of L-Rha, D-Glc, and D-Gal in a molar ratio of 1:3:1.25. The average molecular mass is approximately 9.99×10^6 Da.
b. **Bad368.2 PS** consists of L-Rha, D-Glc, and D-Gal in a molar ratio of 1:1.4:3. The average molecular mass is approximately 1.24×10^4 Da.

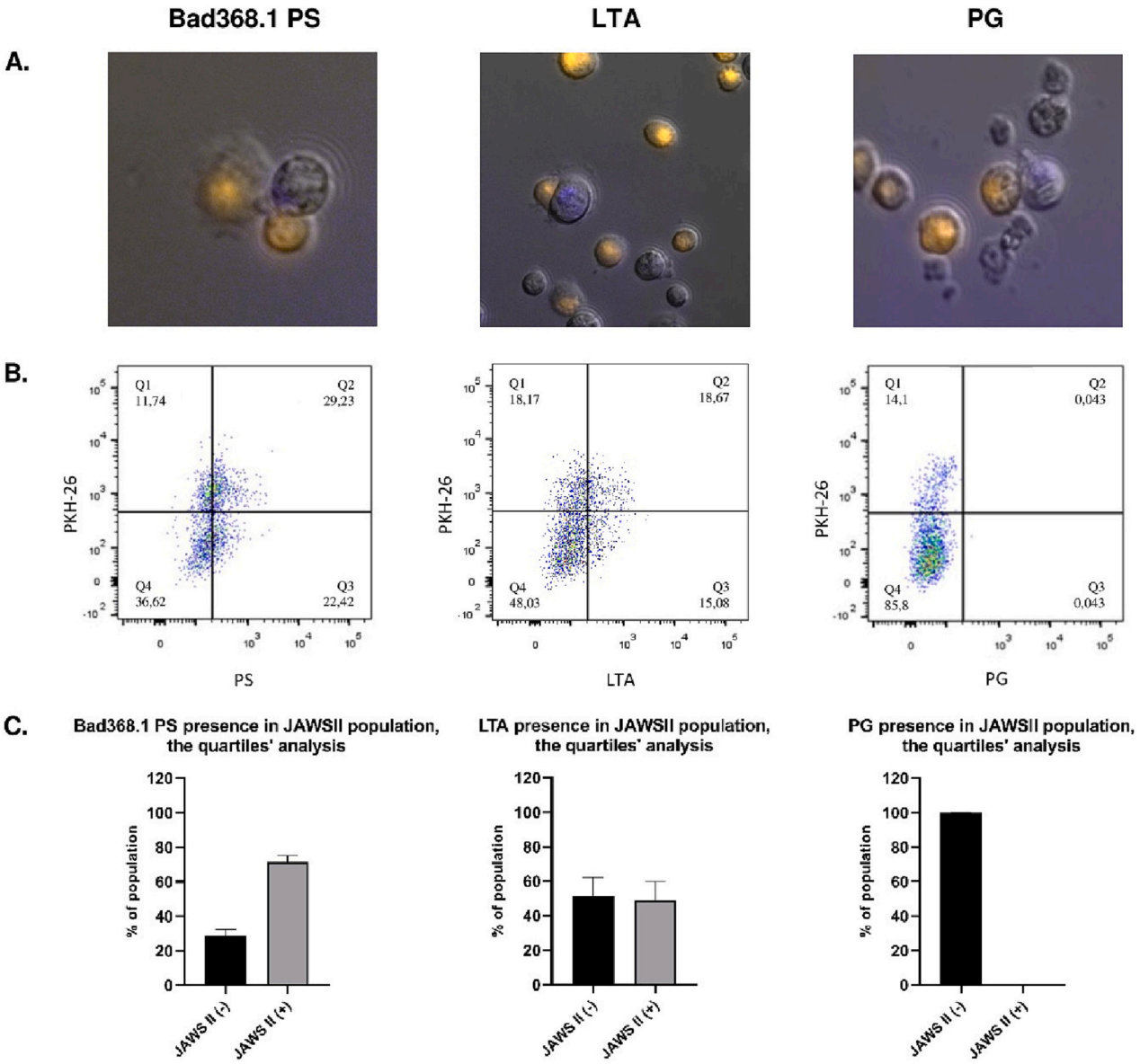

Fig. 4. Antigen transfer from epithelial cells to dendritic cells. A. Fluorescent microscopy results (yellow cells: JAWS II stained with PKH-26; violet cells: TC-1 with labeled antigen). B. Representative dot plots obtained by flow cytometry. C. Flow cytometry results assessed on comparison of the fluorescence signal between quartile Q1 (% of JAWS II cells without antigen - JAWS II (−)) and Q2 (% of JAWS II cells with tested antigen - JAWS II (+)). The experiment was repeated in 2 biological repetitions.

c. **Bad368.3 PS** consists of D-Glc and D-Gal in a molar ratio of 1:2.3. The average molecular mass is approximately 1.27×10^4 Da.

Immunomodulatory studies on splenocytes and BM-DCs revealed interesting immunomodulatory properties only in the case of Bad368.1 PS (Figs. 1 and 2), thus we decided to determine the structure of this PS. At first, methylation analysis was performed to characterize the linkages and substitution positions in this PS. It revealed the presence of 3-Rha*p*, 3-Gal*p*, 2-Glc*p*, and 4-Glc*p*.

The ^{1}H NMR spectrum displayed three different types of signals: the anomeric region (5.6–4.5 ppm), the ring protons region (4.5–3.2 ppm), and the methyl group region. Six distinct signals were present in the anomeric region and two signals in the methyl group region. The absence of ^{31}P signals in the ^{31}P NMR spectrum indicated that Bad368.1 was not phosphorylated.

The ^{1}H-^{13}C HSQC spectrum showed six cross peaks in the region of anomeric resonances corresponding to hexapyranosyl residues indicating that Bad368.1 is made of a hexasaccharide repeating unit (HSQC spectrum with assigned signals is presented in Fig. 5). The chemical shifts of proton and carbon signals from the six sugar residues were assigned from a combination of 2D NMR experiments, COSY, TOCSY at several mixing times, HSQC, HSQC-TOCSY, NOESY, and HMBC (Tables 1 and 2) (Supplementary Figs. S5–S8). The sugar residues were marked with the uppercase letter starting from the most downfield signal in the ^{1}H NMR spectrum.

Analysis of the TOCSY and HSQC-TOCSY spectra showed that residues C, E, and F have *gluco*-configuration as shown by the scalar correlations from the anomeric signal to the other ring signals. Residue A was assigned to the *galacto*-configuration since scalar correlations were observed in the TOCSY and HSQC-TOCSY from the anomeric signal and the other ring signals until the H4/C4 resonance. The H5/C5 signals were assigned from the NOE connectivity from H3 to H5 and from the connectivity in the HMBC spectrum between H1 and C5. The H6/C6 signals were further identified from the scalar connectivities with H5/C5 in the TOCSY and HSQC-TOCSY spectra. Residues B and D were identified as rhamnose by the characteristic methyl resonance of the 6-deoxy

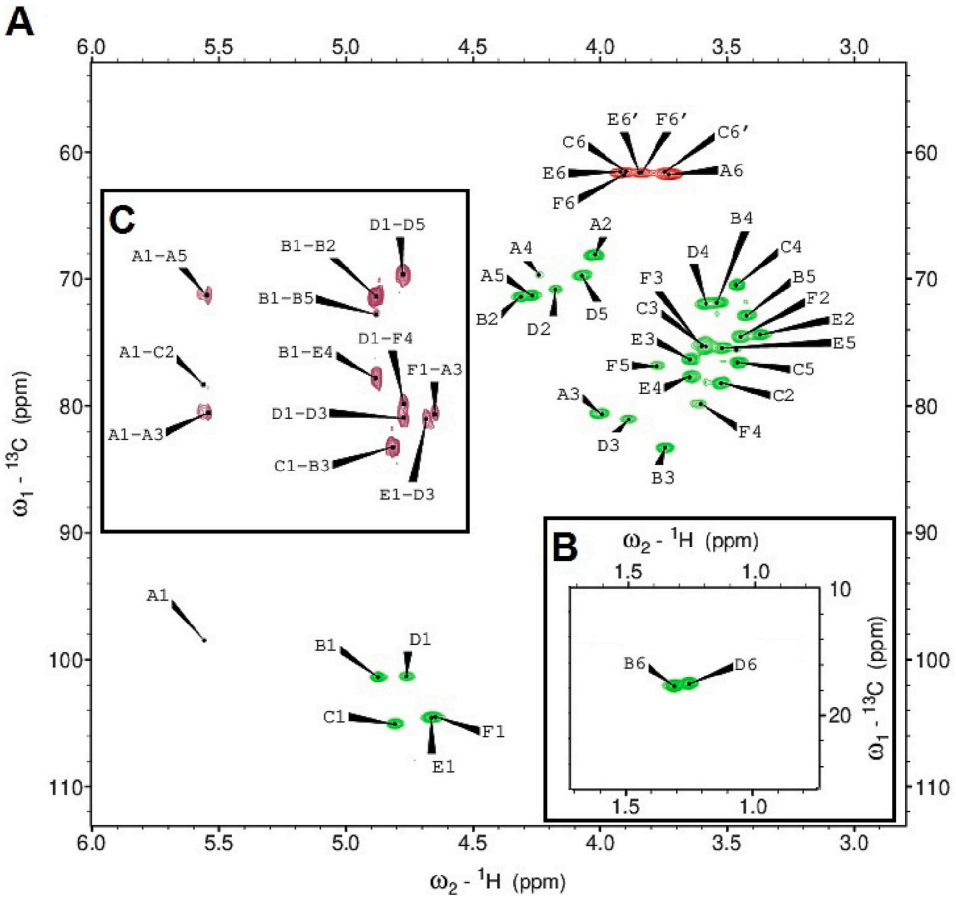

Fig. 5. A. ^{1}H-^{13}C HSQC NMR spectrum of Bad368.1 polysaccharide at 50 °C. The anomeric signals are located in the chemical shift range of 4.2–5.8 ppm and the ring signals between 3.2 and 4.5 ppm. B. The H-6/C-6 signals for rhamnoses (residue B and D). C. The part of the HMBC spectrum which corresponds to the anomeric signals in HSQC spectra.

Table 1
^{1}H and ^{13}C NMR chemical shifts of resonances of Bad368.1 polysaccharide from *Bifidobacterium adolescentis* CCDM 368.

		^{1}H, ^{13}C chemical shifts (ppm)					
Sugar residue		H-1, C-1	H-2, C-2	H-3, C-3	H-4, C-4	H-5, C-5	H-6; H-6', C-6
A	→3)- α-D-Gal*p*-(1→	5.56	4.03	4.01	4.25	4.28	3.74
		98.4	68.1	80.5	69.6	71.2	61.7
B	→3)-β-L-Rha*p*-(1→	4.88	4.32	3.75	3.55	3.43	1.33
		101.2	71.3	83.2	71.8	72.8	17.6
C	→2)-β-D-Glc*p*-(1→	4.82	3.54	3.59	3.47	3.47	3.91; 3.75
		104.9	78.2	75.3	70.4	76.4	61.5
D	→3)-α-L-Rha*p*-(1→	4.78	4.18	3.90	3.59	4.08	1.27
		101.2	70.8	80.9	71.9	69.6	17.4
E	→4)-β-D-Glc*p*-(1→	4.68	3.38	3.65	3.65	3.53	3.93; 3.84
		104.4	74.3	76.3	77.7	75.4	61.6
F	→4)-β-D-Glc*p*-(1→	4.66	3.46	3.59	3.63	3.75	3.93; 3.84
		104.4	74.5	75.3	79.8	77.0	61.6[a]

[a] Could not be assigned unambiguously.

sugar at 1.33 and 1.27 ppm in combination with the observation of only one cross-peak in the TOCSY spectrum from H1 to H2. All spin systems were assigned in the TOCSY and HSQC-TOCSY using the methyl groups as a starting point.

The anomeric configuration of C, E, and F was identified as β due to the $^{3}J_{H1H2}$-values >7 Hz. Residue A has the α-configuration as shown by the small $^{3}J_{H1H2}$-value of 3.0 Hz. For the B and D rhamnose residues, the distinction between α- and β- form is not straightforward since the couplings are <3 Hz and not resolved in the spectra due to line broadening. It has been shown that the position of the signal at C5 can be used

Table 2
Selected inter-residue correlations from ^{1}H,^{1}H NOESY and ^{1}H,^{13}C HMBC spectra of Bad368.1 polysaccharide.

	Residue	H-1/C-1	Connectivity to		Inter-residue
		δ_H/δ_C	δ_C	δ_H	Atom/residue
A	→3)-α-D-Gal*cp*(1→	5.56/98.4	78.2	3.54	C-2, H-2 of **C**
B	→3)-β-L-Rha*p*-(1→	4.88/101.2	77.7	3.65	C-4, H-4 of **E**
C	→2)-β-D-Glc*p*-(1→	4.82/104.9	83.2	3.75	C-3, H-3 of **B**
D	→3)-α-L-Rha*p*-(1→	4.78/101.2	79.8	3.63	C-4, H-4 of **F**
E	→4)-β-D-Glc*p*-(1→	4.68/104.4	80.9	3.90	C-3, H-3 of **D**
F	→4)-β-D-Glc*p*-(1→	4.66/104.4	80.5	4.01	C-3, H-3 of **A**

to distinguish between an α- or a β-linked rhamnose with a C5 at δ 70.5 ppm indicating an α-linked Rha while a C5 with δ at 73.2 ppm indicates a β-Rha*p* (Carillo et al., 2009; Lipkind et al., 1988; Mattos et al., 2001; Senchenkova et al., 1999; Vinogradov et al., 2003). Thus, residue B with C5 at 72.9 ppm can be assigned as β-Rha while residue D with C5 at 69.7 ppm can be assigned as a α-Rha. The α-Rha configuration of residue D was also confirmed by the absence of intraglycosidic NOEs between H1 and H3, H5 while the β-configuration of residue B was confirmed by NOEs from H1 to H3 and H5 (Vinogradov et al., 2003).

The glycosidic bond connections/linkages between the constituent monosaccharides were obtained from the ^{1}H-^{1}H NOESY and ^{1}H-^{13}C HMBC spectra (see Table 2). The glycosylation pattern was confirmed by the downfield shift of the signals of C3 Gal*p* (**A**), C3 Rha*p* (**B** and **D**), C2 Glc*p*, and (**C**) C4 Glc*p* (**E** and **F**) if compared to the non-substituted sugars. To determine the absolute configuration of the Bad368.1 PS monosaccharide moieties ^{13}C NMR chemical shifts were compared with the reference data (Shashkov et al., 1988). The following sequence was thus determined: →2)-β-D-Glc*p*-(1 → 3)-β-L-Rha*p*-(1 → 4)-β-D-Glc*p*-(1 → 3)-α-L-Rha*p*-(1 → 4)-β-D-Glc*p*-(1 → 3)-α-D-Gal*p*-(1→, or with upper-case letters: **C-B-E-D-F-A**. The proposed structure of the repeating unit is presented in Fig. 6.

4. Discussion

The present study was initiated to investigate the immunomodulatory properties of antigens isolated from different *Bifidobacterium* strains that included *B. adolescentis* CCDM 368 and to test their potential as active postbiotics. The idea to investigate the surface molecules of this particular strain was based on *in vitro* experiments performed with untreated and heat-treated bacteria. Obtained results showed that even after heat-inactivation, Bad368 still reduced OVA-induced Th2-related production of IL-5, IL-4, and IL-13 cytokines in splenocytes from OVA-sensitized mice. Since the immunomodulatory properties of the strain were retained in heat-killed bacteria, we aimed at identifying bacteria surface antigens that might be responsible for the observed effect. Thus, we isolated, purified, and evaluated the role of the Bad368 LTAs, PG, and PSs. Interestingly, Bad368.1 PS significantly increased the level of IFN-γ and IL-10 while simultaneously reducing the production of IL-13 and IL-5 in splenocytes isolated from OVA-sensitized mice. In the context of potential anti-allergic properties, a high level of IFN-γ is desirable, because this cytokine can further act as a suppressor for Th2 and switch the response towards Th1 cells (Amrouche et al., 2006; Ivashkiv, 2018). On the contrary, the role of IL-10 is ambiguous. Higher secretion of this cytokine might be related to its production by (1) Treg cells, which leads to the diminished Th2 responses, or (2) Th2 cells and IL-10 function as a guard cytokine that keeps the IFN-γ levels within safe ranges (Robinson et al., 2004). Polymer Bad368.3 exhibited similar properties to Bad368.1 PS but in a weaker manner while Bad368.2 was able to induce neither IFN-γ nor IL-6.

The functions of polysaccharides are mainly affected by their sugar composition and the connections they made within a chain unit. Thus, the chemical structure of Bad368 PSs may impact their biological properties. Our observations are in line with previous studies showing that the ability of PSs from various bifidobacteria to affect immune cell functions depends on their structure. Verma et al. investigated *B. bifidum* and its role in the generation of Foxp3+ cells. Among different PS fractions, only CSGG (consisting of at least 4 different PSs in a form of neutral β-glucans/galactans) was able to activate DCs via TLR2 receptor which resulted in higher levels of TGF-β and IL-10 (Verma et al., 2018). Administration of the PS from *B. longum* subsp. *longum* 35624™ reduced the number of inflammatory cells in peribronchial and perivascular lung tissue in mice with OVA-induced allergic inflammation. Within lung lavages, the eosinophil levels were decreased while the IL-10 level was increased. Moreover, lung tissue studies revealed inhibited expression of Th2-related IL-4 and IL-13 (Schiavi et al., 2018). Our results of BM-DCs and splenocytes stimulation outlined that Bad368.1 PS and PG might be at forefront of interest since they were able to induce the Th1-related response.

Glucose and galactose are the main components of each of the Bad368 PSs. Moreover, rhamnose also occurs in Bad368.1 PS and Bad368.2 PS structures. Polymer Bad368.1 PS with a high average molecular mass of 9.99×10^{6} Da is a linear heteropolysaccharide with a repeating unit consisting of six monosaccharide residues. The remaining Bad368.2 and Bad368.3 are characterized by the low average molecular mass of 1.24×10^{4} Da and 1.27×10^{4} Da, respectively. Both Bad368.1 PS and Bad368.3 PS were strong activators of the TLR2, they were also able to activate TLR4 receptors (Supplementary Fig. S3). Interestingly, Bad368.2 was able to induce only a weak TLR2 response, and no TLR4 or NOD2 response, which indicates that it may be recognized in a different manner. Laws et al. suggested that there is a link between sugar conformation and backbone linkages, and the chemical properties and function of PSs. He indicated that (1–>4) linkages and β-isomers are adding more stiffness to the PSs whereas (1–>3), (1–>2) linkages and α-isomers are more flexible and in general have stronger anti-microbial and anti-oxidant properties (Laws et al., 2001; Zhou et al., 2019). Bad368.1 PS is more abundant in (1–>2) and (1–>3) linkages and β-isomers that might influence its ability to modulate the immune response. Furthermore, some publications connect the role of bacterial PS with its size. Górska et al. showed that high molecular mass PS L900/2 exhibits regulatory properties meanwhile small molecular mass L900/3 induces a pro-inflammatory response in a mouse model of OVA-sensitization (Górska et al., 2017). However, it is inconsistent with our results since high molecular mass Bad368.1 PS was able to elicit both regulatory IL-10 and pro-inflammatory IFN-γ. Another factor that can have a great impact on PS properties is its charge. Studies performed by Speciale et al. on PS isolated from *B. bifidum* PRI1 showed differences in properties between neutral mix (CSGG) fraction that enhanced regulatory functions of the DCs and negatively charged (PBβG) PS that induced proinflammatory cytokine production (IFN-γ) (Speciale et al., 2019). Verma et al. reported that the neutral fraction of *B. bifidum* PS induced the generation of Foxp3+ regulatory T cells in mice when at the same time the negatively charged PS preparations did not exhibit the same properties (Verma et al., 2018). The chemical and NMR analysis did not show any modifications in the Bad368.1 PS chain like phosphorylation that would influence the charge of the PS. It was indicated that the charge of molecules can affect their processing by epithelial or immune cells depending on their polarity. Since the eukaryotic cell membrane is negatively charged, PSs with a positive/neutral charge can be easier internalized than the negatively charged one (Salatin & Yari Khosroushahi, 2017). Along these lines, we observed efficient engulfment of the polymer Bad368.1 PS by epithelial cells and its further transfer to DCs. Generally, PSs are characterized by a high affinity for the mucosal surface, therefore are widespread through the respiratory and gastrointestinal tract (Salatin & Yari Khosroushahi, 2017).

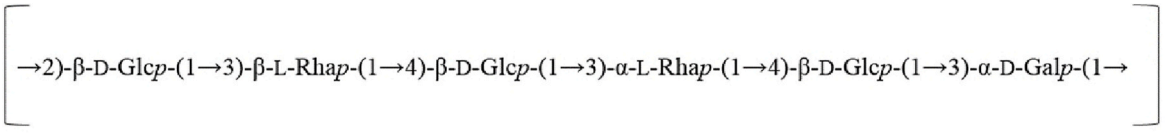

Fig. 6. Structure of the hexasaccharide repeating unit of the Bad368.1 polysaccharide. The approximate number of units in the Bad368.1 polysaccharide equals n = 10,000.

A thorough literature review confirmed that the Bad368.1 PS was not described in different *Bifidobacterium* strains so far. Hosono et al. described water-soluble polysaccharide fraction from *B. adolescentis* M101-4 that in comparison to Bad368.1 PS has furanoses in its structure and no rhamnose residues (Hosono et al., 1977). Another example is a polysaccharide-glycopeptide complex isolated from *B. adolescentis* YIT4011 that contains dTal in the main chain (Nagaoka et al., 1988). Moreover, CSDB (Carbohydrate Structure Database) platform did not indicate the Bad368.1 PS in different organisms. Although, the presence of this structure in different bifidobacteria cannot be excluded. It must be underlined that the effect of the bacteria is the resultant of all of their antigens. The ratio in which the effector molecules are present on the bacteria surface is also important. In our previous studies on the function of *L. rhamnosus* LOCK 0900 polysaccharides we showed that the whole bacteria induced production of IL-10 in BM-DCs, whereas thier PSs did not stimulate the production of IL-10 or IL-12. Surprisingly, PSs due to their chemical features were able to modulate the immune responses to third-party antigens. Exposure to L900/2 enhanced IL-10 production induced by *L. plantarum* WCFS1, while in contrast, L900/3 enhanced the production of IL-12p70 in BM-DCs (Górska et al., 2014).

Results obtained after stimulation of splenocytes and BM-DCs, together with the outcome of the transfer studies, clearly indicate that Bad368.1 PS has the strongest potential among Bad368 antigens to modulate allergic diseases in humans. Due to the potential of newly described structure we decided to name it BAP1 for the further studies.

While discussing PG immunomodulatory properties, it is important to point out that Bad368 PG was able to induce both NOD2 and TLR2 receptors sensing. This is in agreement with Corridoni et al. data indicating that the antigen cross-priming and CD8+ T cells activation are associated with the upregulation of both receptors (Corridoni et al., 2019). We observed that Bad368 PG was able to stimulate the splenocytes to produce a considerable amount of IFN-γ and IL-10 and a significant amount of IL-6. However, the Bad368 PG did not reduce the level of Th2-related cytokines in OVA-sensitized and stimulated splenocytes culture. On the other side, PG improved the production of IL-10, TNF-α, and IL-6 in BM-DCs. Moreover, we have shown, that up to 75 % of TC-1 cells reacted to the PG's presence and internalized the antigen. Also, the PG uptake by the DCs was visible under a microscope up to 12–13 h. It is important to note that we used enzymatically purified PG fraction to minimalize the effect of the antigens present on its surface. Only a few publications describe the role of purified or partially purified PGs. In one of them, Li et al. focused on the role of the PG from *Lactobacillus acidophilus* KLDS 1.0738 on mice sensitized with β-lactoglobulin. Stimulation of murine macrophages with PG revealed its role in the induction of IFN-γ, IL-10, and TGF-β via the TLR2 pathway (Li et al., 2017). Another study performed on lactic acid bacteria extracts showed that selected bacteria strains were able to induce a significant amount of TNF-α and IL-6 in RAW 264.7 cells (Tejada-Simon & Pestka, 1999).

The LTA from the Bad368 strain did not reveal any potential to alleviate OVA-induced Th2-related cytokines in splenocytes nor induced significant cytokine response in BM-DCs. However, this does not exclude its role in the treatment of other diseases. Research focusing on LTA underlines the role of the TLR2 receptors in the recognition of this molecule which is in line with our results (Dessing et al., 2008; Schröder et al., 2003; Zeuthen et al., 2008). There is little information about the bifidobacterial LTAs' impact on the host. Studies of this compound derived from other probiotic bacteria such as lactobacilli confirm its crucial role in physiological and immunomodulatory functions. *Lactobacillus plantarum* L-137 studies indicated the LTA role in phagocytosis and induction of the splenic cells to produce IL-12p40 cytokine which is crucial in the Th1 responses (Hatano et al., 2015). Furthermore, Jeong et al. examined how the LTA structure affects the Th1-related TNF-α and regulatory IL-10 production in RAW 264.7 cells (Jeong et al., 2015). We indicated that LTA derived from *B. adolescentis* CCDM 368 is internalized by epithelial cells at a low level. However, in our model, almost half of the population of dendritic cells (JAWS II) intercepted the antigen from the epithelial cells, which indicates the antigen potential.

5. Conclusions

For the first time we comprehensively compared the biological activity of various *Bifidobacterium* surface antigens. We identified polysaccharide Bad368.1 which was able to efficiently induce the Th1-related response while decreasing the production of Th2 cytokines in allergen-stimulated splenocytes from OVA-sensitized mice. It also induced the Th1 cytokine production after stimulation of naïve BM-DCs. Moreover, this polysaccharide was well recognized by epithelial cells and transferred to DCs. The detailed investigation of its structure pointed out features that may contribute to the biological role of the Bad368.1 PS: lack of electric charge, high mass, monosaccharide content, and linkages. We foresee that this postbiotic molecule may be used in the future in the context of the prevention/treatment of allergy diseases.

Funding

This work was supported by the National Science Centre of Poland (UMO-2017/26/E/NZ7/01202); the Czech Science Foundation (22-04050L); The Ministry of Education, Youth and Sports of the Czech Republic (8JPL19046); the Polish National Agency for Academic Exchange (PPN/BIL/2018/1/00005). The group of MS is supported by The Ministry of Education, Youth and Sports of the Czech Republic (EMBO Installation Grant 4139).

CRediT authorship contribution statement

Katarzyna Pacyga-Prus: Methodology, Formal analysis, Investigation, Resources, Writing – original draft, Visualization. **Dominika Jakubczyk:** Methodology, Formal analysis, Investigation, Writing – original draft. **Corine Sandström:** Investigation, Writing – review & editing. **Dagmar Šrůtková:** Resources, Writing – review & editing. **Marcelina Joanna Pyclik:** Methodology, Investigation, Resources. **Katarzyna Leszczyńska:** Methodology, Resources. **Jarosław Ciekot:** Investigation. **Agnieszka Razim:** Methodology, Resources. **Martin Schwarzer:** Resources, Writing – review & editing, Supervision. **Sabina Górska:** Conceptualization, Validation, Writing – review & editing, Supervision, Project administration, Funding acquisition.

Declaration of competing interest

The authors declare no conflict of interest.

Data availability

Data will be made available on request.

Acknowledgment

We would like to thank Urszula Kozłowska and Aleksandra Bielawska-Pohl for the help in the optimization of the fluorescent microscopy method and Jaroslava Valterova, Kamila Michalickova and Sarka Maisnerova for excellent technical assistance. Graphical abstract was created using BioRender online software (https://biorender.com/).

Appendix A. Supplementary data

Supplementary data to this article can be found online at https://doi.org/10.1016/j.carbpol.2023.120980.

References

Altmann, F., Kosma, P., O'Callaghan, A., Leahy, S., Bottacini, F., Molloy, E., Plattner, S., Schiavi, E., Gleinser, M., Groeger, D., Grant, R., Rodriguez Perez, N., Healy, S., Svehla, E., Windwarder, M., Hofinger, A., O'Connell Motherway, M., Akdis, C. A., Xu, J.O'Mahony, L., … (2016). Genome analysis and characterisation of the exopolysaccharide produced by bifidobacterium longum subsp. Longum 35624TM. *PLOS ONE, 11*(9), Article e0162983. https://doi.org/10.1371/journal.pone.0162983

Amrouche, T., Boutin, Y., Prioult, G., & Fliss, I. (2006). Effects of bifidobacterial cytoplasm, cell wall and exopolysaccharide on mouse lymphocyte proliferation and cytokine production. *International Dairy Journal, 16*(1), 70–80. https://doi.org/10.1016/j.idairyj.2005.01.008

Balaguer, F., Enrique, M., Llopis, S., Barrena, M., Navarro, V., Álvarez, B., Chenoll, E., Ramón, D., Tortajada, M., & Martorell, P. (2022). Lipoteichoic acid from bifidobacterium animalis subsp. Lactis BPL1: A novel postbiotic that reduces fat deposition via IGF-1 pathway. *Microbial Biotechnology, 15*(3), 805–816. https://doi.org/10.1111/1751-7915.13769

Carillo, S., Silipo, A., Perino, V., Lanzetta, R., Parrilli, M., & Molinaro, A. (2009). The structure of the O-specific polysaccharide from the lipopolysaccharide of burkholderia anthina. *Carbohydrate Research, 344*(13), 1697–1700. https://doi.org/10.1016/j.carres.2009.05.013

Ciucanu, I., & Kerek, F. (1984). A simple and rapid method for the permethylation of carbohydrates. *Carbohydrate Research, 131*(2), 209–217. https://doi.org/10.1016/0008-6215(84)85242-8

Clarke, T. B., Davis, K. M., Lysenko, E. S., Zhou, A. Y., Yu, Y., & Weiser, J. N. (2010). Recognition of peptidoglycan from the microbiota by Nod1 enhances systemic innate immunity. *Nature Medicine, 16*(2), 228–231. https://doi.org/10.1038/nm.2087

Corridoni, D., Shiraishi, S., Chapman, T., Steevels, T., Muraro, D., Thézénas, M.-L., Prota, G., Chen, J.-L., Gileadi, U., Ternette, N., Cerundolo, V., & Simmons, A. (2019). NOD2 and TLR2 signal via TBK1 and PI31 to direct cross-presentation and CD8 T cell responses. *Frontiers in Immunology, 10*, 958. https://doi.org/10.3389/fimmu.2019.00958

Dessing, M. C., Schouten, M., Draing, C., Levi, M., von Aulock, S., & van der Poll, T. (2008). Role played by toll-like receptors 2 and 4 in lipoteichoic acid-induced lung inflammation and coagulation. *The Journal of Infectious Diseases, 197*(2), 245–252. https://doi.org/10.1086/524873

DuBois, M., Gilles, K. A., Hamilton, J. K., Rebers, P. A., & Smith, F. (1956). Colorimetric method for determination of sugars and related substances. *Analytical Chemistry, 28*(3), 350–356. https://doi.org/10.1021/ac60111a017

Górska, S., Hermanova, P., Ciekot, J., Schwarzer, M., Srutkova, D., Brzozowska, E., Kozakova, H., & Gamian, A. (2016). Chemical characterization and immunomodulatory properties of polysaccharides isolated from probiotic lactobacillus casei LOCK 0919. *Glycobiology, 26*(9), 1014–1024. https://doi.org/10.1093/glycob/cww047

Górska, S., Jachymek, W., Rybka, J., Strus, M., Heczko, P. B., & Gamian, A. (2010). Structural and immunochemical studies of neutral exopolysaccharide produced by lactobacillus johnsonii 142. *Carbohydrate Research, 345*(1), 108–114. https://doi.org/10.1016/j.carres.2009.09.015

Górska, S., Schwarzer, M., Jachymek, W., Srutkova, D., Brzozowska, E., Kozakova, H., & Gamian, A. (2014). Distinct immunomodulation of bone marrow-derived dendritic cell responses to lactobacillus plantarum WCFS1 by two different polysaccharides isolated from lactobacillus rhamnosus LOCK 0900. *Applied and Environmental Microbiology, 80*(20), 6506–6516. https://doi.org/10.1128/AEM.02104-14

Górska, S., Schwarzer, M., Srutkova, D., Hermanova, P., Brzozowska, E., Kozakova, H., & Gamian, A. (2017). Polysaccharides L900/2 and L900/3 isolated from lactobacillus rhamnosus LOCK 0900 modulate allergic sensitization to ovalbumin in a mouse model. *Microbial Biotechnology, 10*(3), 586–593. https://doi.org/10.1111/1751-7915.12606

Hatano, S., Hirose, Y., Yamamoto, Y., Murosaki, S., & Yoshikai, Y. (2015). Scavenger receptor for lipoteichoic acid is involved in the potent ability of lactobacillus plantarum strain L-137 to stimulate production of interleukin-12p40. *International Immunopharmacology, 25*(2), 321–331. https://doi.org/10.1016/j.intimp.2015.02.011

Hiramatsu, Y., Hosono, A., Konno, T., Nakanishi, Y., Muto, M., Suyama, A., Hachimura, S., Sato, R., Takahashi, K., & Kaminogawa, S. (2011). Orally administered bifidobacterium triggers immune responses following capture by CD11c+ cells in Peyer's patches and cecal patches. *Cytotechnology, 63*(3), 307–317. https://doi.org/10.1007/s10616-011-9349-6

Hosono, A., Adachi, T., & Kaminogawa, S. (1977) (n.d.). In *Characterization of a water-soluble polysaccharide fraction with immunopotentiating activity from Bifidohacterium adolescentis MIOl-4* (p. 5).

Inturri, R., Molinaro, A., Di Lorenzo, F., Blandino, G., Tomasello, B., Hidalgo-Cantabrana, C., De Castro, C., & Ruas-Madiedo, P. (2017). Chemical and biological properties of the novel exopolysaccharide produced by a probiotic strain of bifidobacterium longum. *Carbohydrate Polymers, 174*, 1172–1180. https://doi.org/10.1016/j.carbpol.2017.07.039

Ivashkiv, L. B. (2018). IFNγ: Signalling, epigenetics and roles in immunity, metabolism, disease and cancer immunotherapy. *Nature Reviews Immunology, 18*(9), 545–558. https://doi.org/10.1038/s41577-018-0029-z

Jeong, J. H., Jang, S., Jung, B. J., Jang, K.-S., Kim, B.-G., Chung, D. K., & Kim, H. (2015). Differential immune-stimulatory effects of LTAs from different lactic acid bacteria via MAPK signaling pathway in RAW 264.7 cells. *Immunobiology, 220*(4), 460–466. https://doi.org/10.1016/j.imbio.2014.11.002

Kerry, R., George, Patra, J. K., Gouda, S., Park, Y., Shin, H.-S., & Das, G. (2018). Benefaction of probiotics for human health: A review. *Journal of Food and Drug Analysis, 26*(3), 927–939. https://doi.org/10.1016/j.jfda.2018.01.002

Kohno, M., Suzuki, S., Kanaya, T., Yoshino, T., Matsuura, Y., Asada, M., & Kitamura, S. (2009). Structural characterization of the extracellular polysaccharide produced by bifidobacterium longum JBL05. *Carbohydrate Polymers, 77*(2), 351–357. https://doi.org/10.1016/j.carbpol.2009.01.013

Laws, A., Gu, Y., & Marshall, V. (2001). Biosynthesis, characterisation, and design of bacterial exopolysaccharides from lactic acid bacteria. *Biotechnology Advances, 19*(8), 597–625. https://doi.org/10.1016/S0734-9750(01)00084-2

Li, A.-L., Sun, Y.-Q., Du, P., Meng, X.-C., Guo, L., Li, S., & Zhang, C. (2017). The effect of lactobacillus actobacillus peptidoglycan on bovine β-lactoglobulin-sensitized mice via TLR2/NF-κB pathway. *Iranian Journal of Allergy Asthma and Immunology, 16*(2), 147–158. PMID: 28601055.

Lipkind, G. M., Shashkov, A. S., Knirel, Y. A., Vinogradov, E. V., & Kochetkov, N. K. (1988). A computer-assisted structural analysis of regular polysaccharides on the basis of 13C-n.m.r. data. *Carbohydr. Res., 175*(1), 59–75. https://doi.org/10.1016/0008-6215(88)80156-3

Lu, Q., Guo, Y., Yang, G., Cui, L., Wu, Z., Zeng, X., Pan, D., & Cai, Z. (2022). Structure and anti-inflammation potential of lipoteichoic acids isolated from lactobacillus strains. *Foods, 11*(11), 1610. https://doi.org/10.3390/foods11111610

Martinic, M. M., Caminschi, I., O'Keeffe, M., Thinnes, T. C., Grumont, R., Gerondakis, S., McKay, D. B., Nemazee, D., & Gavin, A. L. (2017). The bacterial peptidoglycan-sensing molecules NOD1 and NOD2 promote CD8 + thymocyte selection. *The Journal of Immunology, 198*(7), 2649–2660. https://doi.org/10.4049/jimmunol.1601462

Mattos, K. A., Jones, C., Heise, N., Previato, J. O., & Mendonça-Previato, L. (2001). Structure of an acidic exopolysaccharide produced by the diazotrophic endophytic bacterium burkholderia brasiliensis: Exopolysaccharide from nitrogen-fixing burkholderia. *European Journal of Biochemistry, 268*(11), 3174–3179. https://doi.org/10.1046/j.1432-1327.2001.02196.x

Morath, S., Geyer, A., & Hartung, T. (2001). Structure-function relationship of cytokine induction by lipoteichoic acid fromStaphylococcus aureus. *Journal of Experimental Medicine, 193*(3), 393–398. https://doi.org/10.1084/jem.193.3.393

Nagaoka, M., Hashimoto, S., Shibata, H., Kimura, I., Kimura, K., Sawada, H., & Yokokura, T. (1996). Structure of a galactan from cell walls of bifidobacterium catenulatum YIT4016. *Carbohydrate Research, 281*(2), 285–291. https://doi.org/10.1016/0008-6215(95)00354-1

Nagaoka, M., Muto, M., Yokokura, T., & Mutai, M. (1988). Structure of 6-deoxytalose-containing polysaccharide from the Cell Wall of bifidobacterium adolescentis. *The Journal of Biochemistry, 103*(4), 618–621. https://doi.org/10.1093/oxfordjournals.jbchem.a122316

Nataraj, B. H., Ali, S. A., Behare, P. V., & Yadav, H. (2020). Postbiotics-parabiotics: The new horizons in microbial biotherapy and functional foods. *Microbial Cell Factories, 19*(1), 168. https://doi.org/10.1186/s12934-020-01426-w

Palomares, O., Akdis, M., Martín-Fontecha, M., & Akdis, C. A. (2017). Mechanisms of immune regulation in allergic diseases: The role of regulatory T and B cells. *Immunological Reviews, 278*(1), 219–236. https://doi.org/10.1111/imr.12555

Pyclik, M. J., Srutkova, D., Razim, A., Hermanova, P., Svabova, T., Pacyga, K., Schwarzer, M., & Górska, S. (2021). Viability status-dependent effect of Bifidobacterium longum ssp. Longum CCM 7952 on prevention of allergic inflammation in mouse model. *Frontiers in Immunology, 12*, 2800. https://doi.org/10.3389/fimmu.2021.707728

Pyclik, M., Srutkova, D., Schwarzer, M., & Górska, S. (2020). Bifidobacteria cell wall-derived exo-polysaccharides, lipoteichoic acids, peptidoglycans, polar lipids and proteins – their chemical structure and biological attributes. *International Journal of Biological Macromolecules, 147*, 333–349. https://doi.org/10.1016/j.ijbiomac.2019.12.227

Raftis, E. J., Delday, M. I., Cowie, P., McCluskey, S. M., Singh, M. D., Ettorre, A., & Mulder, I. E. (2018). Bifidobacterium breve MRx0004 protects against airway inflammation in a severe asthma model by suppressing both neutrophil and eosinophil lung infiltration. *Scientific Reports, 8*(1), 12024. https://doi.org/10.1038/s41598-018-30448-z

Robinson, D. S., Larché, M., & Durham, S. R. (2004). Tregs and allergic disease. *Journal of Clinical Investigation, 114*(10), 1389–1397. https://doi.org/10.1172/JCI200423595

Ruiz, L., Delgado, S., Ruas-Madiedo, P., Sánchez, B., & Margolles, A. (2017). Bifidobacteria and their molecular communication with the immune system. *Frontiers in Microbiology, 8*, 2345. https://doi.org/10.3389/fmicb.2017.02345

Salatin, S., & Yari Khosroushahi, A. (2017). Overviews on the cellular uptake mechanism of polysaccharide colloidal nanoparticles. *Journal of Cellular and Molecular Medicine, 21*(9), 1668–1686. https://doi.org/10.1111/jcmm.13110

Sawardeker, J. S., Sloneker, J. H., & Jeanes, A. (1965). Quantitative determination of monosaccharides as their alditol acetates by gas liquid chromatography. *Analytical Chemistry, 37*(12), 1602–1604. https://doi.org/10.1021/ac60231a048

Schaub, R., & Dillard, J. (2017). Digestion of peptidoglycan and analysis of soluble fragments. *BIO-Protocol, 7*(15). https://doi.org/10.21769/BioProtoc.2438

Schiavi, E., Gleinser, M., Molloy, E., Groeger, D., Frei, R., Ferstl, R., Rodriguez-Perez, N., Ziegler, M., Grant, R., Moriarty, T. F., Plattner, S., Healy, S., O'Connell Motherway, M., Akdis, C. A., Roper, J., Altmann, F., van Sinderen, D., & O'Mahony, L. (2016). The surface-associated exopolysaccharide of bifidobacterium longum 35624 plays an essential role in dampening host proinflammatory responses and repressing local T H 17 responses. *Applied and Environmental Microbiology, 82*(24), 7185–7196. https://doi.org/10.1128/AEM.02238-16

Schiavi, E., Plattner, S., Rodriguez-Perez, N., Barcik, W., Frei, R., Ferstl, R., Kurnik-Lucka, M., Groeger, D., Grant, R., Roper, J., Altmann, F., van Sinderen, D., Akdis, C. A., & O'Mahony, L. (2018). Exopolysaccharide from bifidobacterium

longum subsp. Longum 35624TM modulates murine allergic airway responses. *Beneficial Microbes, 9*(5), 761–773. https://doi.org/10.3920/BM2017.0180

Schröder, N. W. J., Morath, S., Alexander, C., Hamann, L., Hartung, T., Zähringer, U., Göbel, U. B., Weber, J. R., & Schumann, R. R. (2003). Lipoteichoic acid (LTA) of streptococcus pneumoniaeand Staphylococcus aureus activates immune cells via toll-like receptor (TLR)-2, lipopolysaccharide-binding protein (LBP), and CD14, whereas TLR-4 and MD-2 are not involved. *Journal of Biological Chemistry, 278*(18), 15587–15594. https://doi.org/10.1074/jbc.M212829200

Schwarzer, M., Srutkova, D., Schabussova, I., Hudcovic, T., Akgün, J., Wiedermann, U., & Kozakova, H. (2013). Neonatal colonization of germ-free mice with bifidobacterium longum prevents allergic sensitization to major birch pollen allergen bet v 1. *Vaccine, 31*(46), 5405–5412. https://doi.org/10.1016/j.vaccine.2013.09.014

Senchenkova, S. N., Shashkov, A. S., Laux, P., Knirel, Y. A., & Rudolph, K. (1999). The O-chain polysaccharide of the lipopolysaccharide of xanthomonascampestris pv. Begoniae GSPB 525 is a partially l-xylosylated l-rhamnan. *Carbohydrate Research, 319*(1–4), 148–153. https://doi.org/10.1016/S0008-6215(99)00125-1

Shang, N., Xu, R., & Li, P. (2013). Structure characterization of an exopolysaccharide produced by bifidobacterium animalis RH. *Carbohydrate Polymers, 91*(1), 128–134. https://doi.org/10.1016/j.carbpol.2012.08.012

Shashkov, A. S., Lipkind, G. M., Knirel, Y. A., & Kochetkov, N. K. (1988). Stereochemical factors determining the effects of glycosylation on the13C chemical shifts in carbohydrates. *Magnetic Resonance in Chemistry, 26*(9), 735–747. https://doi.org/10.1002/mrc.1260260904

Speciale, I., Verma, R., Di Lorenzo, F., Molinaro, A., Im, S.-H., & De Castro, C. (2019). Bifidobacterium bifidum presents on the cell surface a complex mixture of glucans and galactans with different immunological properties. *Carbohydrate Polymers, 218*, 269–278. https://doi.org/10.1016/j.carbpol.2019.05.006

Tejada-Simon, M. V., & Pestka, J. J. (1999). Proinflammatory cytokine and nitric oxide induction in murine macrophages by Cell Wall and cytoplasmic extracts of lactic acid bacteria. *Journal of Food Protection, 62*(12), 1435–1444. https://doi.org/10.4315/0362-028X-62.12.1435

Tian, X., Fan, R., He, H., Cui, Q., Liang, X., Liu, Q., Liu, T., Lin, K., Zhang, Z., Yi, H., Gong, P., & Zhang, L. (2022). Bifidobacterium animalis KV9 and lactobacillus vaginalis FN3 alleviated β-lactoglobulin-induced allergy by modulating dendritic cells in mice. *Frontiers in Immunology, 13*, Article 992605. https://doi.org/10.3389/fimmu.2022.992605

Verma, R., Lee, C., Jeun, E.-J., Yi, J., Kim, K. S., Ghosh, A., Byun, S., Lee, C.-G., Kang, H.-J., Kim, G.-C., Jun, C.-D., Jan, G., Suh, C.-H., Jung, J.-Y., Sprent, J., Rudra, D., De Castro, C., Molinaro, A., Surh, C. D., & Im, S.-H. (2018). Cell surface polysaccharides of bifidobacterium bifidum induce the generation of Foxp3 + regulatory T cells. *Science Immunology, 3*(28), Article eaat6975. https://doi.org/10.1126/sciimmunol.aat6975

Vinogradov, E., Korenevsky, A., & Beveridge, T. J. (2003). The structure of the O-specific polysaccharide chain of the shewanella algae BrY lipopolysaccharide. *Carbohydrate Research, 338*(4), 385–388. https://doi.org/10.1016/S0008-6215(02)00469-X

Wolf, A. J., & Underhill, D. M. (2018). Peptidoglycan recognition by the innate immune system. *Nature Reviews Immunology, 18*(4), 243–254. https://doi.org/10.1038/nri.2017.136

Xu, R., Shen, Q., Wu, R., & Li, P. (2017). Structural analysis and mucosal immune regulation of exopolysaccharide fraction from bifidobacterium animalis RH. *Food and Agricultural Immunology, 28*(6), 1226–1241. https://doi.org/10.1080/09540105.2017.1333578

Zdorovenko, E. L., Kachala, V. V., Sidarenka, A. V., Izhik, A. V., Kisileva, E. P., Shashkov, A. S., Novik, G. I., & Knirel, Y. A. (2009). Structure of the cell wall polysaccharides of probiotic bifidobacteria bifidobacteriumbifidum BIM B-465. *Carbohydrate Research, 344*(17), 2417–2420. https://doi.org/10.1016/j.carres.2009.08.039

Zeuthen, L. H., Fink, L. N., & Frøkiaer, H. (2008). Toll-like receptor 2 and nucleotide-binding oligomerization domain-2 play divergent roles in the recognition of gut-derived lactobacilli and bifidobacteria in dendritic cells. *Immunology, 124*(4), 489–502. https://doi.org/10.1111/j.1365-2567.2007.02800.x

Zhou, Y., Cui, Y., & Qu, X. (2019). Exopolysaccharides of lactic acid bacteria: Structure, bioactivity and associations: A review. *Carbohydrate Polymers, 207*, 317–332. https://doi.org/10.1016/j.carbpol.2018.11.093

Supplementary materials

Bad368 stimulation of splenocytes isolated from OVA-sensitized mice

1. Material and methods

1.1. Cultivation and heat inactivation of bacterial cells

The strain was cultivated as described in the manuscript in the Material and Methods section. To determine the number of cells, bacteria were seeded on MRS agar plates with 0.05 % L-cysteine for CFU count after 48 h of anaerobic incubation or by QuantomTx Microbial Cell Counter (Logos Biosystems, South Korea). Obtained values were associated with corresponding OD_{600} measurements. Heat inactivation was performed at 65 °C for 1 h, and samples were stored at 4 °C until use. Loss of viability as well as bacterial survival in PBS after 72 h at 4 °C was checked as described previously by CFU count.

1.2. Splenocytes isolation and stimulation

The immunomodulatory potential of Bad368 was tested *ex vivo* on splenocytes derived from ovalbumin (OVA)-sensitized BALB/c mice (8 – 12 weeks of age; n = 3) in four independent experiments. Female mice were sensitized by two intraperitoneal (i.p.) injections of 10 µg of OVA (Sigma Aldrich, grade V) mixed with 0.65 mg/100 µl of Alum (Serva, Germany) in a final volume of 200 µl in a two-week interval. Seven days after the second immunization, mice were anesthetized with 3 % isoflurane and euthanized by cervical dislocation. Splenocyte isolation and restimulation with OVA were performed as described in the manuscript in the Materials and Methods section. Live and heat-inactivated bacteria were added to OVA-treated cells in a ratio of 1 : 10 (cells : bacteria) for 72 h. The concentration of cytokines was measured in supernatants by the Milliplex Map Mouse Cytokine/Chemokine Panel (IL-4, IL-5, IL-13) according to the manufacturer's instructions and analyzed with Luminex 2000 System (Bio-Rad Laboratories). Changes in Th2-related cytokines were presented as a percentage ratio between tested samples and the OVA-control (OVA re-stimulated splenocytes). Unstimulated splenocytes were used as a negative control (medium without OVA).

2. Results

Stimulation of splenocytes with both live and heat-treated Bad368 cells showed the ability of the tested strain to inhibit Th2-related IL-4, IL-5, and IL-13 cytokines in OVA-treated splenocytes derived from OVA-sensitized mice.

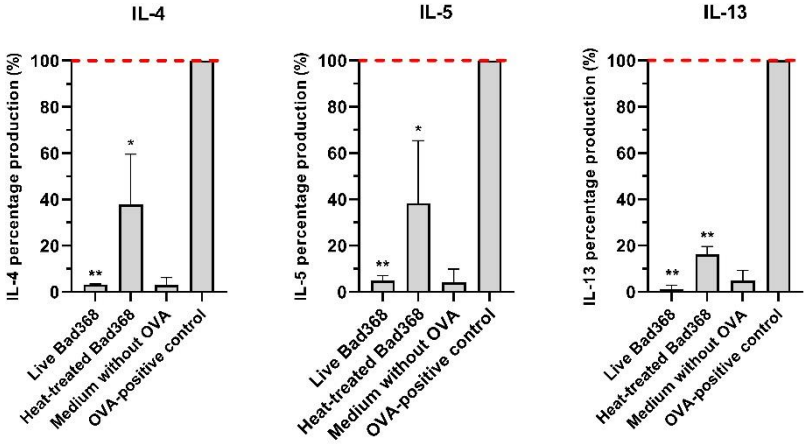

Supplementary Figure S1. Live and heat-treated Bad368 impact on IL-4, IL-5 and IL-13 production by OVA-stimulated splenocytes isolated from OVA-sensitized mice. The stimulation was carried out for 72 h at 37 °C, 5 % CO_2. Bacteria were added to the cells in 1 : 10 ratio (cells : bacteria). Both live and heat-treated Bad368 were able to significantly reduce the Th2-related cytokines when compared to OVA-control (red dashed line). Four separate experiments were performed. Obtained data are shown with mean ± SD. One-way ANOVA and Dunnett's multiple comparison tests to the OVA-control group were performed (**** $p \leq 0.0001$, *** $p \leq 0.001$, ** $p \leq 0.01$, * $p \leq 0.05$).

The ^{1}H-NMR spectra

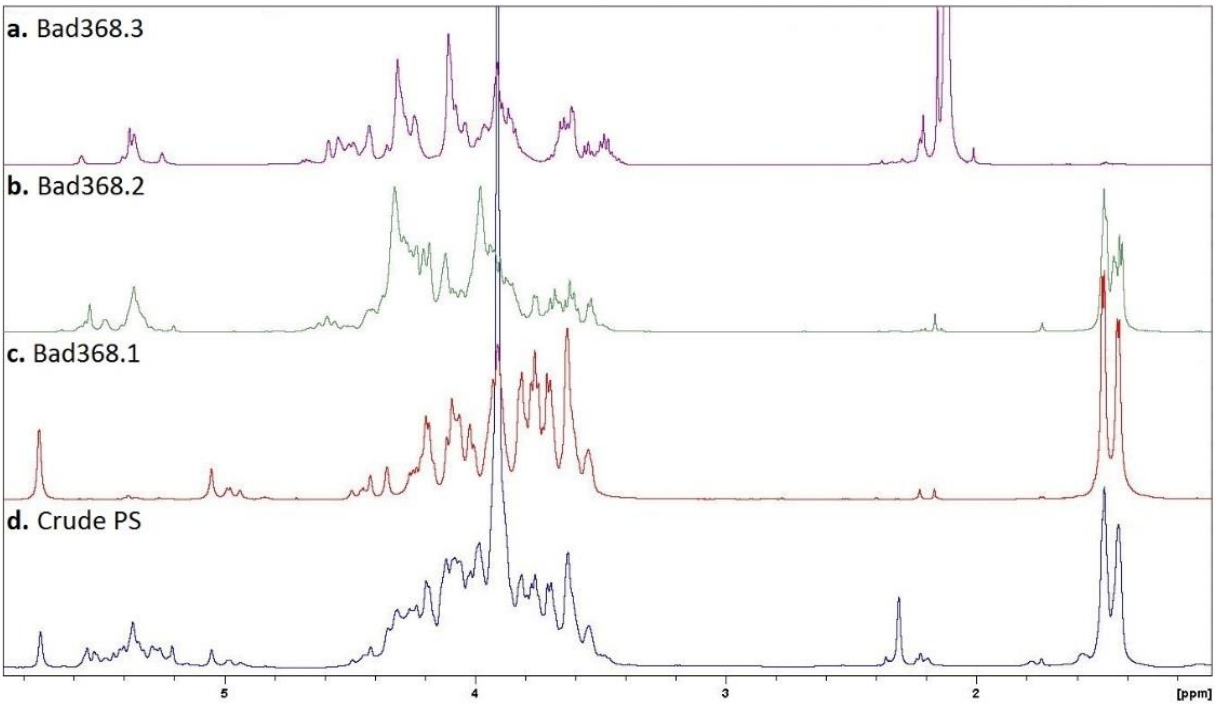

Supplementary Figure S2. ^{1}H-NMR spectra of polysaccharides produced by Bad368. Spectra (a – c) represent fractions after chromatography separations. Spectrum d shows the crude PS.

HEK-Blue™ cells cultivation and stimulation

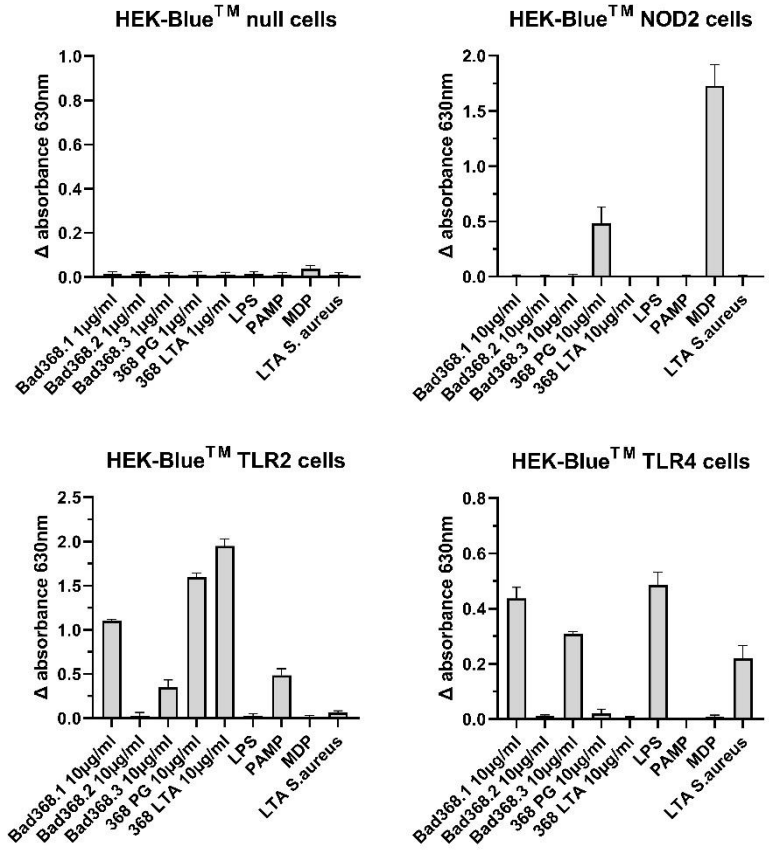

Supplementary Figure S3. Antigens recognition by the innate immune receptors. HEK-Blue cells were stimulated with tested molecules (at concentrations described on a graph) and proper controls: LPS ultra-pure (1 µg/ml), PAMP (Pam3CSK4, 10 ng/ml), MDP (muramyl dipeptide, 1 µg/ml), LTA *S. aureus* (1 µg/ml). Obtained results are presented with mean ± SD as a difference (Δ) between absorbance read for PBS (negative control) and sample. Observation of the colorimetric reaction showed that (1) NOD2 recognizes PG; (2) TLR2 recognizes all PS fractions, PG, and LTA; (3) TLR4 recognizes Bad368.1, Bad368.3, PG, and LTA. Null cells that lack studied receptors were used as a negative control.

Antigens uptake by the epithelial cells (TC-1)

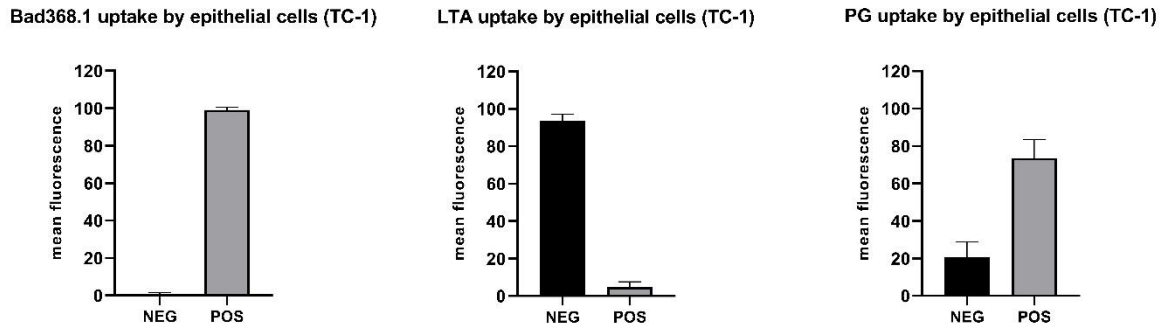

Supplementary Figure S4. Uptake of the Bad368.1 PS, LTA and PG by the epithelial cell line (TC-1). NEG – population of epithelial cells without uptaken antigen; POS – population of epithelial cells with uptaken antigen (after 4h stimulation).

NMR spectra of Bad368.1 polysaccharide

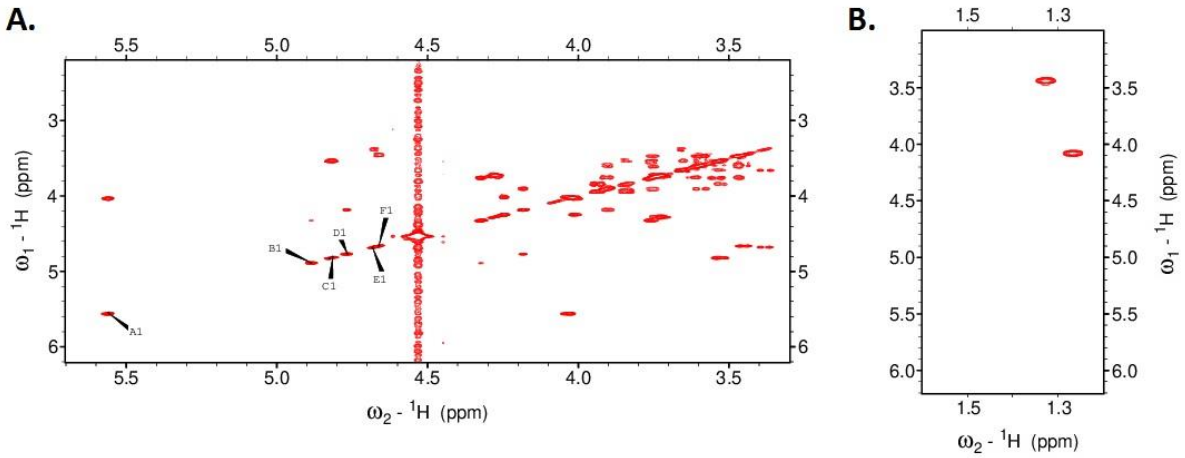

Supplementary Figure S5. ^{1}H-^{1}H COSY spectrum of Bad368.1 polysaccharide. A. The main part of the spectra with the anomeric signals marked from A1 – F1. B. COSY signals for rhamnoses (residue B and D) between 1.2 – 1.6 ppm.

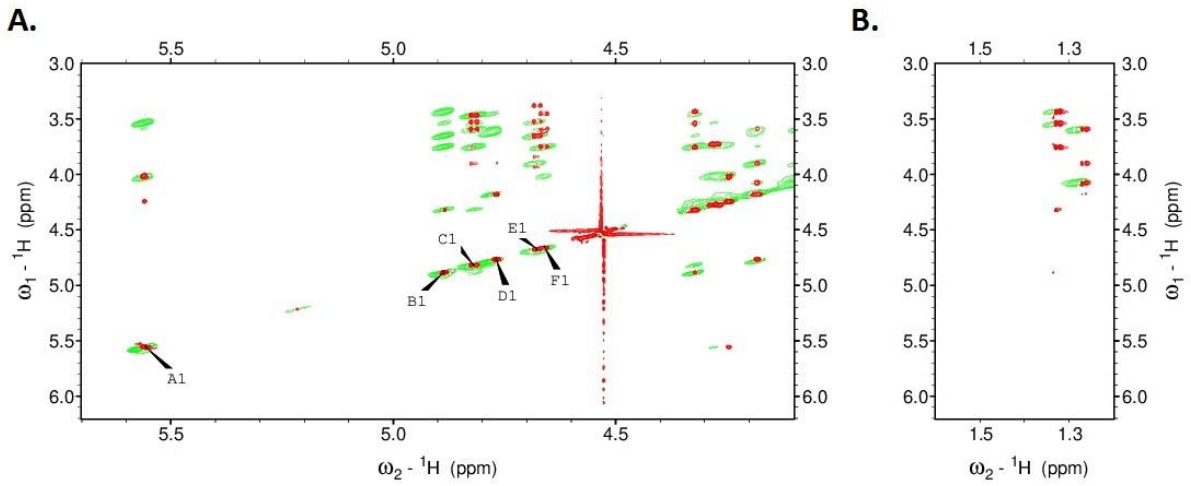

Supplementary Figure S6. 120 ms ^{1}H-^{1}H TOCSY spectrum (green) overlapped with 300 ms ^{1}H-^{1}H NOESY spectrum (red) of Bad368.1 polysaccharide. A. The main part of the spectra with the anomeric signals marked from A1 – F1. B. TOCSY and COSY signals for rhamnoses (residue B and D) between 1.2 – 1.6 ppm.

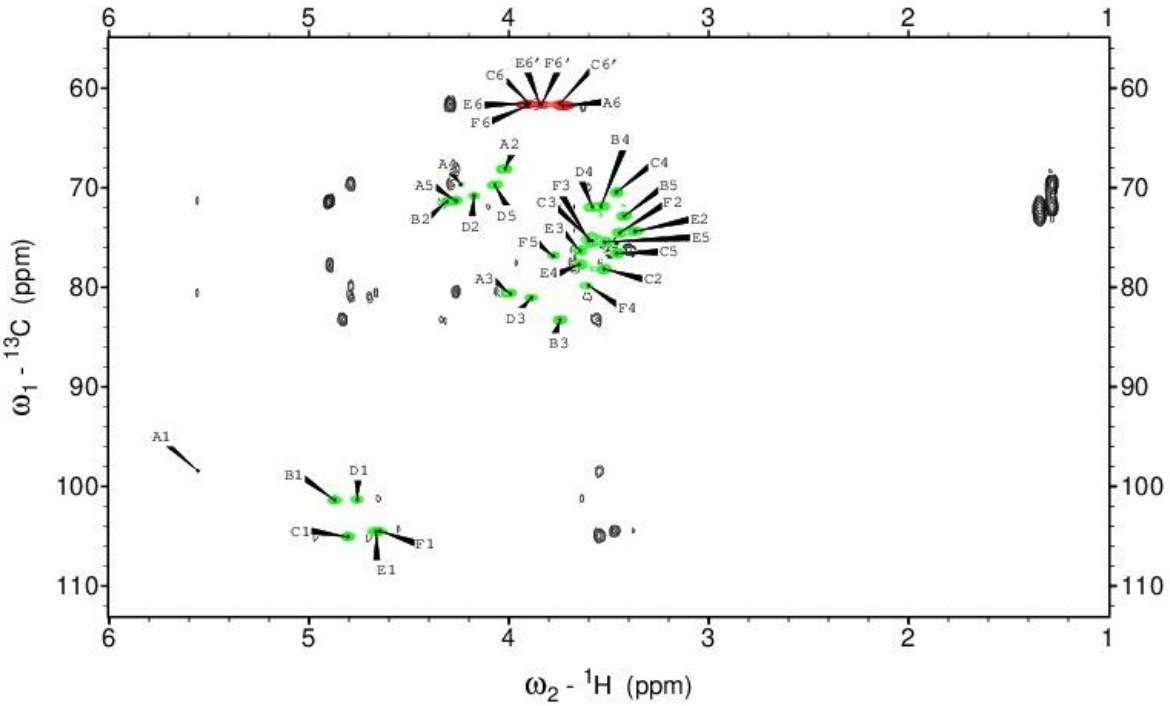

Supplementary Figure S7. ^{1}H-^{13}C HSQC spectrum (green and red) overlapped with ^{1}H-^{13}C HMBC spectrum (black) of Bad368.1 polysaccharide.

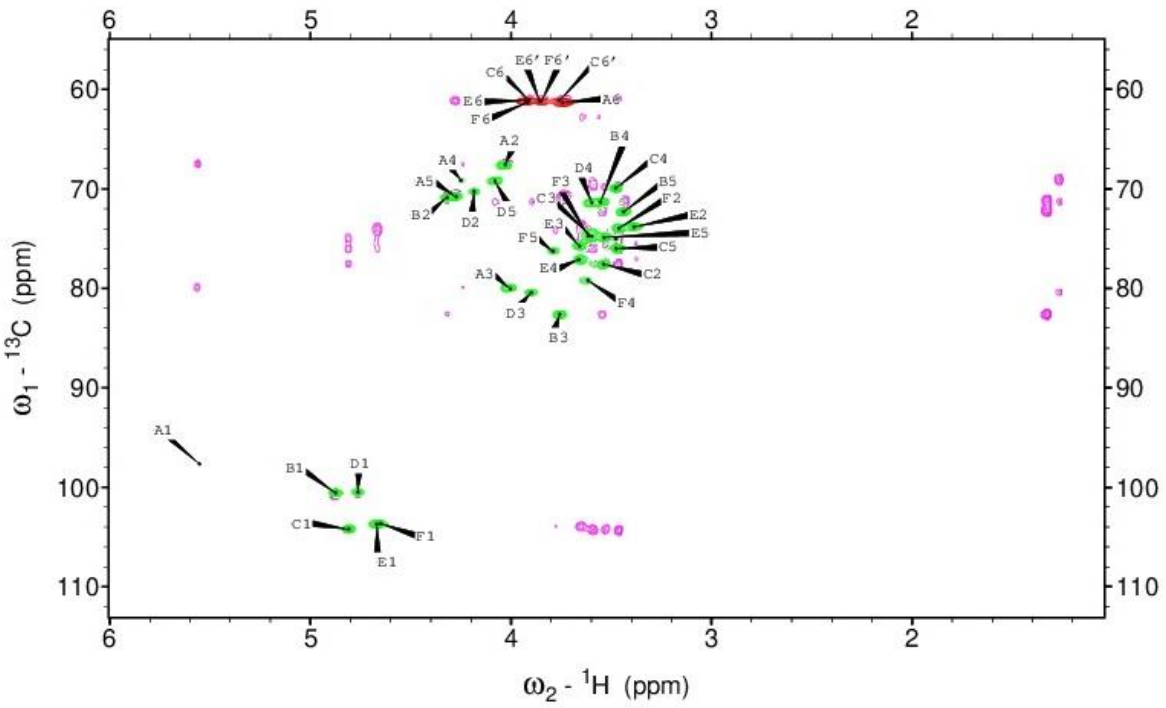

Supplementary Figure S8. ^{1}H-^{13}C HSQC spectrum (green and red) overlapped with HSQC-TOSCY spectrum (magenta) of Bad368.1 polysaccharide.

5. 2nd manuscript

5.1. Foreword to the 2nd manuscript

A. Rationale of research objectives

In some cases, introducing certain modifications (that include acetylation, sulphation or phosphorylation) may enhance the immunomodulatory properties of antigens [35,36]. Structural analysis of the *Bifidobacterium animalis* ssp. *animalis* CCDM 218 surface PSs, revealed that B.PAT is the only phosphorylated PS of the Ban218 strain.

B.PAT was dephosphorylated with 48 % hydrofluoric acid to undermine the function of the phosphorus, creating a B.MAT counterpart. Next, a thorough structural and functional investigation was performed. It contributed to the execution of objectives **O1** and **O2** and to testing whether antigen modifications may improve the properties of native molecules.

B. Methodology:

- Cultivation of the Ban218 strain and bacterial mass collection.
- Isolation, and purification of B.PAT, and dephosphorylation by 48 % hydrofluoric acid.
- Determination of monosaccharide molecule numbers in B.PAT fraction with NMR spectroscopy using- Diffusion-Ordered Spectroscopy (DOSY) method.
- Structure determination and investigation of changes between the B.PAT and B.MAT compounds using chemical methods (GLC-MS), FPLC, and NMR spectroscopy.
- Prediction of B.PAT and B.MAT spatial structure by Carbohydrate Structure Database (CSDB) Structure Editor.
- Determination of cytokine production by BMDCs isolated from naïve BALB/c mice after treatment with tested PSs and in co-culture with known immunostimulant (*L. rhamnosus* GG).
- Cytotoxicity assay to determine BMDCs survival rate after stimulation with studied molecules.
- Investigation of the prophylactic and therapeutic anti-inflammatory effect of B.PAT and B.MAT in the IL-1β-induced inflammatory model of human cell lines (HT-29 and Caco-2).

C. Results:

- Dephosphorylation resulted in the creation of the B.MAT counterpart.
- DOSY experiment allowed the rejection of monosaccharides that did not belong to the B.PAT structure. Further comprehensive NMR analysis of B.PAT revealed a unique

structure of molecular mass of approximately 1.96×10^4 Da consisting of glucose, galactose, and rhamnose, substituted by glycerol phosphate, creating the following repeating unit:

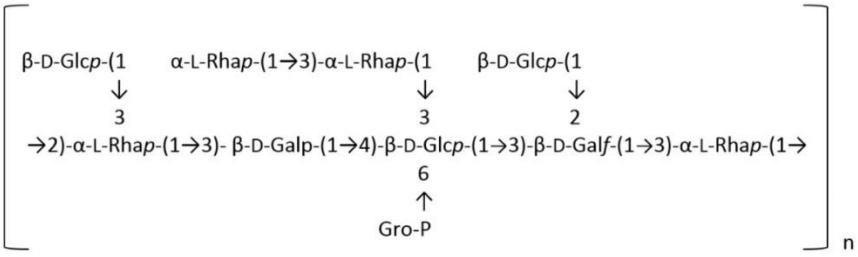

- Structural analysis of B.MAT counterpart revealed changes in the chemical shifts of β-D-Glc*p* as a result of glycerol phosphate loss.
- Prediction of B.PAT and B.MAT spatial structures showed changes after dephosphorylation.
- Dephosphorylated B.MAT resulted in dose-dependent tumor necrosis factor(TNF)-α, IL-6, IL-10, and IL-12 cytokine production. This response was significantly higher than the one induced by B.PAT at the same dose. Moreover, the addition of tested PSs to a known immunostimulant (*L. rhamnosus* GG) increased the cytokine production compared to the strain alone.
- Cytotoxicity assay did not reveal changes in BMDCs survival rate after stimulation with both PSs.
- B.MAT exhibited a stronger anti-inflammatory response than B.PAT when administered to IL-1β-induced HT-29 and Caco-2 cell lines in a preventive model.

D. Conclusions:

The introduction of modifications into a PS structure can change the immunomodulatory properties of the molecule. Dephosphorylation of B.PAT resulted not only in the structural and spatial changes but also in the immunomodulatory differences that favored B.MAT's ability to induce cytokine response and to prevent IL-1β inflammatory response.

5.2. Copy of the 2nd manuscript

Pacyga-Prus, K., Sandström, C., Šrůtková, D., Schwarzer, M., & Górska, S. Phosphorylation-dependent immunomodulatory properties of B.PAT polysaccharide isolated from *Bifidobacterium animalis* ssp. *animalis* CCDM 218. Carbohydr. Polym. 2024 Nov 15; *344*: 122518. https://doi.org/10.1016/j.carbpol.2024.122518.

A. Graphical abstract

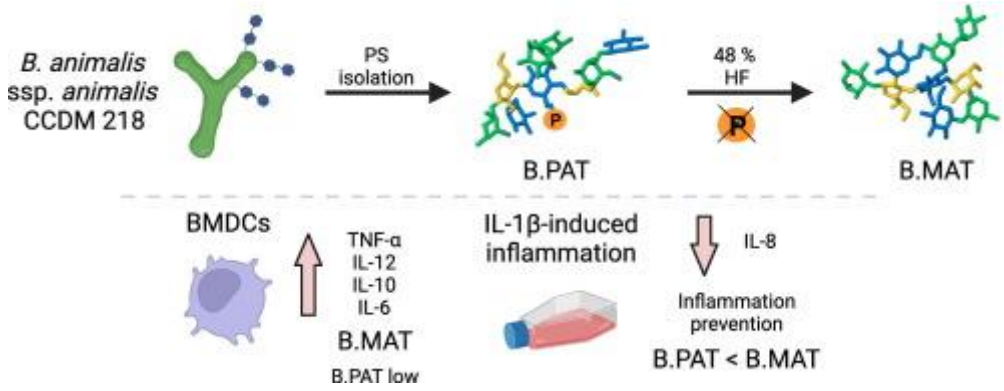

B. Manuscript and supplementary data

Carbohydrate Polymers 344 (2024) 122518

Contents lists available at ScienceDirect

Carbohydrate Polymers

journal homepage: www.elsevier.com/locate/carbpol

Phosphorylation-dependent immunomodulatory properties of B.PAT polysaccharide isolated from *Bifidobacterium animalis* ssp. *animalis* CCDM 218

Katarzyna Pacyga-Prus [a,*], Corine Sandström [b], Dagmar Šrůtková [c], Martin Schwarzer [c], Sabina Górska [a,*]

[a] Laboratory of Microbiome Immunobiology, Hirszfeld Institute of Immunology and Experimental Therapy, Polish Academy of Sciences, 53-114 Wroclaw, Poland
[b] Department of Molecular Sciences, Swedish University of Agricultural Sciences, Box 7015, SE-750 07 Uppsala, Sweden
[c] Laboratory of Gnotobiology, Institute of Microbiology, Czech Academy of Sciences, 549 22 Novy Hradek, Czech Republic

ARTICLE INFO

Keywords:
Polysaccharides
Bifidobacterium
Dephosphorylation
Immunomodulation
Surface antigens
Postbiotics

ABSTRACT

A wide range of articles describe the role of different probiotics in the prevention or treatment of various diseases. However, currently, the focus is shifting from whole microorganisms to their easier-to-define components that can confer similar or stronger benefits on the host. Here, we aimed to describe polysaccharide B.PAT, which is a surface antigen isolated from *Bifidobacterium animalis* ssp. *animalis* CCDM 218 and to understand the relationship between its structure and function. For this reason, we determined its glycerol phosphate-substituted structure, which consists of glucose, galactose, and rhamnose residues creating the following repeating unit:

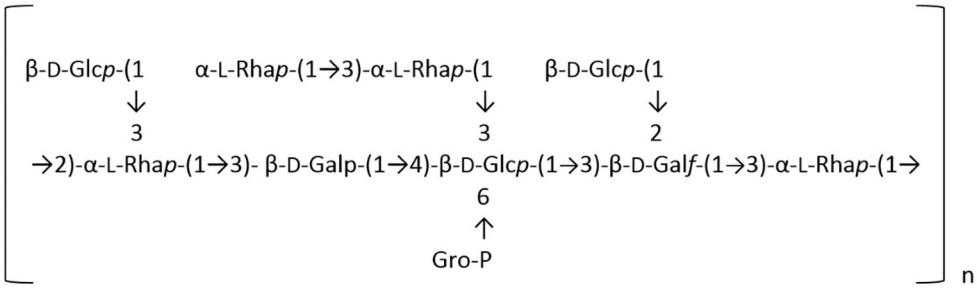

To fully understand the role of glycerol phosphate substitution on the B.PAT function, we prepared the dephosphorylated counterpart (B.MAT) and tested their immunomodulatory properties. The results showed that the loss of glycerol phosphate increased the production of IL-6, IL-10, IL-12, and TNF-α in bone marrow dendritic cells alone and after treatment with *Lacticaseibacillus rhamnosus* GG. Further studies indicated that dephosphorylation can enhance B.PAT properties to suppress IL-1β-induced inflammatory response in Caco-2 and HT-29 cells. Thus, we suggest that further investigation of B.PAT and B.MAT may reveal distinct functionalities that can be exploited in the treatment of various diseases and may constitute an alternative to probiotics.

1. Introduction

The microbiome composition and function have recently gained immense attention, and the number of publications on this topic started to grow extensively after 2010. Currently, not only living and proliferating bacteria (called probiotics) but also their isolated and defined

* Corresponding authors.
E-mail addresses: katarzyna.pacyga-prus@hirszfeld.pl (K. Pacyga-Prus), corine.sandstrom@slu.se (C. Sandström), sabina.gorska@hirszfeld.pl (S. Górska).

https://doi.org/10.1016/j.carbpol.2024.122518
Received 18 March 2024; Received in revised form 15 July 2024; Accepted 17 July 2024
Available online 18 July 2024

components are considered health-promoting factors (Salminen et al., 2021). These molecules are referred to as postbiotics and include surface antigens, for instance, lipoteichoic acids, proteins, glycolipids, and polysaccharides (PSs) (Pyclik et al., 2020). The last group is well described in the literature for both gram-positive and gram-negative bacteria. PSs can be a part of the O-antigen in lipopolysaccharides (LPS, in gram-negative bacteria), can be present in an unattached form in slime, or can be anchored to a cell surface (Bazaka et al., 2011). In general, PSs are composed of monosaccharides connected by glycosidic bonds, creating units that may be modified by different substitutions (Zeidan et al., 2017).

Polysaccharides of microbial origin are widely applied in medicine and industry. Some, like hyaluronic acid produced by bacteria (such as *Streptococci*), are extensively used *e.g.* in cosmetology (Bravo et al., 2022). Others, like dextran (produced by lactic acid bacteria), due to their high viscosity and emulsifying and stabilizing properties, have been tested as potential candidates for modern drug delivery systems (Hu et al., 2021). Additionally, the direct and indirect influence of polysaccharides on apoptotic cell death, antimetastasis, or immunomodulation has been described in the literature (Prateeksha et al., 2022). For instance, the polysaccharide Maitake Z produced by *G. frondosa* improves the Th1-related response against tumor development by upregulating the cytokines IL-12, IL-2, and IFN-γ (Masuda et al., 2009). The immunomodulatory functions of the extracellular PSs of health-promoting bacteria have been extensively described in the literature (Pacyga-Prus et al., 2023; Schiavi et al., 2018; Speciale et al., 2019; Srutkova et al., 2023; Verma et al., 2018). Primarily, their role was directly related to the protection, support, and energy supply for microorganisms. However, more publications have described their host-related functions (Khan et al., 2022). The ability of PSs to influence immune system function by activating different cell subsets or by inducing anti-inflammatory, pro-inflammatory, or regulatory cytokines and chemokines is particularly interesting (Górska et al., 2014; Nishimura-Uemura et al., 2003; Pacyga-Prus et al., 2023; Sato et al., 2004; Speciale et al., 2019; Verma et al., 2018). These functions may be crucial for the prevention or treatment of a wide variety of diseases. For instance, Yue et al. described EPS-1, EPS-2, and EPS-3 PSs from *Bifidobacterium longum* subsp. *infantis* E4 and their role in the inhibition of the pro-inflammatory factors' expression while inducing anti-inflammatory TGF-β and IL-10. These results indicated their role in the alleviation of inflammation. Moreover, they were able to increase the proliferation of mouse spleen lymphocytes and promote NK cell activity (You et al., 2020). On the other hand, BAP1 PS from *Bifidobacterium adolescentis* CCDM 368 exhibited a potential role in allergy treatment by strong induction of IFN-γ and inhibition of Th2-related cytokines in cells isolated from OVA-sensitized mice. More importantly, it was efficiently transferred from epithelial to dendritic cells (Pacyga-Prus et al., 2023).

Depending on their origin, monosaccharide composition, size, spatial structure, or substitutions, PSs can exhibit a wide range of properties, including anti-oxidative, anti-tumor, or anti-microbial functions (Angelin & Kavitha, 2020). These substitutions include, among others, acetylation, sulfation, or phosphorylation. The presence of chemical modifications may influence the charge, molecular weight, or spatial structure of PSs and thus have a great impact on their function and biological activities. In a great number of examples, substitutions can solve the problem of poor solubility or low bioactivity of PSs (Cao et al., 2020; Liu et al., 2023). However, the natural occurrence of chemically modified PSs is low, as is the degree of substitution of the PS chain. For this reason, to improve PSs' functions, non-substituted PSs are modified in the research and industry fields to obtain new PSs that acquire enhanced functionalities (Laffargue et al., 2023). Among bacteria, there are naturally occurring PSs that bear phosphorylation in their structure, however, only a few publications have investigated the influence of this substitution on PSs function (Nishimura-Uemura et al., 2003; Sato et al., 2004; Speciale et al., 2019). Moreover, there is little information on the structure-function relationships. This can be caused by the complex, hard-to-characterize backbones that make the structure very difficult to determine (Laffargue et al., 2023).

The beneficial effects of probiotics in inflammatory disorders (such as inflammatory bowel disease or allergy) are well described in the literature, however, their use is not without drawbacks. Researchers are therefore focusing on finding alternative molecules that will inherit the immunomodulatory effect of whole microorganisms and overcome emerging obstacles. One solution focuses on the use of postbiotics that have decisive advantages over whole microorganisms. First, polysaccharides are inanimate molecules that cannot reproduce and thus cause bacteremia (Salminen et al., 2021). Second, their structure is much easier to define, which allows a detailed examination of their safety and exact functions. Moreover, PSs are stable molecules that are heat resistant and can be stored at room temperature (RT), which makes them easier to transport than probiotics (Rafique et al., 2023). Although microbial PSs have gained increased amounts of attention over the past decade, there are no known available probiotic alternatives. However, immunomodulatory results are promising for quick changes.

Here, we propose that the presence of phosphate substitution impacts the immunomodulatory function of PSs isolated from *Bifidobacterium animalis* ssp. *animalis* CCDM 218 (Ba218). Therefore, in this study, a PS called B.PAT was isolated from the surface of the Ba218 strain. Its structure was described with the use of NMR and GLC-MS methods, and the presence of glycerol phosphate substitution was confirmed by ^{31}P NMR and ^{1}H—^{13}C HSQC experiments. To fully understand the role of phosphorus substitution, B.PAT was dephosphorylated with the use of 48 % hydrofluoric acid. The differences in the immunomodulatory properties between B.PAT (phosphorylated PS) and B.MAT (dephosphorylated PS) were tested on bone marrow-derived dendritic cells (BMDCs) from BALB/c mice. Finally, to investigate the potential anti-inflammatory functions, both PSs were studied in the Caco-2/HT-29 cell line model of IL-1β-induced inflammation. As expected, B.PAT and B.MAT exhibited distinct properties depending on the presence of the phosphate substitution.

2. Materials and methods

2.1. *Bifidobacterium animalis ssp. animalis CCDM 218 culture*

Ba218, originally isolated from a healthy human fecal sample (Srutkova et al., 2015), was obtained from the Czech Collection of Dairy Microorganisms (CCDM, Laktoflora, Milcom, Tábor, Czech Republic). Bacteria were cultivated on MRS broth (Sigma Aldrich) supplemented with 0.05 % L-cysteine (Merc Millipore) for 72 h at 37 °C under anaerobic conditions (anaerobic chamber, Oxoid, 80 % N_2, 10 % CO_2, 10 % H_2). For bacterial mass collection, Ba218 was centrifuged at 4500 ×*g* (15 min, 4 °C; Hermle Centrifuge Z 36 HK) and washed twice with sterile phosphate-buffered saline (PBS), after which the resulting pellet was frozen and freeze-dried.

2.2. *Polysaccharide isolation and purification*

The Ba218 PSs were isolated as described previously according to the method commonly used in our laboratory (Pacyga-Prus et al., 2023). Briefly, the crude PS mixture was extracted by bacterial incubation in 10 % trichloroacetic acid (2.5 h, RT) and centrifugation (15,000 ×*g*, 4 °C, 20 min; Hermle Centrifuge Z 36 HK). For higher efficiency, the extraction was repeated twice. The collected supernatant was treated with 5 volumes of ethanol and kept overnight at −20 °C. Then, the suspension was centrifuged (15,000 ×*g*, 4 °C, 50 min, Hermle Centrifuge Z 36 HK), dissolved and dialyzed with miliQ water (24 h, 4 °C) (MWCO 6–8 kDa, Roth). The obtained crude mixture was frozen, freeze-dried, and subsequently subjected to ion exchange (DEAE-Sephadex A-25 column; 1.6 × 20 cm (Pharmacia); buffer A: 20 mM Tris-HCl, buffer B: 2 M NaCl; linear-gradient (0 % B – 100 % B); 23 °C) and size exclusion (TSK HQ-55S column; 1.6 × 100 cm (Amersham Pharmacia Biotech);

eluted with 0.1 M ammonium acetate; 23 °C) chromatography with the use of the NGS Chromatography System (Bio-Rad) equipped with a UV detector. To detect sugars, the fractions collected after separations were tested with the phenol-sulfuric acid method (DuBois et al., 1956). Finally, the PS fractions were analyzed using classical chemical methods and NMR spectroscopy.

To obtain a dephosphorylated fraction, 5 mg of B.PAT PS was treated with 48 % hydrofluoric acid for 48 h at 4 °C. Afterward, the dephosphorylated sample (B.MAT) was dialyzed overnight with miliQ water using Slide-A-Lyzer™ Dialysis Cassettes (2 K MWCO, Thermo Scientific). The efficiency of dephosphorylation was assessed by ^{31}P NMR and ^{1}H—^{31}P HSQC NMR experiments.

The average molecular mass of the PS was determined as described previously by GPC (Dionex Ultimate 3000) on an OHpak SB-806 M HQ column (8 × 300 mm, maximum pore size 15,000 Å; Shodex) equipped with a refractive index detector (RI 102; Shodex). Briefly, dextran standards (MW 12, 25, 50, 80, 150, and 270 kDa) were administered on a column together with PS, and 0.1 M ammonium acetate buffer was used as the eluent. The run was performed at 0.5 ml/min. The working detector temperature was 25 °C, and the sensitivity was 512×. Chromeleon software (Dionex) was used for data acquisition and processing (Górska et al., 2016).

Moreover, UV–vis analysis was performed to investigate PS contamination by nucleic acids and proteins (BioPhotometer, Eppendorf).

2.3. Structure analysis

2.3.1. NMR

All NMR data were obtained with a Bruker 600 Hz Avance III spectrometer using a 5 mm QCI probe equipped with a z-gradient. TopSpin 3.1pl6 software was used for data acquisition, while TopSpin 4.0.7 and SPARKY were used for spectra processing (Lee et al., 2015). For analysis, 5 mg of lyophilized PSs were dissolved in deuterium oxide and placed in 5 mm NMR tubes. Each sample was subjected to one- (^{1}H, ^{31}P) and two-dimensional NMR experiments (^{1}H–^{1}H-COSY, ^{1}H—^{1}H TOCSY, ^{1}H—^{1}H NOESY, ^{1}H—^{13}C HSQC, ^{1}H—^{13}C HMBC, ^{1}H—^{31}P HSQC, and ^{1}H—^{13}C HSQC-TOSCY) using pulse sequences from the Bruker library. Several mixing times were used for TOCSY (30, 60, 100 ms) and NOESY (100, 300 ms) experiments. Diffusion-Ordered Spectroscopy (DOSY) was performed using the ledbpgp2s pulse sequence with a diffusion time of 50 ms and a gradient length of 2 ms. All the data were collected at 25 °C, and the chemical shifts of the NMR signals were referenced by using acetone as an internal reference (δ_H 2.225 ppm, δ_C 31.05 ppm). The absolute configurations of the monosaccharides were obtained by comparison of their ^{13}C NMR chemical shifts with reference data (Shashkov, Lipkind, Knirel, Kochetkov, 1988a, 1988b).

2.3.2. Chemical analysis

The monosaccharide content was investigated according to the method of Sawardeker et al. (Sawardeker et al., 1965) with modifications as described in our previous studies (Pacyga-Prus et al., 2023). First, 0.3 mg of PS was hydrolyzed with 10 M HCl (80 °C, 25 min). The nitrogen-dried sample was then reduced by overnight treatment with 10 mg/ml $NaBH_4$ at 10 °C, and the reaction was stopped by adding 80 % acetic acid. Free -OH groups were acetylated with methylimidazole and acetic anhydride. Finally, the sugar residues were extracted with a water : dichloromethane (1:1, *v*/v) mixture, and the organic phase was collected.

The monosaccharide linkage and substitution positions were obtained by methylation analysis. Briefly, NaOH was added to 2 mg of PS in DMSO, and the mixture was sonicated. The sample was then cooled, iodomethane was added, and the mixture was vortexed (3 × 3 min). Then, the neutral pH was restored with 1 M acetic acid, and methylated sugars were extracted 3 times with a mixture of chloroform and water (1:1, v/v) (Ciucanu & Kerek, 1984). The organic phase was collected and dried under a nitrogen stream. Then, the sample was treated with 10 M HCl, reduced with $NaBH_4$, and neutralized with 80 % acetic acid as described for the sugar analysis. The methylated sugars were extracted with a water : dichloromethane (1:1, v/v) mixture, and the organic phase was collected.

The samples obtained after sugar and methylation analyses were dried under a nitrogen stream and kept at 4 °C until further investigation. For gas–liquid chromatography–mass spectrometry (GLC-MS), the samples were dissolved in ethyl acetate. The analysis was performed on an ITQ 700 Thermo Focus GC system equipped with a Zebron ZB-5HT Inferno capillary column (Phenomenex) with a temperature gradient from 150 °C to 270 °C (8 °C/min). All the data were obtained and analyzed with Xcalibur™ software (Thermo Fisher). Additionally, sugar standards were tested with the samples after sugar analysis to verify the monosaccharide content.

2.3.3. Carbohydrate structure database analysis

The structural units of B.PAT and B.MAT were encoded and pasted to the Carbohydrate Structure Database (CSDB) to confirm that their unique structure was not previously described (as of 15.03.2024) (Toukach, 2011). Additionally, a Structure Editor (a part of CSDB) was used to visualize 3D models of the isolated PS (as of 15.03.2024) (Bochkov & Toukach, 2021).

2.4. Mouse cell isolation and stimulation

To investigate the immunomodulatory properties of the isolated PSs, bone marrow dendritic cells (BMDCs) precursors were isolated from 8- to 10-week-old naïve female BALB/c mice according to methods commonly used in our laboratory (Górska et al., 2014; M. J. Pyclik et al., 2021). For the procedure, the mice were euthanized by cervical dislocation after 3 % isoflurane anesthesia. All experiments were performed following the EU Directive 2010/63/EU for animal experiments. Animal experiments were approved by the Committee for the protection and use of experimental animals of the Institute of Microbiology, The Czech Academy of Sciences (No. 91/2019).

BMDCs were prepared as previously described (Górska et al., 2014). Briefly, femurs and tibias were cleaned from skin and muscles, and cells were rinsed from bones with the use of RPMI 1640 medium. Cells were seeded on a Petri dish in an RPMI 1640 medium (4 × 10^6 cells/plate) supplemented with 10 % FBS, 100 U/ml penicillin, 100 μg/ml streptomycin, 10 mM HEPES and 20 ng/ml murine granulocyte-macrophage colony-stimulating factor (GM-CSF, Invitrogen). Precursor cells were differentiated for one week with the addition of fresh medium on the 3rd and 6th day. On the 7th day, BMDCs were collected from Petri dishes, counted, and seeded on a 96-well plate (0.5 × 10^6 cells per well). Next, the cells were treated with the studied PSs (30 and 90 μg/ml) alone or in combination with *Lacticaseibacillus rhamnosus GG* (10:1, bacteria : BMDCs). Non-stimulated cells were used as a negative control, and cells treated with 1 μg/ml ultra-pure LPS (Invivogen) served as a positive control. BMDCs were incubated for 20 h at 37 °C and 5 % CO_2. The levels of the cytokines IL-10, IL-6, IL-12p70, and TNF-α in culture supernatants were detected with ELISA (Ready-Set-Go! Kits (eBioscience) according to the manufacturer's instructions. Moreover, cells after stimulation with B.PAT and B.MAT (30 μg/ml and 120 μg/ml) were subjected to cytotoxicity analysis *via* the SRB assay (Vichai & Kirtikara, 2006). Briefly, after stimulation, the cells were fixed with 10 % trichloroacetic acid and left at 4 °C for 1 h. Next, the plate was washed four times with water, and 0.06 % sulforhodamine B was added to dye the cells (30 min, RT, in darkness). Finally, the plate was washed four times with 1 % acetic acid to remove the excess dye, and the remaining protein-bound reagent was dissolved in 10 mM Tris base solution (pH = 10.5). Finally, the absorbance was read at 490, 510, and 530 nm.

2.5. Human cell lines stimulation in the IL-1β inflammatory model

The adherent, immortalized epithelial cell lines of male human colorectal adenocarcinoma (Caco-2) and the female human, adherent, immortalized epithelial colon cancer cell line (HT-29) were used (after the 10th passage) to test the potential anti-inflammatory properties of B. PAT and B.MAT. First, 0.5 × 10^6 cells/well were seeded on a 12-well plate in DMEM/F12 (Gibco) supplemented with 10 % FBS (Gibco) and a 1 % L-glutamine-Penicillin-Streptomycin solution for HT-29 cells, and EMEM/DMEM high glucose (Sigma Aldrich) supplemented with 10 % FBS, 1 × non-essential amino acids (100 × concentrated, Sigma Aldrich), and 10 mM HEPES (Sigma Aldrich) for Caco-2 cells. After, the Caco-2 cells were incubated for 24 h, and the HT-29 cells were allowed to adhere to the plate for 48 h.

2.5.1. Prophylactic model

The cells adherent to the plate were stimulated with B.PAT and B. MAT at a 10 μg/ml concentration. The cells were incubated for 18 h (37 °C, 5 % CO_2). Then, 10 ng/ml IL-1β was added to the cells, and after an additional 18 h of incubation (37 °C, 5 % CO_2), the media above the cells were collected and frozen. Finally, to measure the levels of IL-8 in culture supernatants, an ELISA Ready-Set-Go! Kit (BD Biosciences) was used according to the manufacturer's instructions.

2.5.2. Therapeutic model

The cells adherent to the plate were stimulated with 10 ng/ml IL-1β. The cells were incubated for 18 h (37 °C, 5 % CO_2). Then, B.PAT and B. MAT were added to the cells, and an additional 18 h of incubation (37 °C, 5 % CO_2) was performed. The media above the cells were collected and frozen. Finally, to measure the levels of IL-8 in culture supernatants, an ELISA Ready-Set-Go! Kit (BD Biosciences) was used according to the manufacturer's instructions.

2.6. Statistical analysis

All experiments were repeated with at least two technical and two biological repetitions. The data were presented as the mean ± SD and differences were analyzed with an unpaired *t*-test. All the statistical analyses and visualizations were prepared with Graph Pad Prism version 9.

3. Results

3.1. Structural analysis of B.PAT polysaccharide

B.PAT was separated from a complex PS blend that was isolated from the surface of the Ba218 strain. The crude PS mixture was submitted to ion exchange and size exclusion chromatography and subsequently analyzed by NMR spectroscopy. This led to the determination of the three distinct PS fractions. The ^{31}P NMR spectra showed that B.PAT was the only PS containing phosphorus in its structure. Since the main idea behind this study was to investigate changes in the immunomodulatory properties of phosphorylated PSs and their dephosphorylated counterparts, the phosphate-substituted B.PAT was selected for further experiments.

Sugar analysis indicated that B.PAT consists of L-Rha, D-Glc, and D-Gal in a molar ratio of 1:1.5:3. An average molecular mass of *ca.* 1.96 × 10^4 Da was determined.

Analysis of the ^{1}H—^{13}C HSQC spectrum showed 12 cross peaks in the anomeric region. Since some of the signals in the ^{1}H NMR spectrum and in the 2D HSQC spectrum were significantly broader than others, DOSY experiments that allow the separation of molecules based on their different sizes or mobilities were performed (Fig. 1, Supplementary Fig. S1).

The DOSY spectra showed that the B.PAT PS consists of a non-asaccharide repeating unit with 8 hexapyranosyl and 1 hexafuranosyl residues as determined from the ^{1}H—^{13}C HSQC NMR spectrum (Fig. 2).

The structure of the PS was obtained from analysis of the 2D NMR spectra, including COSY, TOCSY, and NOESY at several mixing times, HSQC, HSQC-TOCSY, and HMBC (Supplementary Fig. 2–5). In Table 1, the sugar residues of B.PAT are marked with an uppercase letter starting from the most downfield signal in the ^{1}H NMR spectrum.

Analysis of the TOCSY and HSQC-TOCSY spectra allowed us to determine the type of sugar residues constituting B.PAT. Residue A was assigned as a hexafuranose due to the strong downfield shift of the anomeric carbon signal with the *galacto*-configuration. For residues B, C, E, and F, the characteristic methyl resonances of 6-deoxy sugars were observed at 1.28, 1.33, 1.32, and 1.26, respectively. In the TOCSY spectra, only one cross-peak was found between H1 and H2 of those residues, indicating that they are rhamnoses. Therefore, the spin systems for residues B, C, E, and F were obtained from the TOCSY and HSQC-

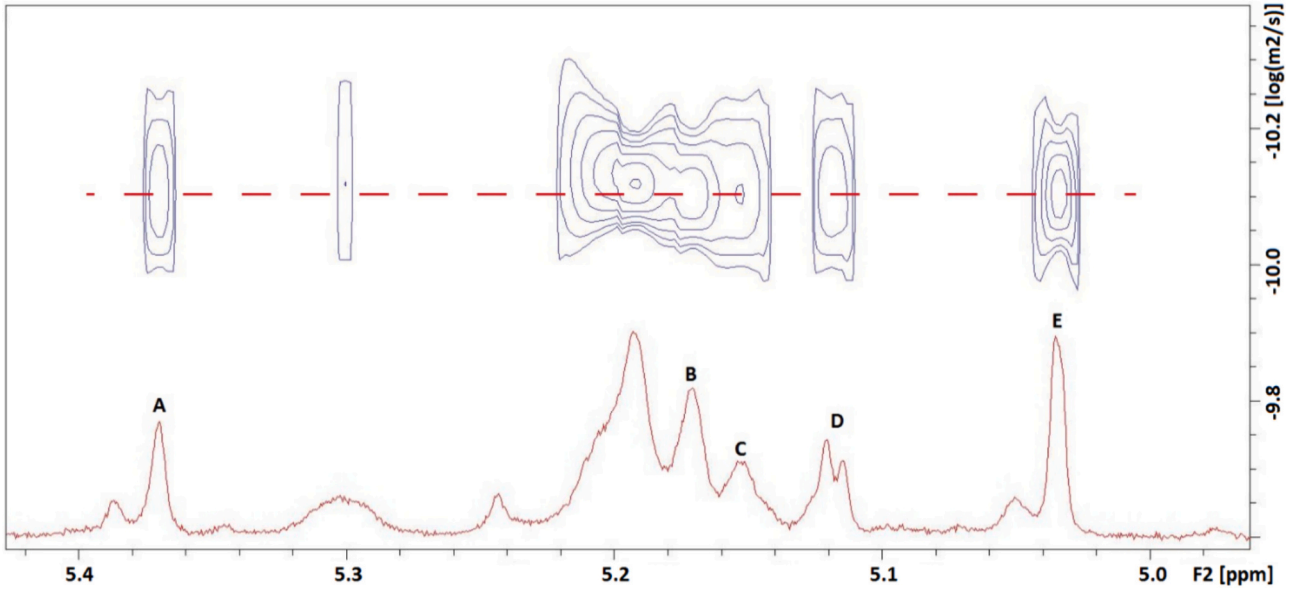

Fig. 1. A part of the DOSY spectrum of B.PAT showing the anomeric region of the PS (blue). The experimental ^{1}H NMR spectrum is shown in red. Signals on the same level (red, dashed line) belong to B.PAT structure (marked as A-E).

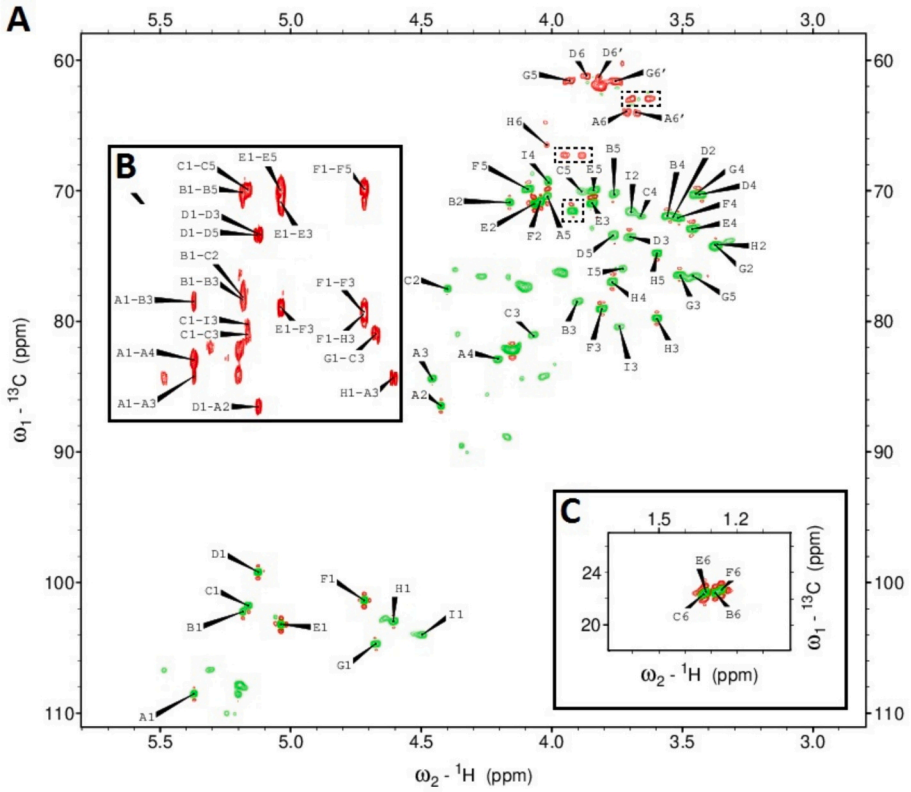

Fig. 2. A. Part of the $^{1}H—^{13}C$ HSQC NMR spectrum of B.PAT at 25 °C. The anomeric signals are located in the chemical shift range of 4.2–5.8 ppm and the ring signals are between 3.2 and 4.5 ppm. The black dashed line indicates the signals corresponding to the glycerol substitution. B. The part of the HMBC spectrum corresponds to the anomeric signals in the HSQC spectra. C. H-6/C-6 signals for rhamnoses (residues B, C, E, and F).

TOCSY spectra using the methyl groups as starting points. An analysis of scalar correlations for residues D, G, and H showed resonances characteristic for the *gluco*-configuration. Finally, residue I was assigned to the *galacto*-configuration since the analysis of the TOCSY and HSQC-TOCSY spectra showed scalar correlations from the anomeric signal only until the H4/C4 resonance. The H5/C5 chemical shifts for residue I were determined from the connectivity between H3 and H5 in the NOESY spectra and from the connectivity between H1 and C5 in the HMBC spectrum.

The anomeric configuration of residue A was identified as β due to the downfield shift of the anomeric carbon lower than δ 105 ppm, which is observed only for the β-configuration of galactofuranoside (Gorin & Mazurek, 1975; Nagaoka et al., 1996). For the rhamnoses (residues B, C, E, and F) the $^{3}J_{H1H2}$-values were small (< 3.0 Hz) and not resolved in the NMR spectra due to line broadening and therefore could not be used to determine the anomeric configuration. However, it has been shown that the chemical shift of the C5 signal can be used to distinguish between α- or β-linkages. The C5 resonance at δ 70.5 ppm indicates the α-configuration, while the C5 resonance at δ 73.2 ppm is attributed to the β-configuration (Carillo et al., 2009; Lipkind et al., 1988; Mattos et al., 2001; Senchenkova et al., 1999; Vinogradov et al., 2003). Since residues B, C, E, and F have C5 resonances <70.5 ppm, they were assigned as α-rhamnoses. The α-configuration was also confirmed by the absence of intraglycosidic NOEs between H1 and H3, H5 (Vinogradov et al., 2003). The glucose residues G, H, and galactose I have $^{3}J_{H1H2}$-values >7 Hz, indicating a β, while residue D, with a small $^{3}J_{H1H2}$-value of 3 Hz, was assigned an α. The chemical shift of C6 from the H residue could not be assigned unambiguously due to the lack of scalar connectivities between H5/C5 and H6/C6. The reason might be that the C-6 substitution by glycerol phosphate affects the conformation around the C5-C6 bond.

The connections between the monosaccharides in the B.PAT unit were determined from NOESY and HMBC spectra (Table 2). The glycosylation pattern was further confirmed by the downfield shift of signals belonging to C2 and C3 of Gal*f* (A), C3 of Rha*p* (B), C2 and C3 of Rha*p* (C), C3 of Rha*p* (F), C3 and C4 of Glc*p* (H), and C3 of Gal*p* (I) compared to those of the non-substituted sugars. Moreover, a strong downfield shift was observed for the C6 signal of Glc*p* (H), indicating substitution at this position. Analysis of the $^{1}H—^{13}C$ HSQC spectrum together with the $^{1}H—^{31}P$ HSQC spectrum revealed that phosphorus substituted both glycerol at 3.95 and 3.88 ppm (δ 67.3 ppm, glycerol) and H6 at 4.02 and 4.07 ppm (δ 66.4 ppm, residue H).

The absolute configuration of B.PAT monosaccharide moieties was tentatively obtained from the ^{13}C NMR chemical shifts and compared with reference data (Shashkov, Lipkind, Knirel, Kochetkov, 1988a). Thus, the following sequence for the B.PAT's repeating unit was proposed: →2)-[β-D-Glc*p*-(1 → 3)-]α-L-Rha*p*-(1 → 3)-β-D-Gal*p*-(1 → 4)-[D-Gro(→P → 6)-,α-L-Rha*p*-(1 → 3)-]α-L-Rha*p*-(1 → 3)-]β-D-Glc*p*-(1 → 3)-[α-D-Glc*p*-(1 → 2)-]β-D-Gal*f*-(1 → 3)-α-L-Rha*p*-(1→, or with the uppercase letters: [G-]C-I-[Gro-P-,*E*-F-]H-[D-]A-B. The obtained structure was consistent with the methylation analysis results, thus, the proposed structure of the repeating unit was proposed (Fig. 3).

To better understand the influence of phosphorylation on B.PAT, it underwent dephosphorylation for 48 h at 4 °C. The dephosphorylation process was confirmed by ^{31}P NMR experiments. Analysis of 2D NMR spectra allowed us to assess the impact of glycerol phosphate on B.PAT structure (Fig. 4).

Dephosphorylation of B.PAT did not affect the main chain of PS. Differences between the B.PAT and B.MAT structures focus on residue H only and lead to changes in the HSQC, TOCSY, and HSQC-TOCSY spectra, confirming that phosphorylation is related to this sugar in B.PAT's repeating unit (Table 3). However, even after dephosphorylation, chemical shifts for C6 of residue H could not be assigned unambiguously.

Moreover, a search in an online database (CSDB) confirmed that the

Table 1
^{1}H and ^{13}C NMR chemical shifts of the resonances of B.PAT from *Bifidobacterium animalis* ssp. *animalis* CCDM 218.

		^{1}H, ^{13}C chemical shifts (ppm)					
Sugar residue		H-1, C-1	H-2, C-2	H-3, C-3	H-4, C-4	H-5, C-5	H-6, H-6′ C-6
A	→2,3)-β-D-Gal*f*-(1→	5.37 108.5	4.42 86.5	4.45 84.4	4.21 82.9	4.02 70.4	3.71, 3.67 64.0
B	→3)-α-L-Rha*p*-(1→	5.18 102.2	4.16 70.9	3.90 78.5	3.54 71.9	3.76 70.3	1.28 17.5
C	→2,3)-α-L-Rha*p*-(1→	5.16 101.8	4.4 77.5	4.07 81.0	3.66 72.0	3.89 70.1	1.33 17.6
D	α-D-Glc*p*-(1→	5.12 99.2	3.56 71.9	3.70 73.5	3.44 70.3	3.76 73.4	3.82, 3.86 61.3
E	α-L-Rha*p*-(1→	5.04 103.2	4.07 71.0	3.85 70.9	3.46 72.9	3.84 70.0	1.32 17.5
F	→3)-α-L-Rha*p*-(1→	4.72 101.3	4.04 70.8	3.81 79.0	3.52 72.1	4.09 69.8	1.26 17.3
G	β-D-Glc*p*-(1→	4.68 104.7	3.37 74.2	3.51 76.4	3.44 70.3	3.46 76.6	3.75, 3.93 61.6
H	→3,4,6)-β-D-Glc*p*-(1→	4.61 103.0	3.37 74.2	3.60 79.7	3.77 77.0	3.60 74.8	4.02, 4.07 66.4
I	→3)-β-D-Gal*p*-(1→	4.5 104.0	3.7 71.6	3.74 80.4	4.01 69.3	3.73 76.0	
	Glycerol phosphate	3.69, 3.63 62.9	3.92 71.5	3.95, 3.88 67.3			
	^{31}P	0.7					

Table 2
Selected inter-residue correlations from ^{1}H—^{1}H NOESY and ^{1}H—^{13}C HMBC spectra of B.PAT.

		H-1 / C-1	Connectivity to		Inter-residue
	Residue	δ_H / δ_C	δ_C	δ_H	Atom / Residue
A	→2,3)-β-D-Gal*f*-(1→	5.37 / 108.5	78.5	3.90	C-3, H-3 of B
B	→3)-α-L-Rha*p*-(1→	5.18 / 102.2	81.0	4.07	C-2, H-2 of C
C	→2,3)-α-L-Rha*p*-(1→	5.16 / 101.8	80.4	3.74	C-3, H-3 of I
D	α-D-Glc*p*-(1→	5.12 / 99.2	86.5	4.42	C-2, H-2 of A
E	α-L-Rha*p*-(1→	5.04 / 103.2	79.0	3.81	C-3, H-3 of F
F	→3)-α-L-Rha*p*-(1→	4.72 / 101.3	79.7	3.60	C-3, H-3 of H
G	β-D-Glc*p*-(1→	4.68 / 104.7	81.0	4.07	C-3, H-3 of C
H	→3,4,6)-β-D-Glc*p*-(1→	4.61 / 103.0	84.4	4.45	C-3, H-3 of A
I	→3)-β-D-Gal*p*-(1→	4.5 / 104.0	70.8	4.04	C-4, H-4 of H
	Glycerol phosphate	3.95, 3.88 / 67.3	66.4	4.02, 4.07	C-6, H-6 of H

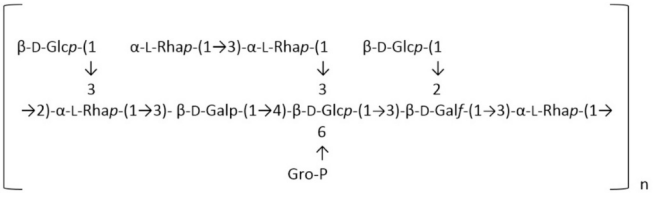

Fig. 3. Structure of the nonasaccharide repeating unit of B.PAT. The approximate number of units in B.PAT equals $n = 7$.

structure of B.PAT and B.MAT were not described previously. The CSDB Structure Editor allowed the prediction of 3D models of both PSs variants. The obtained 3D models indicate that the loss of Gro-P in dephosphorylated PS affects the spatial structure of B.PAT with a more open structure, which may influence the differences in the properties of both PSs (Fig. 5).

Finally, UV–vis analysis was performed to ensure that the PS fractions were free of nucleic acid and protein contamination (Supplementary Table T1).

3.2. Distinct immunomodulatory properties of B.PAT and B.MAT

A strong, dose-dependent production of TNF-α, IL-6, and IL-10 cytokines was the result of BMDCs stimulation with B.MAT (Fig. 6A). Furthermore, B.MAT was the only one able to induce IL-12 production at 90 μg/ml. B.PAT, on the other hand, induced low levels of IL-6 and TNF-α without inducing IL-10 or IL-12 production. To confirm the distinct modulatory properties of B.PAT and B.MAT, BMDCs were stimulated with a strain known for its immunomodulatory properties – *Lacticaseibacillus rhamnosus* GG – with the addition of the studied compounds (Fig. 6B). Both B.PAT and B.MAT were able to enhance cells' response to stimulation with the selected strains in a dose-dependent manner for isolated PSs as well as in favor of the dephosphorylated compound. A significantly greater production of TNF-α (** $p \leq 0.01$) was observed for B.MAT at the highest concentration in comparison to B.PAT (when stimulated with a lactobacilli strain). Moreover, B.MAT at 90 μg/ml in the same variant of the experiment showed a stronger tendency than B.PAT to intensify IL-12 and IL-10 production. No differences in enhancing lactobacilli strain immunomodulatory properties were observed for either PS for IL-6 levels.

Moreover, the viability assay confirmed the safety of B.PAT and B.MAT, since the survival rate did not significantly differ between the control cells (untreated cells, 100 %) and the cells treated with the tested PSs (Supplementary Fig. S6).

3.3. Dephosphorylation enhances the anti-inflammatory properties of B.PAT

To fully understand the potential of B.PAT and B.MAT, their anti-inflammatory properties were tested in Caco-2 and HT-29 cells. Both cell lines are widely used as models of the intestinal epithelial barrier in which inflammation is induced with the use of IL-1β. Isolated PSs were administered before (prophylactic) or after (therapeutic) IL-1β treatment to investigate their possible role in the prevention or treatment of inflammatory responses. Notably, the phosphorylated compound was able to inhibit the development of inflammatory responses in prophylactic settings, which resulted in lower levels of IL-8 in both HT-29 cells and Caco-2 cells. Dephosphorylation significantly enhanced the ability of B.PAT to prevent inflammation by even stronger suppression of IL-8 production in both cell lines (** $p \leq 0.01$ for HT-29 cells and * $p \leq 0.05$ for Caco-2 cells). Moreover, B.MAT showed a tendency to reduce IL-8 production in HT-29 cells in therapeutic settings after stimulation with IL-1β (Fig. 7) ($p = 0.09$, in comparison to the IL-1β control).

4. Discussion

The presented study was based on the idea that modifications of PSs can greatly influence their functions. To prove this hypothesis, PSs were isolated from the surface of *Bifidobacterium animalis* ssp. *animalis* CCDM 218 and purified by chromatography methods. The obtained fractions were subjected to NMR analysis, which showed that one of the structures, B.PAT, is phosphorylated. The first step in understanding the presence of phosphorus on B.PAT was to determine the PS structure. Studies of human-derived *Bifidobacterium* strains have shown that the typical size of bifidobacterial PSs is between 10^4 and 10^6 Da and that the most common sugars that build a PS chain unit are glucose, galactose,

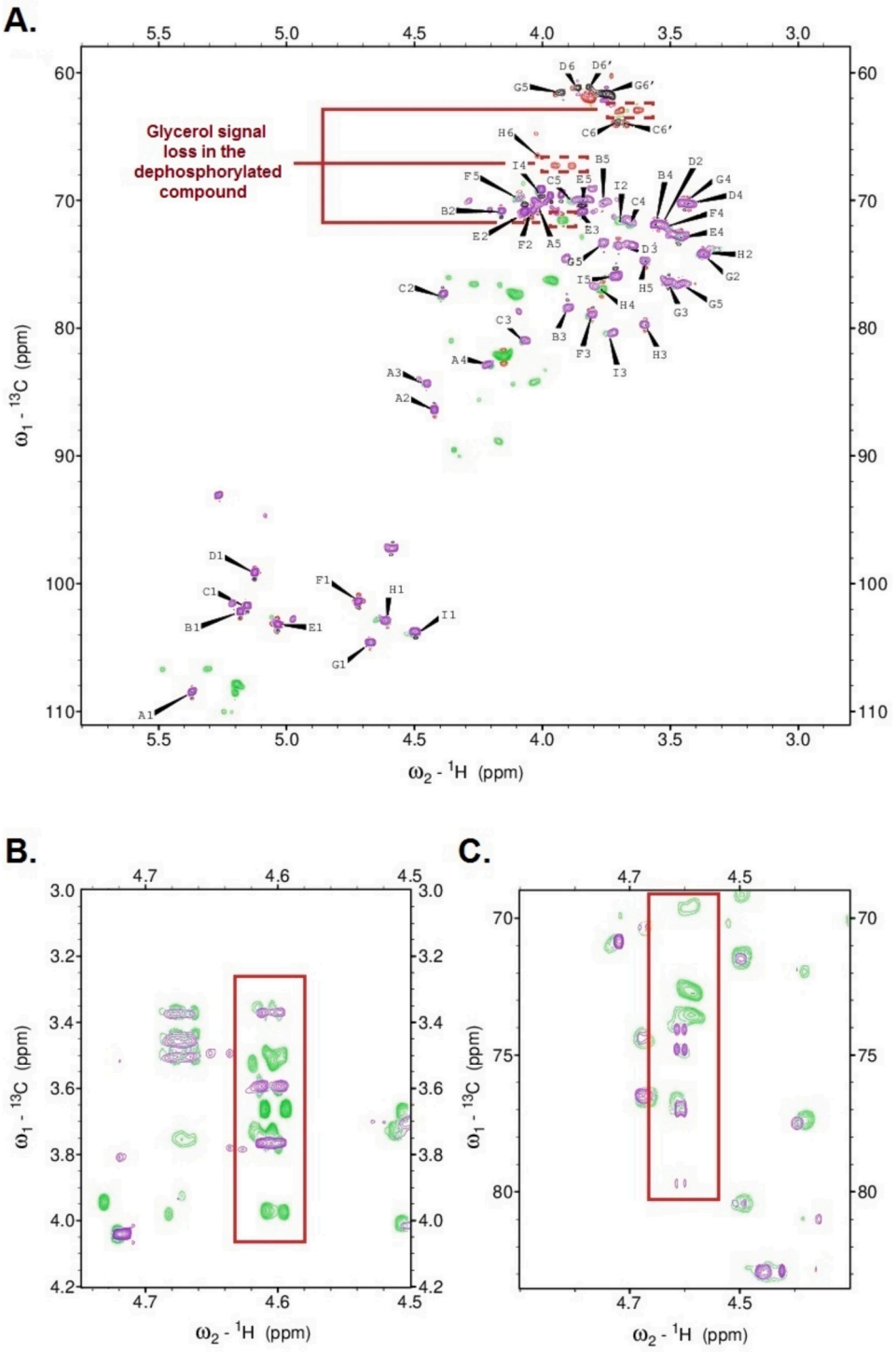

Fig. 4. Differences between B.PAT and B.MAT. A. Overlapped $^{1}H—^{13}C$ HSQC spectra of B.PAT and B.MAT. There is a loss of glycerol signals (red, dashed line) in the dephosphorylated compound, as well as a loss of additional signals present in B.PAT. B. Overlapped TOCSY spectrum of the residue H region of B.PAT and B.MAT (red box). C. Overlapped HSQC-TOCSY spectrum of residue H region of B.PAT and B.MAT (red box). The green and red spectra correspond to B.PAT, while purple and black ones – to B.MAT.

and rhamnose (Salazar et al., 2009). B.PAT is a small PS of 1.96×10^4 Da, and sugar analysis revealed the presence of only glucose, galactose, and rhamnose in its structure. The small size of the PS may be the first indicator of its possible properties. As described previously by Górska et al. (2014), PSs with small molecular sizes are associated with pro-inflammatory responses, while PSs with high molecular masses exhibit regulatory properties (Górska et al., 2014). Given the relatively small molecular mass of our PSs, we also considered them to have pro-inflammatory properties. In contrast to the findings of Górska et al., our results obtained in the IL-1β inflammatory model showed prophylactic effects of both B.PAT and B.MAT, indicating their anti-inflammatory effect. Therefore, the function of PS might be based not only on its size and sugar composition but also on the molar ratio of its components, the order of sugars in a PS chain unit, the spatial structure, and, most importantly, on the non-sugar substitutions of the PS chain. The structure determination of B.PAT revealed a highly branched PS

Table 3
Comparison of the B.PAT's and B.MAT's differences in chemical shifts for residue H.

Sugar residue		^{1}H, ^{13}C chemical shifts (ppm)					
		H-1, C-1	H-2, C-2	H-3, C-3	H-4, C-4	H-5, C-5	H-6, H-6' C-6
B.PAT							
H	→3,6)-β-D-Glc*p*-(1→	4.61 103.0	3.37 74.2	3.60 79.7	3.77 77.0	3.60 74.8	4.02, 4.07 66.4
B.MAT							
H	→3)-β-D-Glc*p*-(1→	4.61 102.9	3.36 73.8	3.6 79.7	3.80 76.75	3.54 71.82	

with 4 rhamnose, 3 glucose, and 1 galactose residues in the pyranose form, and 1 galactose residue in the furanose form. Most of its sugar residues have an alpha configuration, and there is a majority of 1 → 3 glycosidic bonds that positively influence the flexibility of PS and may result in increased anti-microbial and anti-oxidant properties (Laws et al., 2001; Zhou et al., 2019). Moreover, chemical modifications can greatly improve the spatial configuration of PS and influence its physiological properties and functions. There is a broad spectrum of modifications that can occur on the PS chain, including acetylation, sulfation, and phosphorylation. B.PAT was found to be substituted by glycerol phosphate connected to β-D-Glc*p* (residue H) at the 6th position. Phosphorylated PSs, such as B.PAT, are not abundant in nature, and the degree of substitution in a phosphorylated PS is usually low. Phosphorus-containing PSs are often more complex, and their structure is difficult to determine (Laffargue et al., 2023). There are even fewer examples of glycerol phosphate substitutions in bacterial PSs. Edgar et al. (2019) described *Streptococcus mutans* rhamnose PSs that contain glycerol phosphate modifications on approximately 25 % of the GlcNAc residues (Edgar et al., 2019). Furthermore, Speciale et al. (2019) described an 8 × 10^4 Da phospho-glycero-β-galactofuronian (PGβG) substituted by glycerol phosphate at the 6th position and produced by *Bifidobacterium bifidum* PRI1 (Speciale et al., 2019).

To better understand the role of glycerol phosphate substitution on B.PAT, the PS was dephosphorylated. Comparison of NMR data for B.PAT (with phosphorus) and B.MAT (after dephosphorylation) showed that dephosphorylation caused significant changes in the chemical shifts of the carbons belonging to the residue, which is consistent with the literature data (Fig. 4, Table 3) (Kołodziejska et al., 2006; Speciale et al., 2019). Further investigation of the 3D models predicted by the Structure Editor showed that the loss of glycerol phosphate substitution may result in spatial changes in isolated PSs, and the structure became less condensed since the H residue lost its substitution at the C6 position (Fig. 5). This may be the cause of better recognition of B.MAT and increased cytokine production in the tested cells.

Liu et al. (2023) discussed in detail the impact of phosphorylation on PSs and emphasized that adding phosphorus to the structure can lead to spatial changes and affect PSs function (Liu et al., 2023). Few publications have compared the functions of phosphorylated and dephosphorylated PSs. Even fewer studies have expanded their research by structure investigation. The majority of related research indicates that the phosphorylation of PSs results in an improvement in their activity. Neutral (NPS) and phosphorylated (APS) PSs were described for *Lactobacillus delbrueckii* ssp. *bulgaris* OLL1073E-1. Both consist of the same structure with galactose and glucose residues in a molar ratio of 3:2 (Nishimura-Uemura et al., 2003). The only difference was the presence of 0.1 % phosphorus in the APS fraction. Studies performed on the mouse macrophage-like cell line J774.1 revealed that APS is a stronger immunomodulator than NPS, as it can significantly increase IL-6, IL-10, and IL-12p40 while decreasing IL-12p35 levels. To prove that the effect of APS is caused by the presence of phosphorus substitution, APS was subjected to dephosphorylation, which led to the inhibition of its mitogenic and cytostatic activity (Nishimura-Uemura et al., 2003). Another immunomodulatory effect was observed by Makino et al. (2006), who isolated neutral (NPS) and phosphorylated (H-APS) high molecular mass PSs from the same strain as Nishimura-Uemura et al. These PSs consisted of glucose, galactose, mannose, and xylose (for NPS) and glucose, galactose, and 0.01 % phosphorus substitution (for H-APS). In C3H/HeJ mouse spleen cells, compared with NPS, APS caused a significant increase in IFN-γ. Moreover, *in vivo* analysis of murine splenocytes isolated from BALB/c mice previously administered with H-APS revealed a dose-dependent increase in NK cell induction. Furthermore, compared with the control treatment, treatment with concanavalin A positively affected the production of IFN-γ and the inhibition of IL-4 (Makino et al., 2006). Another interesting example is the introduction of phosphorus to dextran at a degree level of 1.7–2 %. It induced mitogenic activity in mouse splenocytes. In addition, it was able to induce the expression of CD86 as well as the gene expression of IL-10 and IFN-γ in comparison to non-phosphorylated dextran (Sato et al., 2004). However, dephosphorylation is not always associated with the suppression of PS function. Speciale et al. (2019) isolated surface PSs from *Bifidobacterium bifidum* PRI1 that led to the purification of structurally different fractions. The first fraction contained at least 4 different β-glucan/galactan PSs with an average molecular mass of 4 × 10^4 Da (CSGG). The second one was determined to be phosphor-glycero-β-galactofuronian (PGβG), which has an average molecular mass of 8 × 10^4 Da. Studies investigating CSGG and PGβG activities have shown that the neutral fraction can induce Foxp3$^+$ cells in spleen-derived mouse DCs. Moreover, CSGG improved the production of IL-10, suggesting that this PS has regulatory properties (Speciale et al., 2019). This effect was confirmed by Verma et al. (2018), who described the suppressive effect of this PS on the development of colitis in mice. In contrast, the

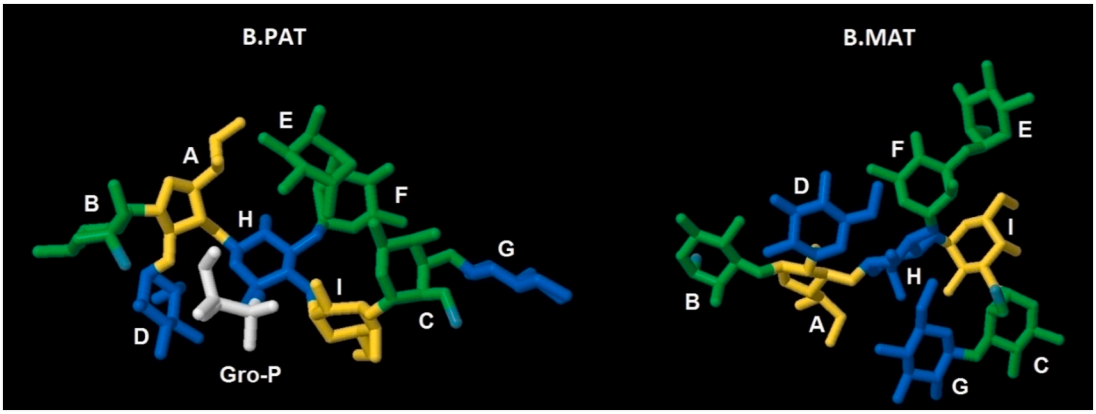

Fig. 5. 3D models of B.PAT and B.MAT predicted by CSDB Structure Editor. After dephosphorylation, the spatial structure of B.PAT is significantly changed.

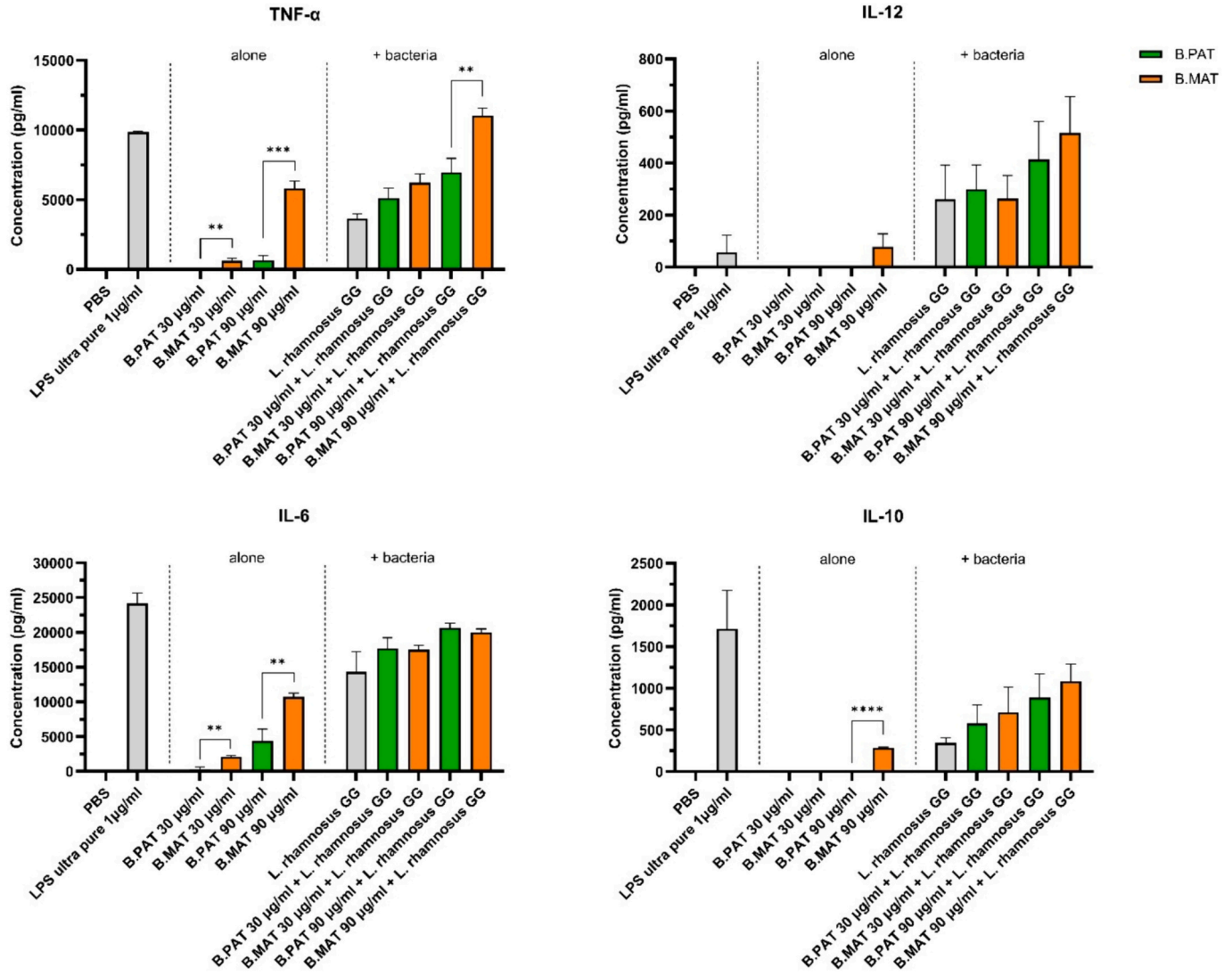

Fig. 6. Cytokine production after immune cells stimulation with B.PAT and B.MAT. Mouse BMDCs stimulation with PBS (negative control), LPS ultra-pure (positive control, Invivogen), or PSs at a concentration of 30 and 90 μg/ml alone or with the addition of *Lacticaseibacillus rhamnosus* GG. B.PAT was marked in green, while B. MAT was marked in orange. An unpaired *t*-test was performed, and significant differences between phosphorylated and dephosphorylated compounds (90 μg/ml) were calculated (**** $p \leq 0.0001$, *** $p \leq 0.001$, ** $p \leq 0.01$).

phosphorylated fraction did not affect Foxp3^{+} expression, however, it was able to significantly increase IFN-γ levels, while IL-10 remained unaffected. This may indicate that, unlike regulatory CSGG, it has potential pro-inflammatory properties (Verma et al., 2018). Stimulation of mouse BMDCs with isolated PS resulted in significantly greater production of IL-10, IL-6, and TNF-α in response to B.MAT (90 μg/ml) than in response to B.PAT. More interestingly, B.MAT also induced the production of IL-12 at 90 μg/ml, while at the same time, B.PAT was not able to induce either IL-12 or IL-10 at any of the tested doses (Fig. 6A).

To investigate the abilities of B.PAT and B.MAT to enhance the function of known immunomodulators, BMDCs were stimulated with *Lacticaseibacillus rhamnosus* GG, which is known for its health-promoting properties (Capurso, 2019). Both PSs dose-dependently strengthened the effect of the whole bacteria. However, greater cytokine production was observed after the addition of dephosphorylated PS, which is consistent with previous results (Fig. 6B). In the case of IL-10 and IL-12 production, B.PAT alone was not capable of inducing high levels of these cytokines at the tested doses. Simultaneously, B.MAT induced low IL-10 and IL-12 levels at 90 μg/ml. However, stimulation with lactobacilli proved that both PSs can act as costimulators of different antigens, improving the effect of other known immunomodulators. Górska et al. (2014) described two PSs from *Lacticaseibacillus rhamnosus* LOCK 900 (Górska et al., 2014). Both were negatively charged, but L900/2 was a large (8.3×10^6 Da), pyruvylated, branched PS with 7 monosaccharide residues, and L900/3 was a small ($1{,}8 \times 10^4$ Da) PS containing 5 monosaccharides and phosphomonoester substitution. Both PSs were tested in mouse BMDCs together with *Lactobacillus plantarum* WCFS-1. The results showed that the high molecular weight L900/2 PS increased IL-10 production, whereas the small molecular weight L900/3 PS increased IL-12p70 cytokine levels, compared to the strain alone. Thus, the authors indicated that L900/2 might be a possible anti-inflammatory factor in conditions such as inflammatory bowel disease, while L900/3 could play a role in the treatment of allergies (Górska et al., 2014).

To investigate the possible anti-inflammatory properties of isolated PSs, the IL-1β-induced inflammation model was used in Caco-2 and HT-29 human cell lines. IL-1β is known to impair the integrity of intestinal epithelial cells and to enhance the inflammatory response by upregulating IL-8 cytokine production (Al-Sadi & Ma, 2007; Sunil et al., 2010). The addition of isolated PSs prevented the outburst of IL-8 in both HT-29 cells and Caco-2 cells. Interestingly, the dephosphorylated compound had a significantly stronger downregulatory effect on IL-8 production,

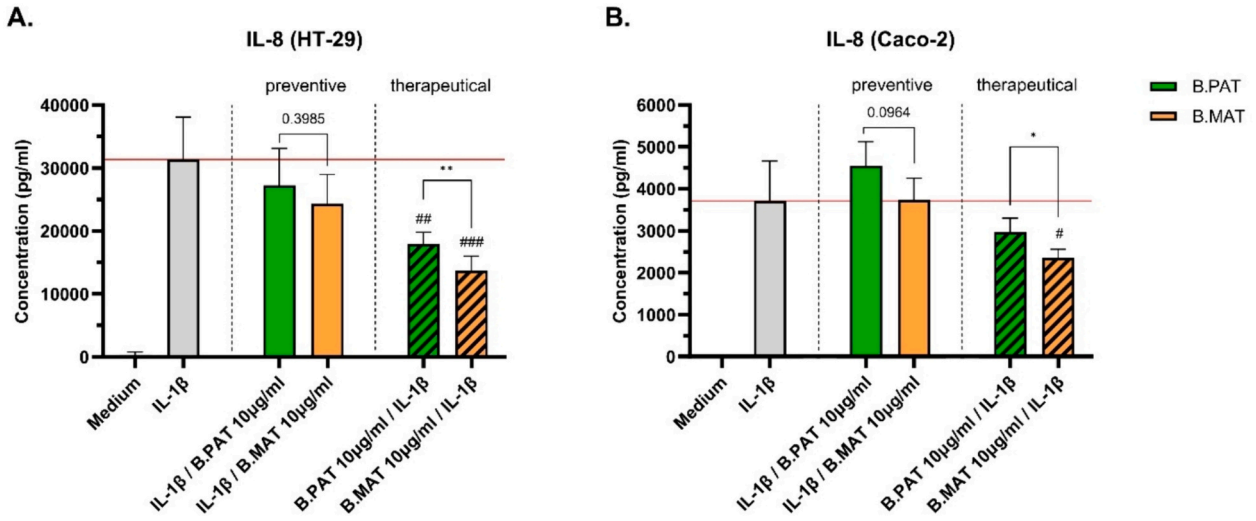

Fig. 7. IL-8 cytokine production after cell lines stimulation with B.PAT and B.MAT. A. Stimulation of HT-29 cell line with tested PS before (preventive) or after (therapeutical) the induction of inflammation with IL-1β. B. Stimulation of Caco-2 cell line with tested PS before (preventive) or after (therapeutical) the induction of inflammation with IL-1β. B.PAT is marked in green, while B.MAT is marked in orange. The red line shows the level of IL-8 after cell treatment with IL-1β only (positive control). An unpaired t-test was performed, and significant differences between phosphorylated and dephosphorylated compounds were calculated (** $p \leq 0.01$, * $p \leq 0.05$). Significance in comparison to positive control was marked with # (### $p \leq 0.001$, ## $p \leq 0.01$, # $p \leq 0.05$).

indicating its anti-inflammatory effects in the presented model.

The immunomodulatory properties of the presented PSs and, in particular, the dephosphorylated B.MAT molecule show potential for future use in the prevention or treatment of various diseases. The greatest advantages of these molecules are the well-described structures introduced in this research. Moreover, the knowledge presented in this manuscript provides a strong foundation for future detailed structure–function investigations, which are not possible for whole microorganisms. This approach also provides opportunities for *in vivo* studies. In comparison to probiotics, postbiotics lack virulence factors and cannot transfer antibiotic resistance genes. Overall, their high stability, efficient and easy isolation, and definable structure make them perfect alternatives to probiotics (Rafique et al., 2023).

5. Conclusions

In this work, we comprehensively studied a glycerol phosphate-substituted polysaccharide (PS) called B.PAT isolated from *Bifidobacterium animalis* ssp. *animalis* CCDM 218 and thoroughly described its structure. To fully understand the immunomodulatory potential of B.PAT, we investigated the biological activities of this compound and its dephosphorylated counterpart – B.MAT. The results showed that dephosphorylation strongly influenced the spatial structure of B.PAT. Moreover, studies of BALB/c mouse BMDCs indicated the possible immunomodulatory potential of B.MAT that is stronger than that of B.PAT. Further experiments performed on Caco-2 and HT-29 cells in an IL-1β-induced inflammation model showed the enhanced effect of B.MAT to prevent the development of an inflammatory response. Therefore, our results demonstrated that the dephosphorylation of PSs does not have to be associated with the suppression of PS's function but may also be responsible for the enhancement of the existing properties and different functionalities depending on the tested model.

Funding

This work was supported by the National Science Centre of Poland (UMO-2017/26/E/NZ7/01202); and the Ministry of Education, Youth and Sports of the Czech Republic (CZ.02.01.01/00/22_008/0004597).

CRediT authorship contribution statement

Katarzyna Pacyga-Prus: Writing – original draft, Visualization, Resources, Methodology, Investigation, Formal analysis. **Corine Sandström:** Writing – review & editing, Investigation. **Dagmar Šrůtková:** Writing – review & editing, Resources. **Martin Schwarzer:** Writing – review & editing, Supervision, Resources. **Sabina Górska:** Writing – review & editing, Validation, Supervision, Project administration, Funding acquisition, Conceptualization.

Declaration of competing interest

The authors declare that they have no known competing financial interests or personal relationships that could have appeared to influence the work reported in this paper.

Data availability

Data will be made available on request.

Acknowledgments

Graphical abstract was created using BioRender online software (https://biorender.com/).

Appendix A. Supplementary data

Supplementary data to this article can be found online at https://doi.org/10.1016/j.carbpol.2024.122518.

References

Al-Sadi, R. M., & Ma, T. Y. (2007). IL-1β causes an increase in intestinal epithelial tight junction permeability. *The Journal of Immunology, 178*(7), 4641–4649. https://doi.org/10.4049/jimmunol.178.7.4641

Angelin, J., & Kavitha, M. (2020). Exopolysaccharides from probiotic bacteria and their health potential. *International Journal of Biological Macromolecules, 162*, 853–865. https://doi.org/10.1016/j.ijbiomac.2020.06.190

Bazaka, K., Crawford, R. J., Nazarenko, E. L., & Ivanova, E. P. (2011). Bacterial extracellular polysaccharides. In D. Linke, & A. Goldman (Eds.), *Vol. 715. Bacterial adhesion* (pp. 213–226). Netherlands: Springer. https://doi.org/10.1007/978-94-007-0940-9_13.

Bochkov, A. Y., & Toukach, P. V. (2021). CSDB/SNFG structure editor: An online glycan builder with 2D and 3D structure visualization. *Journal of Chemical Information and Modeling, 61*(10), 4940–4948. https://doi.org/10.1021/acs.jcim.1c00917

Bravo, B., Correia, P., Gonçalves Junior, J. E., Sant'Anna, B., & Kerob, D. (2022). Benefits of topical hyaluronic acid for skin quality and signs of skin aging: From literature review to clinical evidence. *Dermatologic Therapy, 35*(12). https://doi.org/10.1111/dth.15903

Cao, Y.-Y., Ji, Y.-H., Liao, A.-M., Huang, J.-H., Thakur, K., Li, X.-L., Hu, F., Zhang, J.-G., & Wei, Z.-J. (2020). Effects of sulfated, phosphorylated and carboxymethylated modifications on the antioxidant activities in-vitro of polysaccharides sequentially extracted from Amana edulis. *International Journal of Biological Macromolecules, 146*, 887–896. https://doi.org/10.1016/j.ijbiomac.2019.09.211

Capurso, L. (2019). Thirty years of Lactobacillus rhamnosus GG: A review. *Journal of Clinical Gastroenterology, 53*(Supplement 1), S1–S41. https://doi.org/10.1097/MCG.0000000000001170

Carillo, S., Silipo, A., Perino, V., Lanzetta, R., Parrilli, M., & Molinaro, A. (2009). The structure of the O-specific polysaccharide from the lipopolysaccharide of Burkholderia anthina. *Carbohydrate Research, 344*(13), 1697–1700. https://doi.org/10.1016/j.carres.2009.05.013

Ciucanu, I., & Kerek, F. (1984). A simple and rapid method for the permethylation of carbohydrates. *Carbohydrate Research, 131*(2), 209–217. https://doi.org/10.1016/0008-6215(84)85242-8

DuBois, M., Gilles, K. A., Hamilton, J. K., Rebers, P. A., & Smith, F. (1956). Colorimetric method for determination of sugars and related substances. *Analytical Chemistry, 28*(3), 350–356. https://doi.org/10.1021/ac60111a017

Edgar, R. J., Van Hensbergen, V. P., Ruda, A., Turner, A. G., Deng, P., Le Breton, Y., … Korotkova, N. (2019). Discovery of glycerol phosphate modification on streptococcal rhamnose polysaccharides. *Nature Chemical Biology, 15*(5), 463–471. https://doi.org/10.1038/s41589-019-0251-4

Gorin, P. A. J., & Mazurek, M. (1975). Further studies on the assignment of signals in ^{13}C magnetic resonance spectra of aldoses and derived methyl glycosides. *Canadian Journal of Chemistry, 53*(8), 1212–1223. https://doi.org/10.1139/v75-168

Górska, S., Hermanova, P., Ciekot, J., Schwarzer, M., Srutkova, D., Brzozowska, E., Kozakova, H., & Gamian, A. (2016). Chemical characterization and immunomodulatory properties of polysaccharides isolated from probiotic *Lactobacillus casei* LOCK 0919. *Glycobiology, 26*(9), 1014–1024. https://doi.org/10.1093/glycob/cww047

Górska, S., Schwarzer, M., Jachymek, W., Srutkova, D., Brzozowska, E., Kozakova, H., & Gamian, A. (2014). Distinct immunomodulation of bone marrow-derived dendritic cell responses to Lactobacillus plantarum WCFS1 by two different polysaccharides isolated from Lactobacillus rhamnosus LOCK 0900. *Applied and Environmental Microbiology, 80*(20), 6506–6516. https://doi.org/10.1128/AEM.02104-14

Hu, Q., Lu, Y., & Luo, Y. (2021). Recent advances in dextran-based drug delivery systems: From fabrication strategies to applications. *Carbohydrate Polymers, 264*, Article 117999. https://doi.org/10.1016/j.carbpol.2021.117999

Khan, R., Shah, M. D., Shah, L., Lee, P.-C., & Khan, I. (2022). Bacterial polysaccharides—A big source for prebiotics and therapeutics. *Frontiers in Nutrition, 9*, 1031935. https://doi.org/10.3389/fnut.2022.1031935

Kołodziejska, K., Perepelov, A. V., Zabłotni, A., Drzewiecka, D., Senchenkova, S. N., Zych, K., … Sidorczyk, Z. (2006). Structure of the glycerol phosphate-containing O-polysaccharides and serological studies of the lipopolysaccharides of *Proteus mirabilis* CCUG 10704 (OE) and *Proteus vulgaris* TG 103 classified into a new *Proteus* serogroup, O54. *FEMS Immunology & Medical Microbiology, 47*(2), 267–274. https://doi.org/10.1111/j.1574-695X.2006.00084.x

Laffargue, T., Moulis, C., & Remaud-Siméon, M. (2023). Phosphorylated polysaccharides: Applications, natural abundance, and new-to-nature structures generated by chemical and enzymatic functionalisation. *Biotechnology Advances, 65*, Article 108140. https://doi.org/10.1016/j.biotechadv.2023.108140

Laws, A., Gu, Y., & Marshall, V. (2001). Biosynthesis, characterisation, and design of bacterial exopolysaccharides from lactic acid bacteria. *Biotechnology Advances, 19*(8), 597–625. https://doi.org/10.1016/S0734-9750(01)00084-2

Lee, W., Tonelli, M., & Markley, J. L. (2015). NMRFAM-SPARKY: Enhanced software for biomolecular NMR spectroscopy. *Bioinformatics, 31*(8), 1325–1327. https://doi.org/10.1093/bioinformatics/btu830

Lipkind, G. M., Shashkov, A. S., Knirel, Y. A., Vinogradov, E. V., & Kochetkov, N. K. (1988). A computer-assisted structural analysis of regular polysaccharides on the basis of 13C-n.m.r. Data. *Carbohydrate Research, 175*(1), 59–75. https://doi.org/10.1016/0008-6215(88)80156-3

Liu, T., Ren, Q., Wang, S., Gao, J., Shen, C., Zhang, S., Wang, Y., & Guan, F. (2023). Chemical modification of polysaccharides: a review of synthetic approaches, biological activity and the structure–activity relationship. *Molecules, 28*(16), 6073. https://doi.org/10.3390/molecules28166073

Makino, S., Ikegami, S., Kano, H., Sashihara, T., Sugano, H., Horiuchi, H., … Oda, M. (2006). Immunomodulatory effects of polysaccharides produced by Lactobacillus delbrueckii ssp. Bulgaricus OLL1073R-1. *Journal of Dairy Science, 89*(8), 2873–2881. https://doi.org/10.3168/jds.S0022-0302(06)72560-7

Masuda, Y., Matsumoto, A., Toida, T., Oikawa, T., Ito, K., & Nanba, H. (2009). Characterization and antitumor effect of a novel polysaccharide from Grifola frondosa. *Journal of Agricultural and Food Chemistry, 57*(21), 10143–10149. https://doi.org/10.1021/jf9021338

Mattos, K. A., Jones, C., Heise, N., Previato, J. O., & Mendonça-Previato, L. (2001). Structure of an acidic exopolysaccharide produced by the diazotrophic endophytic bacterium *Burkholderia brasiliensis*. *European Journal of Biochemistry, 268*(11), 3174–3179. https://doi.org/10.1046/j.1432-1327.2001.02196.x

Nagaoka, M., Hashimoto, S., Shibata, H., Kimura, I., Kimura, K., Sawada, H., & Yokokura, T. (1996). Structure of a galactan from cell walls of Bifidobacterium catenulatum YIT4016. *Carbohydrate Research, 281*(2), 285–291. https://doi.org/10.1016/0008-6215(95)00354-1

Nishimura-Uemura, J., Kitazawa, H., Kawai, Y., Itoh, T., Oda, M., & Saito, T. (2003). Functional alteration of murine macrophages stimulated with extracellular polysaccharides from Lactobacillus delbrueckii ssp. Bulgaricus OLL1073R-1. *Food Microbiology, 20*(3), 267–273. https://doi.org/10.1016/S0740-0020(02)00177-6

Pacyga-Prus, K., Jakubczyk, D., Sandström, C., Šrůtková, D., Pyclik, M. J., Leszczyńska, K., … Górska, S. (2023). Polysaccharide BAP1 of Bifidobacterium adolescentis CCDM 368 is a biologically active molecule with immunomodulatory properties. *Carbohydrate Polymers, 315*, Article 120980. https://doi.org/10.1016/j.carbpol.2023.120980

Prateeksha, Sharma, V. K., Liu, X., Oyarzún, D. A., Abdel-Azeem, A. M., Atanasov, A. G., … Singh, B. N. (2022). Microbial polysaccharides: An emerging family of natural biomaterials for cancer therapy and diagnostics. *Seminars in Cancer Biology, 86*, 706–731. https://doi.org/10.1016/j.semcancer.2021.05.021

Pyclik, M., Srutkova, D., Schwarzer, M., & Górska, S. (2020). Bifidobacteria cell wall-derived exo-polysaccharides, lipoteichoic acids, peptidoglycans, polar lipids and proteins – Their chemical structure and biological attributes. *International Journal of Biological Macromolecules, 147*, 333–349. https://doi.org/10.1016/j.ijbiomac.2019.12.227

Pyclik, M. J., Srutkova, D., Razim, A., Hermanova, P., Svabova, T., Pacyga, K., … Górska, S. (2021). Viability status-dependent effect of Bifidobacterium longum ssp. Longum CCM 7952 on prevention of allergic inflammation in mouse model. *Frontiers in Immunology, 12*, 2800. https://doi.org/10.3389/fimmu.2021.707728

Rafique, N., Jan, S. Y., Dar, A. H., Dash, K. K., Sarkar, A., Shams, R., … Hussain, S. Z. (2023). Promising bioactivities of postbiotics: A comprehensive review. *Journal of Agriculture and Food Research, 14*, Article 100708. https://doi.org/10.1016/j.jafr.2023.100708

Salazar, N., Prieto, A., Leal, J. A., Mayo, B., Bada-Gancedo, J. C., De Los Reyes-Gavilán, C. G., & Ruas-Madiedo, P. (2009). Production of exopolysaccharides by Lactobacillus and Bifidobacterium strains of human origin, and metabolic activity of the producing bacteria in milk. *Journal of Dairy Science, 92*(9), 4158–4168. https://doi.org/10.3168/jds.2009-2126

Salminen, S., Collado, M. C., Endo, A., Hill, C., Lebeer, S., Quigley, E. M. M., … Vinderola, G. (2021). The international scientific Association of Probiotics and Prebiotics (ISAPP) consensus statement on the definition and scope of postbiotics. *Nature Reviews Gastroenterology & Hepatology, 18*(9), 649–667. https://doi.org/10.1038/s41575-021-00440-6

Sato, T., Nishimura-Uemura, J., Shimosato, T., Kawai, Y., Kitazawa, H., & Saito, T. (2004). Dextran from Leuconostoc mesenteroides augments Immunostimulatory effects by the introduction of phosphate groups. *Journal of Food Protection, 67*(8), 1719–1724. https://doi.org/10.4315/0362-028X-67.8.1719

Sawardeker, J. S., Sloneker, J. H., & Jeanes, A. (1965). Quantitative determination of monosaccharides as their Alditol acetates by gas liquid chromatography. *Analytical Chemistry, 37*(12), 1602–1604. https://doi.org/10.1021/ac60231a048

Schiavi, E., Plattner, S., Rodriguez-Perez, N., Barcik, W., Frei, R., Ferstl, R., … O'Mahony, L. (2018). Exopolysaccharide from *Bifidobacterium longum* subsp. *Longum* 35624™ modulates murine allergic airway responses. *Beneficial Microbes, 9*(5), 761–773. https://doi.org/10.3920/BM2017.0180

Senchenkova, S. N., Shashkov, A. S., Laux, P., Knirel, Y. A., & Rudolph, K. (1999). The O-chain polysaccharide of the lipopolysaccharide of Xanthomonascampestris pv. Begoniae GSPB 525 is a partially l-xylosylated l-rhamnan. *Carbohydrate Research, 319*(1–4), 148–153. https://doi.org/10.1016/S0008-6215(99)00125-1

Shashkov, A. S., Lipkind, G. M., Knirel, Y. A., & Kochetkov, N. K. (1988a). Stereochemical factors determining the effects of glycosylation on the ^{13}C chemical shifts in carbohydrates. *Magnetic Resonance in Chemistry, 26*(9), 735–747. https://doi.org/10.1002/mrc.1260260904

Shashkov, A. S., Lipkind, G. M., Knirel, Y. A., & Kochetkov, N. K. (1988b). Stereochemical factors determining the effects of glycosylation on the13C chemical shifts in carbohydrates. *Magnetic Resonance in Chemistry, 26*(9), 735–747. https://doi.org/10.1002/mrc.1260260904

Speciale, I., Verma, R., Di Lorenzo, F., Molinaro, A., Im, S.-H., & De Castro, C. (2019). Bifidobacterium bifidum presents on the cell surface a complex mixture of glucans and galactans with different immunological properties. *Carbohydrate Polymers, 218*, 269–278. https://doi.org/10.1016/j.carbpol.2019.05.006

Srutkova, D., Kozakova, H., Novotna, T., Gorska, S., Hermanova, P. P., Hudcovic, T., … Schwarzer, M. (2023). Exopolysaccharide from *Lacticaseibacillus rhamnosus* induces IgA production in airways and alleviates allergic airway inflammation in mouse model. *European Journal of Immunology, 53*(7), 2250135. https://doi.org/10.1002/eji.202250135

Srutkova, D., Schwarzer, M., Hudcovic, T., Zakostelska, Z., Drab, V., Spanova, A., … Schabussova, I. (2015). Bifidobacterium longum CCM 7952 promotes epithelial barrier function and prevents acute DSS-induced colitis in strictly strain-specific manner. *PLoS One, 10*(7), Article e0134050. https://doi.org/10.1371/journal.pone.0134050

Sunil, Y., Ramadori, G., & Raddatz, D. (2010). Influence of NFκB inhibitors on IL-1β-induced chemokine CXCL8 and −10 expression levels in intestinal epithelial cell lines: Glucocorticoid ineffectiveness and paradoxical effect of PDTC. *International Journal of Colorectal Disease, 25*(3), 323–333. https://doi.org/10.1007/s00384-009-0847-3

Toukach, P. V. (2011). Bacterial carbohydrate structure database 3: Principles and realization. *Journal of Chemical Information and Modeling, 51*(1), 159–170. https://doi.org/10.1021/ci100150d

Verma, R., Lee, C., Jeun, E.-J., Yi, J., Kim, K. S., Ghosh, A., … Im, S.-H. (2018). Cell surface polysaccharides of *Bifidobacterium bifidum* induce the generation of Foxp3 $^{+}$

regulatory T cells. *Science Immunology, 3*(28), Article eaat6975. https://doi.org/10.1126/sciimmunol.aat6975

Vichai, V., & Kirtikara, K. (2006). Sulforhodamine B colorimetric assay for cytotoxicity screening. *Nature Protocols, 1*(3), 1112–1116. https://doi.org/10.1038/nprot.2006.179

Vinogradov, E., Korenevsky, A., & Beveridge, T. J. (2003). The structure of the O-specific polysaccharide chain of the Shewanella algae BrY lipopolysaccharide. *Carbohydrate Research, 338*(4), 385–388. https://doi.org/10.1016/S0008-6215(02)00469-X

You, X., Li, Z., Ma, K., Zhang, C., Chen, X., Wang, G., Yang, L., Dong, M., Rui, X., Zhang, Q., & Li, W. (2020). Structural characterization and immunomodulatory activity of an exopolysaccharide produced by Lactobacillus helveticus LZ-R-5. *Carbohydrate Polymers, 235*, Article 115977. https://doi.org/10.1016/j.carbpol.2020.115977

Zeidan, A. A., Poulsen, V. K., Janzen, T., Buldo, P., Derkx, P. M. F., Øregaard, G., & Neves, A. R. (2017). Polysaccharide production by lactic acid bacteria: From genes to industrial applications. *FEMS Microbiology Reviews, 41*(Supp_1), S168–S200. https://doi.org/10.1093/femsre/fux017

Zhou, Y., Cui, Y., & Qu, X. (2019). Exopolysaccharides of lactic acid bacteria: Structure, bioactivity and associations: A review. *Carbohydrate Polymers, 207*, 317–332. https://doi.org/10.1016/j.carbpol.2018.11.093

NMR spectra of B.PAT

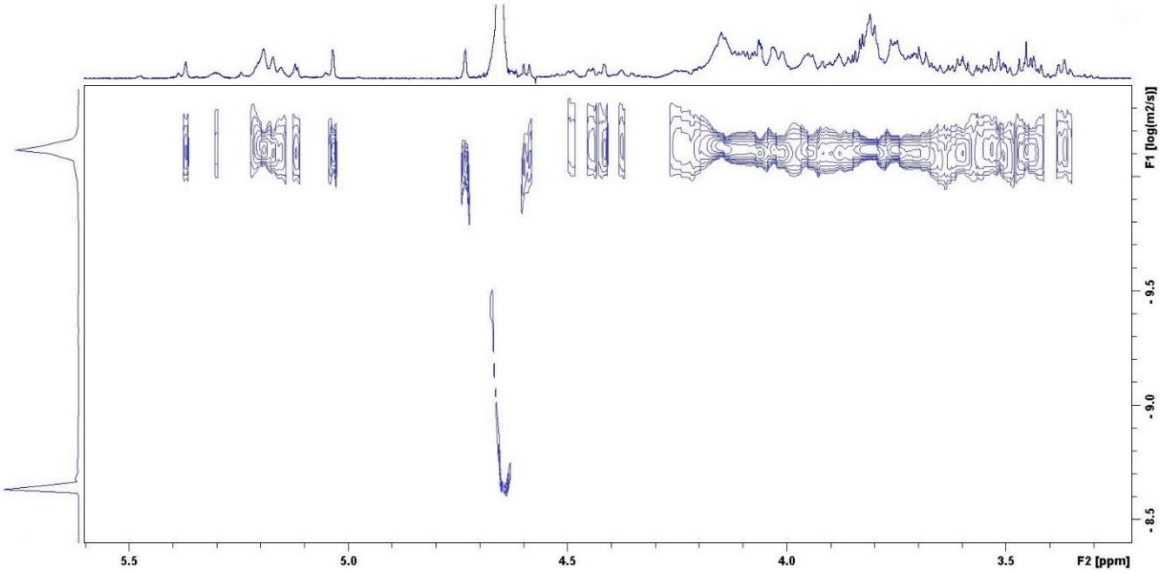

Supplementary Figure S1. Full DOSY spectrum of B.PAT.

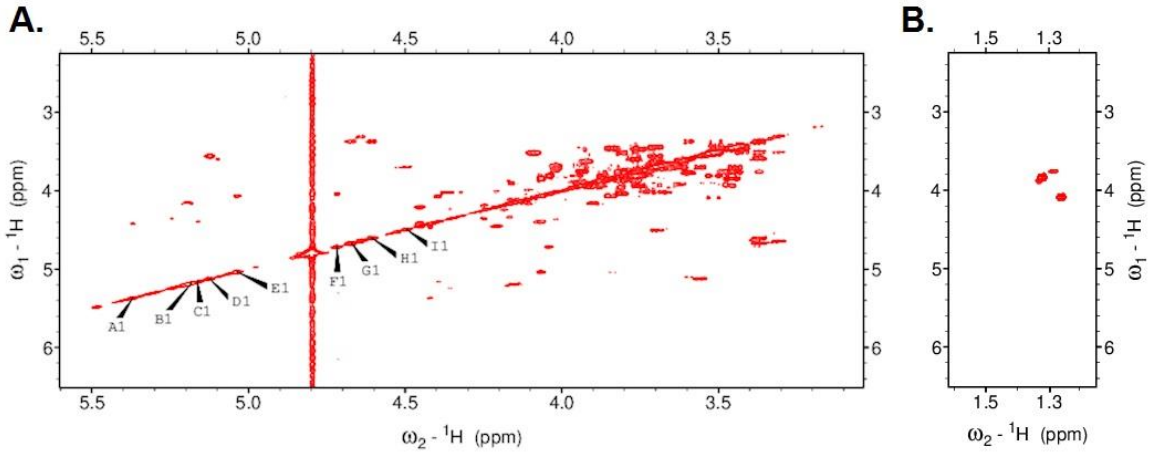

Supplementary Figure S2. ^{1}H-^{1}H COSY spectrum of B.PAT. **A.** The main part of the spectra with the anomeric signals marked from A1 – I1. **B.** COSY signals for rhamnoses (residues B, C, E, and F) between 1.2 and 1.6 ppm.

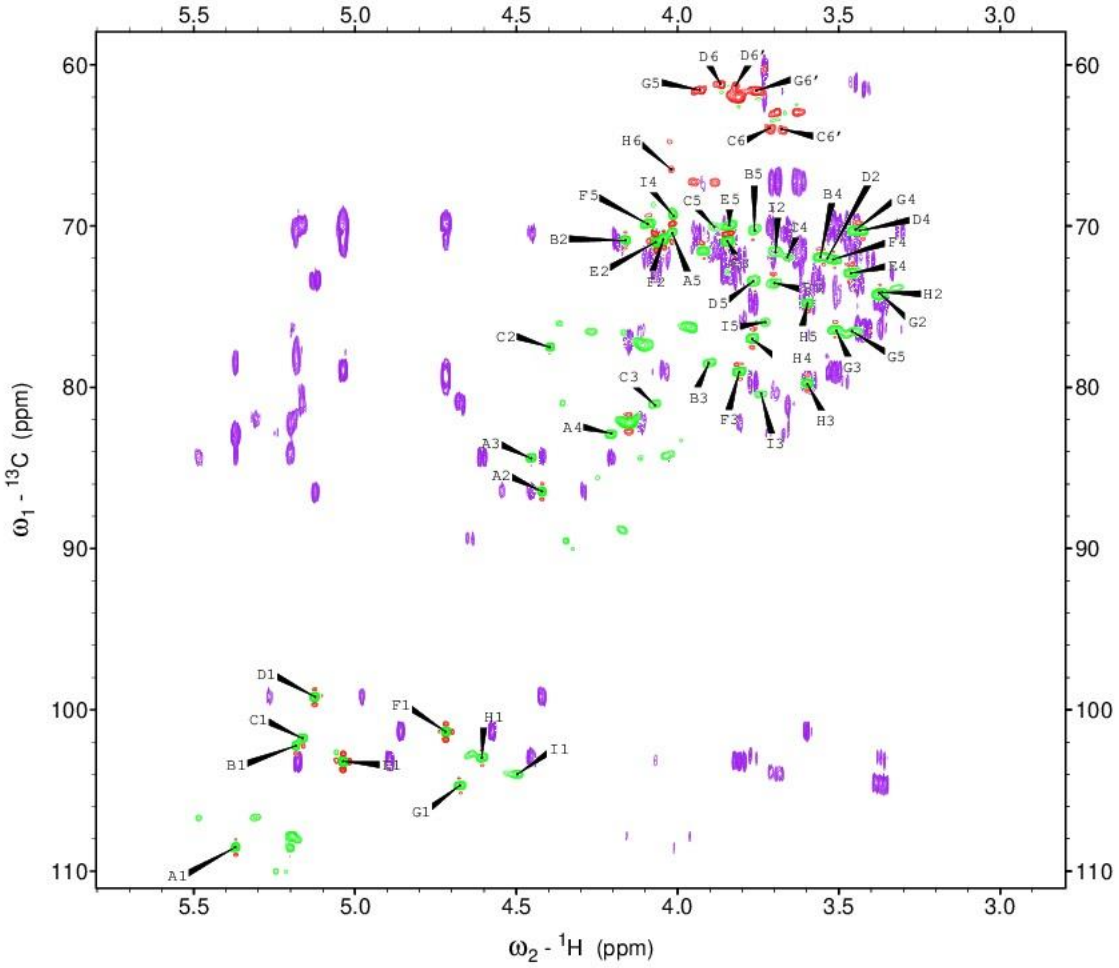

Supplementary Figure S3. ^{1}H-^{13}C HSQC spectrum (green and red) overlapped with ^{1}H-^{13}C HMBC spectrum (purple) of B.PAT.

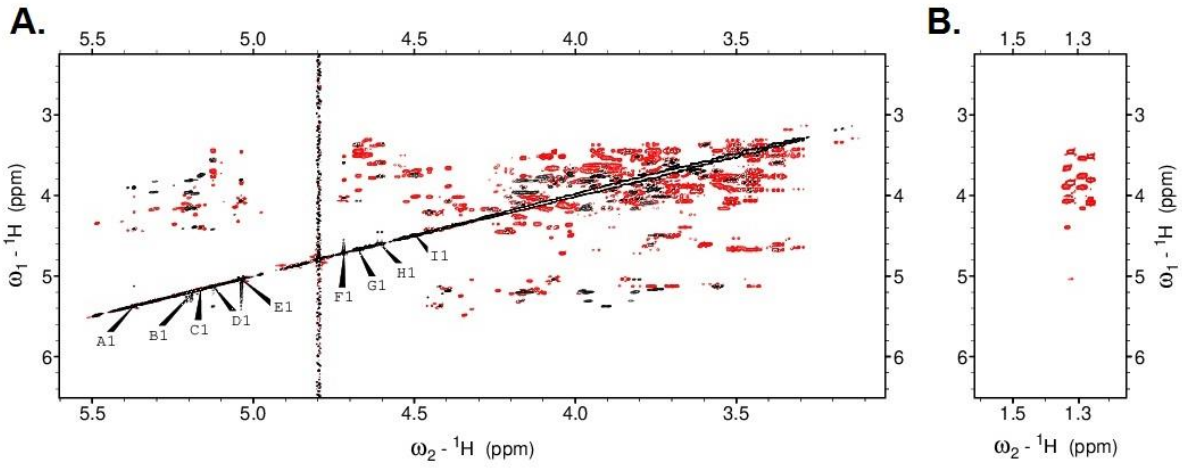

Supplementary Figure S4. 120 ms ^{1}H-^{1}H TOCSY spectrum (red) overlapped with 100 ms ^{1}H-^{1}H NOESY spectrum (black) of B.PAT. **A.** The main part of the spectra with the anomeric

signals marked from A1 – I1. **B.** TOCSY and COSY signals for rhamnoses (residue B, C, E, and F) between 1.2 – 1.6 ppm.

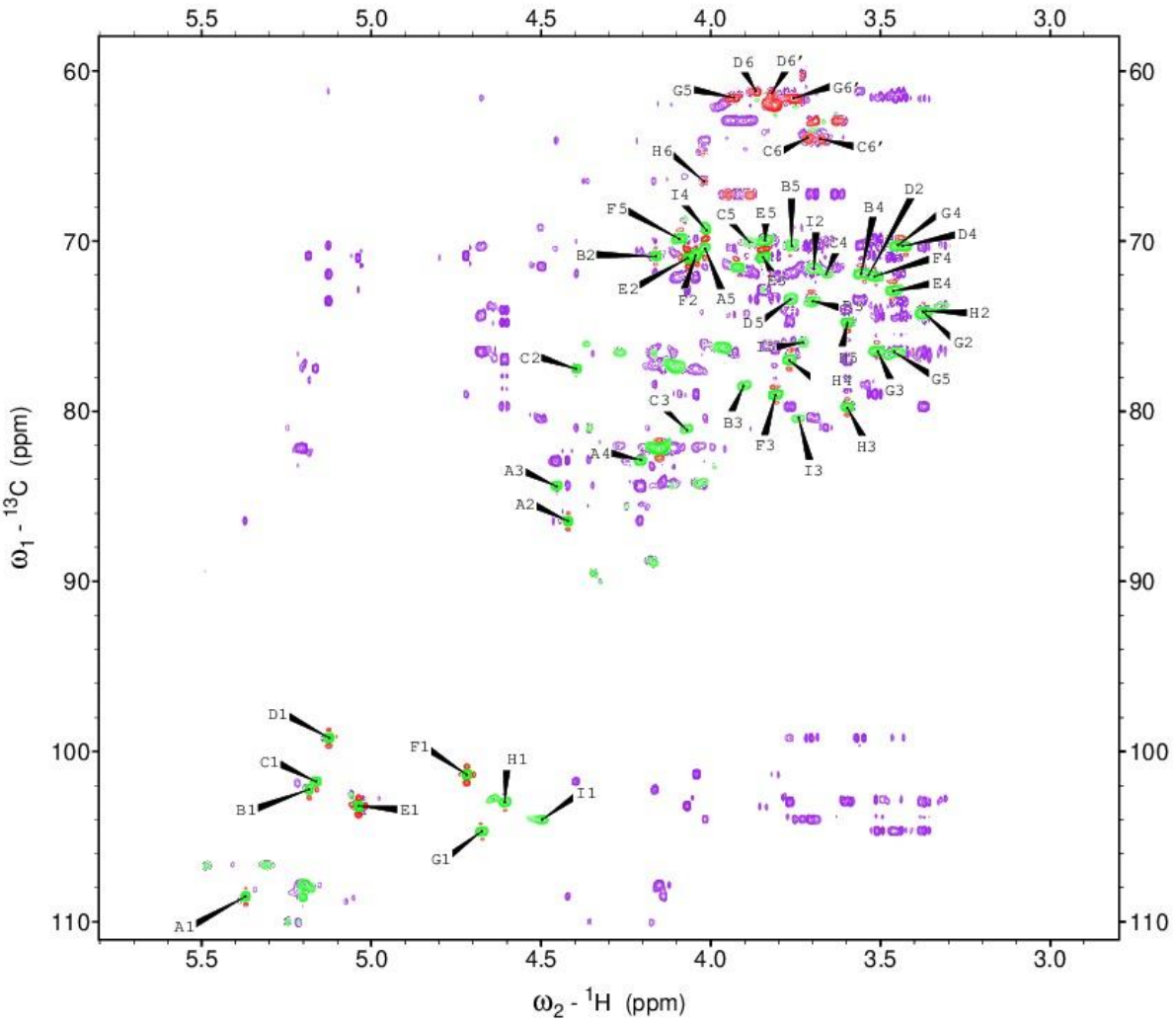

Supplementary Figure S5. ^{1}H-^{13}C HSQC spectrum (green and red) overlapped with HSQC-TOSCY spectrum (purple) of B.PAT.

BMDCs viability after stimulation with B.PAT and B.MAT

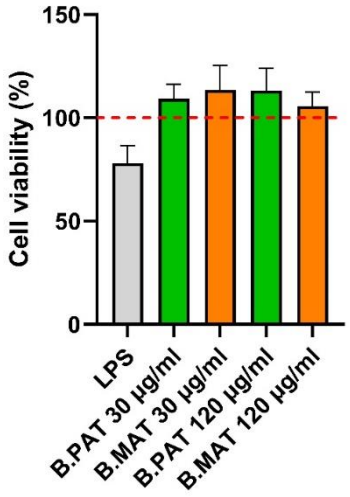

Supplementary Figure S6. BMDCs viability after treatment with B.PAT and B.MAT (30 and 120 µg/ml). Results of the SRB assay showed no changes in viability in PS-treated cells compared to the control (medium only, 100 %, red dashed line).

UV–vis analysis of the B.PAT and B.MAT

Supplementary Table T1. Results of UV–vis analysis of B.PAT and B.MAT.

	230 nm	**260 nm**	**280 nm**	**320 nm**
B.PAT	0.023	0.015	0.017	0.008
B.MAT	0.039	0.029	0.029	0.023

6. 3rd manuscript (preprint)

6.1. Foreword to the 3rd manuscript

A. Rationale of research objectives

Previous studies presented in the 1st manuscript led to the selection of BAP1 as an antigen with the most promising anti-allergic properties. To confirm its functions, it was crucial to test it in a more complex environment. However, before conducting animal studies, an extensive literature review was needed to decide on the antigens' administration method. Since, in the treatment of airway allergies it is necessary to target both local and immune responses, for this study intranasal delivery was chosen **(Chapter 1.4)**. In the next step, antigen-specific response was tested in GF mice **(Chapter 1)**. Subsequently, local and systemic responses to BAP1 were evaluated in the mice model of OVA-induced allergy.

The abovementioned tasks were performed to fulfill objectives **O3** and **O4** and therefore, contributed to proving the initially established hypothesis by selecting a bacterial antigen that can be responsible for the anti-allergic effect of the whole bacteria and provide an alternative for available treatments.

B. Methodology:

Treatment of GF and OVA-allergy mice with BAP1 antigen:

- Isolation and stimulation of splenocytes and lung cells.
- Determination of cytokines levels in splenocytes and lung cells supernatants after treatment with BAP1 by the Milliplex Map Mouse Cytokine/Chemokine Panels.
- Histopathology evaluation of lungs.
- Evaluation of bronchoalveolar lavage (BAL):
    - BAL cell differential count,
    - Immunological analysis of BALF – determination of total and OVA-specific antibodies.
- Evaluation of blood sera:
    - Immunological analysis – determination of total and OVA-specific antibodies.
- Analysis of gene expression in lungs.

C. Results:

Treatment of GF mice with BAP1:

- tended to increase total IgA in sera,
- did not impact chemokine and cytokine production in splenocytes,
- did not induce cell infiltration in BAL, however, significantly increased IgA in BALF,
- showed no impact on the lung inflammation,
- significantly increased chemokine (C-C motif) ligand 5 (CCL5), decreased IL-6, and CCL2 levels, and tended to inhibit eotaxin production in lung cells,
- significantly increased *Rorc* and tended to enhance *Tbx21* expression.

Treatment of OVA-allergy mice with BAP1:

- tended to decrease total IgE, IgA, and OVA-specific IgA antibodies, while significantly reducing OVA-specific IgE in sera,
- inhibited Th2-related cytokine production in splenocytes (with significant inhibition of IL-5) and tended to reduce IL-10 levels,
- decreased cell infiltration in BAL (with significant reduction of eosinophil and macrophage numbers), thus, restraining lung inflammation,
- significantly decreased IL-5 and IL-10 levels, while tending to inhibit IL-4 and IL-13 production.
- tended to increase *Rorc* and significantly reduced *Il10* expression.

D. Conclusions:

Comprehensive analysis of BAP1 conducted throughout 1st manuscript allowed the selection of a high molecular mass antigen with a unique structure that showed the ability to alleviate OVA sensitization. Investigation of GF mice confirmed the neutral effect of BAP1 on the naïve immune system, despite the decrease of allergy-associated CCL2 production and increase of the *Rorc* gene expression. Further analysis of BAP1 in the OVA-allergy mouse model demonstrated the anti-allergic properties of this molecule, manifested by a systemic reduction of OVA-specific IgE in sera and inhibition of Th2-related cytokines production in splenocytes. Moreover, locally, BAP1 restricted lung inflammation by limiting eosinophil infiltration and IL-5, IL-4, and IL-13 levels. A closer look at the IL-10 showed an inhibitory effect of BAP1 on the production of this cytokine, known for its pleiotropic function in allergies. Finally, gene expression analysis confirmed the possible role of *Rorc* in BAP1 signaling and confirmed the impact of the tested PS on the *Il10* inhibition. These findings could make a significant contribution to developing alternative treatments for respiratory allergies.

6.2. Copy of the 3rd manuscript (preprint)

Pacyga-Prus, K., Hornikova, T., Srutkova, D., Leszczyńska-Nowak, K., Zabłocka, A., Schwarzer, M., Górska, S. (2024). Polysaccharide BAP1 of Bifidobacterium adolescentis CCDM 368 attenuates ovalbumin-induced allergy through inhibition of Th2 immunity in mice. *bioRxiv*, 1 Jan 2024, 2024.09.14.613063. https://doi.org/10.1101/2024.09.14.613063.

A. Graphical abstract

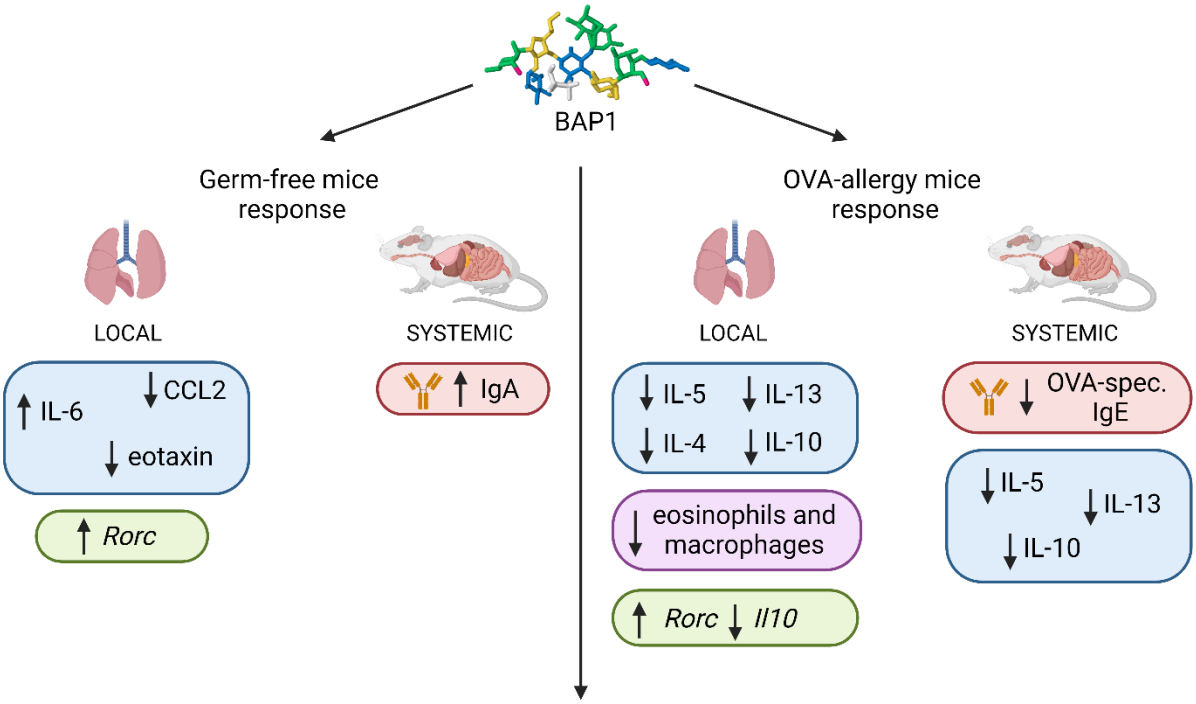

Anti-allergic properties of BAP1 polysaccharide

B. Manuscript and supplementary data

Polysaccharide BAP1 of *Bifidobacterium adolescentis* CCDM 368 attenuates ovalbumin-induced allergy through inhibition of Th2 immunity in mice

Katarzyna Pacyga-Prus[a*], Tereza Hornikova[b], Dagmar Šrůtková[b], Katarzyna Leszczyńska-Nowak[a], Agnieszka Zabłocka[a], Martin Schwarzer[b], Sabina Górska[a*]

[a]Laboratory of Microbiome Immunobiology, Hirszfeld Institute of Immunology and Experimental Therapy, Polish Academy of Sciences, 53-114, Wroclaw, Poland

[b]Laboratory of Gnotobiology, Institute of Microbiology, Czech Academy of Sciences, 549 22, Novy Hradek, Czech Republic

*Corresponding author:

Katarzyna Pacyga-Prus: (katarzyna.pacyga-prus@hirszfeld.pl, (+48) 713371172 (183))

Sabina Górska: sabina.gorska@hirszfeld.pl

Katarzyna Pacyga-Prus: katarzyna.pacyga-prus@hirszfeld.pl; ORCID: 0000-0002-9400-9297

Tereza Hornikova: tereza.svabova@biomed.cas.cz; ORCID: 0000-0002-1643-4837

Dagmar Srutkova: srutkova@biomed.cas.cz; ORCID: 0000-0003-0054-5396

Katarzyna Leszczyńska-Nowak: katarzyna.leszczynska@hirszfeld.pl; ORICD: 0000-0003-3208-9559

Agnieszka Zabłocka: agnieszka.zablocka@hirszfeld.pl; ORCID: 0000-0002-5707-9886

Martin Schwarzer: schwarzer@biomed.cas.cz; ORCID: 0000-0002-1401-6578

Sabina Górska: sabina.gorska@hirszfeld.pl; ORCID: 0000-0002-3206-0695

Abstract

Allergies have become a growing problem and the number of cases is increasing yearly. Administration of postbiotics, well-defined bacterial molecules, is gaining attention as a novel and promising strategy to ameliorate the allergic burden. The BAP1 polysaccharide (PS) of *Bifidobacterium adolescentis* CCDM 368, was previously characterized by us regarding its structure and *in vitro* immunomodulatory properties. Here, to decipher the effect of BAP1 on immune system development, it was intranasally (i.n.) administered to germ-free mice. We observed increased IgA in bronchoalveolar lavage (BAL) fluid, decreased CCL2 production, and higher *Rorc* gene expression in the lung. The intranasal administration of BAP1 reduced lung inflammation and decreased eosinophils numbers in BAL in the ovalbumin-induced allergy mouse model. Moreover, BAP1 decreased OVA-specific IgE levels in sera and Th2-related cytokines in OVA-stimulated splenocytes and lung cells. Finally, increased *Rorc* and inhibited *Il10* gene expression were observed in lung tissue indicating their possible role in BAP1 function. Our findings support and expand on our previous *in vitro and ex vivo* studies by demonstrating that BAP1, with a unique chemical structure, induces a specific immunomodulatory effect in the host and could be potentially used for alleviating allergic diseases.

Keywords:

Bifidobacterium; airway allergies; polysaccharide; BAP1; postbiotics

Graphical abstract

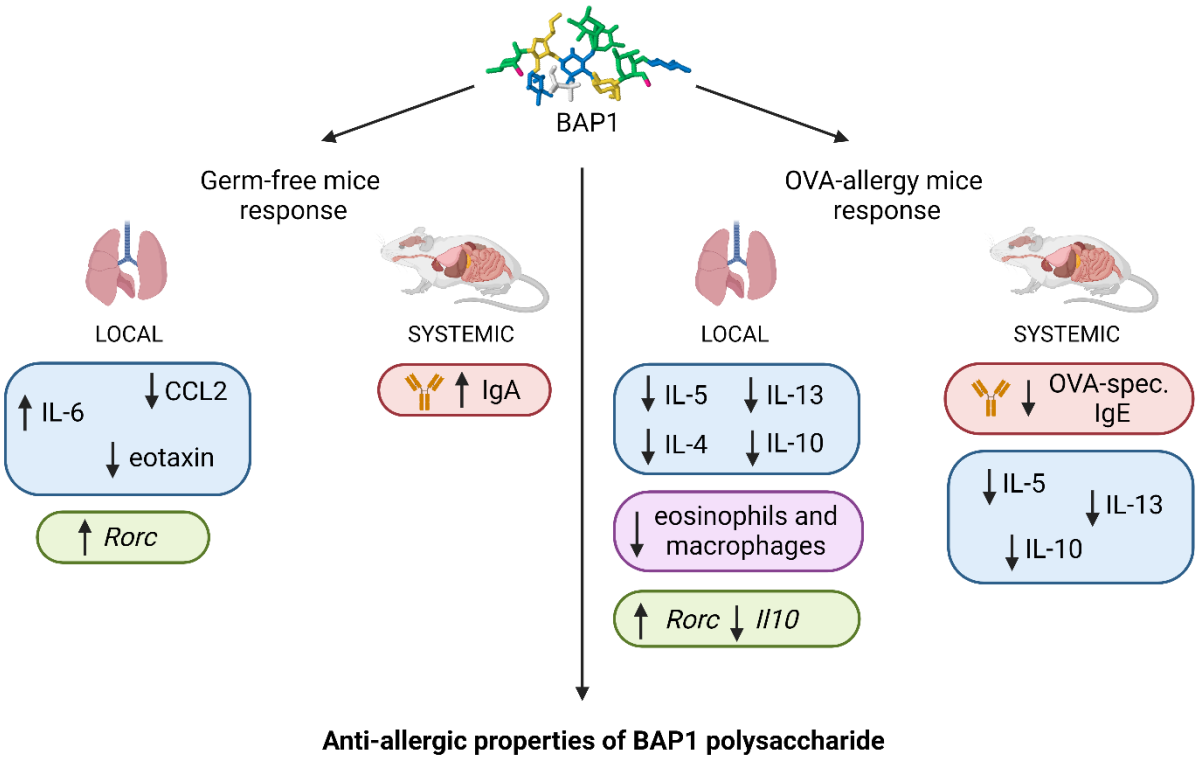

Anti-allergic properties of BAP1 polysaccharide

1. Introduction

Airway allergies have become a major healthcare problem affecting people worldwide. According to data collected by the European Academy of Allergy and Clinical Immunology (EAACI), in 2019 up to 40% of the world's population suffered from allergic rhinitis, while over 300 million people were diagnosed with asthma[1]. However, the number of cases is increasing every year affecting patients' quality of life, and ability to work, while having a significant impact on the global economy [2,3]. Available allergy treatments are often described as inefficient or as causing side effects. Thus, it is necessary to search for alternative therapies[2]. In recent years, more studies have highlighted the role of healthy microbiota of the intestinal and airway tract in the prevention of allergy outcomes. Well-described are the differences between the microbiome composition of healthy and allergic patients[4]. Moreover, available studies indicate that the shape of the infant microbiome predicts allergic disease susceptibility in later life[5,6]. For instance, the Copenhagen Prospective Study on Asthma in Childhood (COPSAC) studied asthma susceptibility in infants and showed that hypopharynx colonization by pathogenic bacteria including *Streptococcus pneumoniae* or *Haemophilus influenzae* increased the risk of asthma development[7]. On the other hand, the nasal presence of *Lactobacillus* strains is associated with a lower risk of allergic asthma[4]. These breakthroughs have led to a new way of thinking, namely, introducing a health-beneficial bacteria to rebalance the microbiome and thus treat/prevent allergies. These microorganisms include bifidobacteria, which are anaerobic commensal bacteria well known for their immunomodulatory and health-promoting properties[8]. Also, they were proven to exhibit promising anti-allergic properties[9]. For instance, in an ovalbumin(OVA)-allergic mouse model, we have shown the preventive effect of *Bifidobacterium longum* ssp. *longum* CCM 7952 on the development of allergic sensitization and OVA-induced lung inflammation[10,11]. The additive effect of different bifidobacterial strains in reducing symptoms and improving quality of life in children with allergic rhinitis has also been shown in a clinical study[12]. Also, Ouwehand et al. (2009) described the combined influence of *Bifidobacterium lactis* Bl-04 and *Lactobacillus acidophilus* NCFM™ on the alleviation of respiratory allergy symptoms and eosinophilic infiltration into nasal mucosa in children with birch pollen allergy [13].

Despite the promising results obtained for probiotics administration, several limitations remain. First, as the definition of probiotics claims, they are "live microorganisms that, when administered in adequate amounts, confer a health benefit on the host"[14]. Live organisms are more difficult to maintain and also their stability is low. Furthermore, they still possess the ability to reproduce, causing a risk of bacteriemia or the transfer of antibiotic-resistance genes[15,16]. Moreover, the complexity of a whole bacterial cell makes it impossible to determine its structure-function relationship in detail. For this reason, a new attempt has been proposed. So-called postbiotics started to gain attention in recent

years and have been described by the International Association of Probiotics and Prebiotics as the "preparation of inanimate microorganisms and/or their components that confers a health benefit on the host"[15]. This definition includes different antigens present on the bacterial surface, such as proteins, glycolipids, lipoteichoic acids, and polysaccharides (PS).

We have recently described BAP1, the PS isolated from the surface of *Bifidobacterium adolescentis* CCDM 368, as a linear hexasaccharide with a unique structure consisting of glucose, galactose, and rhamnose residues, and a molecular mass of approximately 9.99 x 10^6 [17]. This polymer has been shown to be efficiently engulfed by airway epithelial cells and transferred to dendritic cells in *in vitro* assay. Treatment of bone marrow dendritic cells with the tested PS resulted in higher levels of TNF-α, IL-10, and IL-6. Further *ex vivo* immunomodulatory studies in OVA-restimulated splenocytes from OVA-sensitized BALB/c mice showed the ability of BAP1 to restore the balance between Th1/Th2-related cytokines, making it a very interesting molecule with anti-allergic potential.

Here, we first investigated the role of BAP1 in the naïve immune system development of germ-free (GF) mice, which, due to the sterile environment, were a perfect model for a precise study of the specific molecule-host reaction[18]. We further investigated the impact of BAP1 on the prevention and modulation of allergic (local and systemic) immune responses to OVA in a mouse model of allergy. The obtained results indicated the ability of BAP1 to alleviate allergic symptoms by re-establishing the Th1/Th2 balance.

2. Materials and methods

2.1. BAP1 PS

BAP1 is a surface PS from *Bifidobacterium adolescentis* CCDM 368 (Bad368) derived from human adult feces and made available for research by the Czech Collection of Dairy Microorganisms (CCDM, Laktoflora, Milcom, Tábor, Czech Republic). The bacteria cultivation and the PS isolation and purification were performed following the methods described previously[17].

2.2. Animals

All animal procedures were performed following the EU Directive 2010/63/EU for animal experiments and were approved by the committee for the protection and use of experimental animals of the Institute of Microbiology, The Czech Academy of Sciences (no. 91/2019).

2.2.1. GF mice

GF BALB/c mice (females, 3 weeks old) were kept under sterile conditions in Trexler-type plastic isolators and exposed to a 12 h light : 12 h dark cycle with unlimited access to autoclaved water and sterile irradiated diet (V1124-300, Ssniff Spezialdiäten GmbH, Germany).

2.2.2. Specific-pathogen free mice

Specific-pathogen free (SPF) BALB/c mice (females, 6-8 weeks old) were kept in cages (IVC, Tecniplast, Italy) exposed to a 12 h light : 12 h dark cycle with unlimited access to water and sterile irradiated diet (V1124-300, Ssniff Spezialdiäten GmbH, Germany). SPF mice were regularly checked for the absence of potential pathogens according to an internationally established standard (FELASA).

2.3. Experimental designs

2.3.1. GF mice treatment

GF mice (n = 6 per group) were divided into two experimental groups: PBS and BAP1. The experiment started with the intranasal (i.n.) administration of 30 µg/30 µl of BAP1 or PBS to 3-week-old mice anesthetized by isoflurane. PS administration was repeated an additional 2 times at one-week intervals (experimental design, Figure 1A). A week after the last treatment, mice were sacrificed and samples were collected.

2.3.2. Model of allergic airway inflammation to OVA

SPF mice (n = 5 – 6 per group) were divided into two experimental groups: OVA and BAP1. OVA-allergy model was introduced by 2 intraperitoneal (i.p.) injections of 10 µg of OVA (grade V, Sigma Aldrich, USA) in PBS (100 µl) mixed with Alum (100 µl; Alu-gel-S, SERVA Electrophoresis, GmbH, Germany) in a 14-day interval. Third boosting immunization was performed with 15 µg of OVA (grade V, Sigma

Aldrich) in PBS (100 µl) mixed with Alum (100 µl) one week after the second injection. 4 hours before each i.p. sensitization, mice were treated intranasally with 30 µl of BAP1 (30 µg per dose) or PBS (OVA group). 7 days after the third immunization, 30 µl of PBS (OVA group) or BAP1 (30 µg /30 µl) were applied intranasally 4 hours before the OVA challenge (100 µg per dose, 30µl, intranasally) and repeated for 3 consecutive days. The following day, mice were sacrificed and samples were collected (experimental design, Figure 4A).

2.4. Splenocyte isolation

Splenocyte isolation was performed on aseptically removed spleens according to the method described by Pyclik et al. [11]. Isolated cells were counted and seeded on a 96-well plate (1×10^7 cells/ml, 100 µl/well) in RPMI 1640 medium (Sigma Aldrich) supplemented with 10 % FBS (Fetal Bovine Serum, Gibco), 100 U/ml of penicillin, 100 µg/ml streptomycin, and 10 mM HEPES (Sigma Aldrich). Splenocytes derived from GF mice were incubated without additional treatment, with a total volume of 200 µl of medium per well. Splenocytes isolated from the OVA-sensitized mice were restimulated on a plate with 100 µg of OVA (100 µl/well in a total volume of 200 µl). Finally, cells were incubated for 72 h at 37 °C (5 % CO_2, appropriate humidity). The concentration of cytokines was measured in supernatants by the Milliplex Map Mouse Cytokine/Chemokine Panel including CCL2, CCL5, CCL3, IL-6, IL-1β, TNF-α, IL-17E, IL-4 for GF mice and IL-10, IFN-γ, IL-4, IL-5, and IL-13 for OVA-allergy model. The procedure was performed according to the manufacturer's instructions and analyzed with the Luminex 2000 System (Bio-Rad Laboratories, USA). Unstimulated cells were used as a background for restimulated cells.

2.5. Lung cells

The left lung lobe was aseptically collected from BALB/c mice, and placed in a digestion buffer containing Liberase TL (0.05 mg/ml, Sigma Aldrich) and DNAse (0.5 mg/ml, Sigma Aldrich) dissolved in RPMI 1640 medium supplemented with 100 U/ml of penicillin, 100 µg/ml streptomycin, and 2 mM L-glutamine. To increase the efficiency of the process, the lungs were cut into smaller pieces with sterile scissors and left for 45 min at 37 °C. Digested cells were pressed through a 70 µm cell strainer and centrifuged (1300 rpm, 10 min, 4 °C). Pellet was treated with ACK lysis buffer for 3 min and the reaction was stopped with supplemented RPMI 1640 medium completed with 10 % FBS. Finally, centrifuged cells were counted and seeded on a 96-well plate (0.2×10^6 cells/well).

Cells derived from GF mice were incubated without additional treatment, with a total volume of 200 µl of medium per well. Cells from the OVA-allergy model were restimulated on a plate by 100 µg of OVA (100 µl/well in a total volume of 200 µl). Finally, plates were incubated for 72 h at 37 °C (5 % CO_2, appropriate humidity). The concentration of cytokines was measured in supernatants by the Milliplex

Map Mouse Cytokine/Chemokine Panel including CCL2, CCL5, IP-10, CCL3, CCL11, IL-6, IL-1β, TNF-α, IL-17A, IL-17E, IL-4 for GF mice and IL-10, IFN-γ, IL-4, IL-5, and IL-13 for OVA-allergy model. The procedure was performed according to the manufacturer's instructions and analyzed with the Luminex 2000 System (Bio-Rad Laboratories). Unstimulated cells were used as a background for restimulated cells.

2.6. Histopathological evaluation of lungs

The middle lobe of the lungs collected from the GF and OVA-allergy mouse model was fixed in 4 % paraformaldehyde for 24 h and stored in 80 % ethanol. Fixed lungs were embedded in paraffin, cut into 5 µm-thick slides, and subjected to periodic acid-Schiff staining (PAS). Prepared sections were assessed for a histological score with light microscopy (100 x magnification) as described by Srutkova et al. [18]. Samples were viewed under Olympus BX 40 microscope equipped with an Olympus Camedia DP 70 digital camera, and the images were analyzed using Olympus DP-Soft. The average histological score was assessed in 5 fields of the slide per each mouse and expressed as the sum of single parameters (perivascular and peribronchiolar inflammation, number of cells in alveolar spaces, and a number of PAS-positive cells) described in Table 1 and divided by 3.

Table 1. Principles of histological sections assessment.

Score	Perivascular and peribronchiolar inflammation	Number of leukocytes in alveolar spaces	Number of PAS(+) cells / 50 bronchoalveolar epithelial cells
0	no changes	0	0
1	few perivascular and peribronchiolar inflammatory cells	2 – 4 cells	< 12 cells
2	moderate numbers of cell infiltrations on several perivascular and peribronchiolar sites	4 – 10 cells	12 – 25 cells
3	a large number of diffusely infiltrated cell cuffs	> 10 cells	> 25 cells

2.7. Investigation of bronchoalveolar lavage (BAL)

To collect bronchoalveolar lavage fluid (BALF), the lungs were gently flushed with 2 × 0.5 ml of sterile Dulbecco's Phosphate Buffered Saline (D-PBS, Gibco) through trachea cannulation. The obtained suspension was centrifuged (400 × g, 7 min, 4°C) and the supernatant was separated from the pellet and stored at – 80 °C. The cell pellet was resuspended in 200 µl of RPMI 1640 medium (Sigma Aldrich) and used for cell differential count. Briefly, BAL cells were transferred to a microscope slide with a cytospin, left to dry, fixed with methanol, and stained with a Dip-Quick-stain kit following the

manufacturer's instructions (Medical Products, Czech Republic). BAL cells were evaluated with light microscopy following standard morphologic criteria (200 cells observed per cytospin preparation) [19].

2.8. Immunological evaluation of sera and BALF

Total IgA, IgG-Fc, and IgE antibody levels were detected with Bethyl kit (Bethyl Laboratories, Inc), according to the manufacturer's recommendations. Briefly, goat anti-mouse antibodies were used to coat the 96-well microtiter plates (Nunc MaxiSorp, Thermo Fisher Scientific), wells were blocked with 1 % bovine serum albumin (BSA), and tested sera or BALFs were added. After rinsing the excess reagents, HRP-conjugated detection antibodies were incubated on the plate for 1 h, and TMB substrate was used to develop a colorimetric reaction. Finally, the reaction was stopped with 2 M H_2SO_4 and the absorbance was read at 450 and 570 nm.

Antigen-specific IgA, IgE, IgG-Fc, IgG1, and IgG2a antibody levels were detected with Bethyl reagents (Bethyl Laboratories, Inc), according to the manufacturer's recommendations. Briefly, 0.5 µg/well of OVA in PBS was used to coat the 96-well microtiter plates, wells were blocked with 1 % BSA in PBS, and diluted sera or BALFs were added. HRP-conjugated anti-mouse detection antibodies were used and TMB substrate was used. The reaction was stopped by adding 2 M H_2SO_4 and the results were assessed by an absorbance read at 450 and 570 nm.

2.9. RT-qPCR

RNA was isolated from the superior lobe of the lung with a NucleoSpin® RNA kit (Macherey-Nagel) and cDNA was prepared with the use of SuperScript™ II Reverse Transcriptase (Invitrogen) kit according to the manufacturer's instructions. For Real-Time PCR, a master mix was prepared for each of the tested genes including *Actb* – reference gene, *Rorc*, *Gata3*, *Tbx21*, *Foxp3*, and *Il10*, that included (for 1 well): 5 µl of the SYBR Green Real-Time PCR master mix (Promega), 1.25 µl of the forward and reverse primer (standardized KiCqStart™ primers, Merck). 7.5 µl of the prepared mixes were added to white 96-well qPCR plate wells with 2.5µl of the tested cDNA. The mRNA expression was calculated with the 2–ΔΔCT. Analysis was performed with CFX Connect™ Real Time System equipped with Thermal Cycler (Serial No. BR002307; BioRad) and Optical Module (Serial No. 788BR02394; BioRad). Gene expression was counted in relation to the mean of negative control mice (PBS-treated GF and OVA-treated mice).

2.10. Statistical analysis

All data are presented as boxes and whiskers with median + minimal and maximal values. An unpaired Student's t-test was used to compare results between PBS- and BAP1-treated GF mice and between PBS- and BAP1-treated OVA-sensitized and challenged mice. All statistically significant results were marked on the graphs (∗∗∗∗$p < 0.0001$, ∗∗∗$p < 0.001$, ∗∗$p < 0.01$, ∗$p < 0.05$). GraphPad Prism 10 Software (San Diego, CA, USA) was used for statistical calculations and visualizations.

3. Results

3.1. BAP1 treatment increases IgA levels in GF mice

To evaluate the impact of BAP1 on the naïve immune system, we tested it in GF mice. PS was administered to mice on the experimental day 1, 7, and 14. On the 21st day, mice were sacrificed and spleen, lungs, sera, and BALF were collected (Figure 1A). To assess the systemic responses, the levels of total IgA, IgG-Fc, and IgE antibodies were measured in sera. Results showed a trend to increase total IgA compared to mice treated with PBS only (Figure 1B, Supplementary Figure 1). We examined the BAP1-specific recall response in the spleen and observed that there were no significant changes in spontaneous cytokine/chemokine production when compared to the control group (Figure 1C).

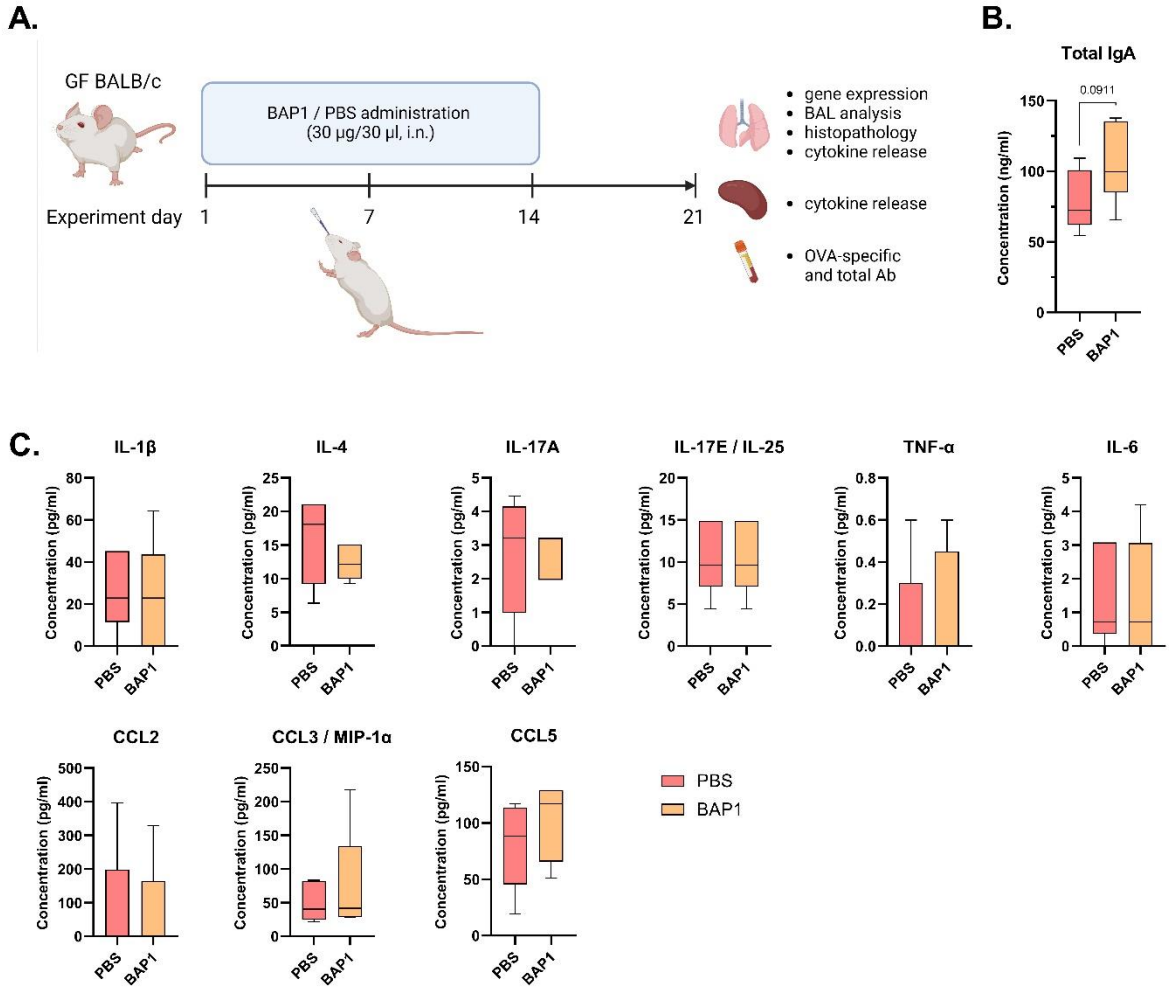

Figure 1. Systemic response of the GF mice to BAP1 i.n. application. **A.** Experimental design of GF mice treatment with PBS (control group) or BAP1 (30 µg / 30 µl / mouse). **B.** Total IgA serum antibodies tested by ELISA. **C.** Spontaneous cytokines and chemokines production in BAP1 and PBS-treated mice measured in splenocytes cultures by Luminex. An unpaired t-test was performed and significant differences between PBS- and BAP1-treated mice were calculated.

3.2. BAP1 administration does not induce inflammatory lung responses in GF mice but activates Rorc expression

Further evaluation of the BAP1 influence on the lung immune responses of GF mice showed no differences in the total cell or different immune cell types (such as macrophages or lymphocytes) count in the BAL (Figure 2A). Importantly, we did not observe an undesirable infiltration of inflammatory neutrophils or eosinophils to the lung tissue. Simultaneously, we detected a significant increase in the total IgA antibody levels in BALF (Figure 2B). Histopathological examination of the lung tissue confirmed the absence of aberrant immune cell infiltration or other morphological changes in response to BAP1 treatment (Figure 2C). In the lung cell culture, administration of BAP1 to GF mice was associated with a significant decrease in IL-6 and CCL-2 levels and a tendency to inhibit eotaxin production. On the other hand, BAP1 administration increased the spontaneous CCL5 production (Figure 2D). To investigate the impact of BAP1 on the activation of certain transcription factors, the upper lobe of the lung was subjected to RNA isolation. We examined four transcription factors *Gata3*, *Tbx21*, *Foxp3*, and *Rorc*, which are involved in Th1, Th2, Treg, and Th17 responses respectively. Our results indicated that PS treatment significantly induced the *Rorc* gene and showed a tendency to increase *Tbx21* expression in comparison to the PBS control group (Figure 2E).

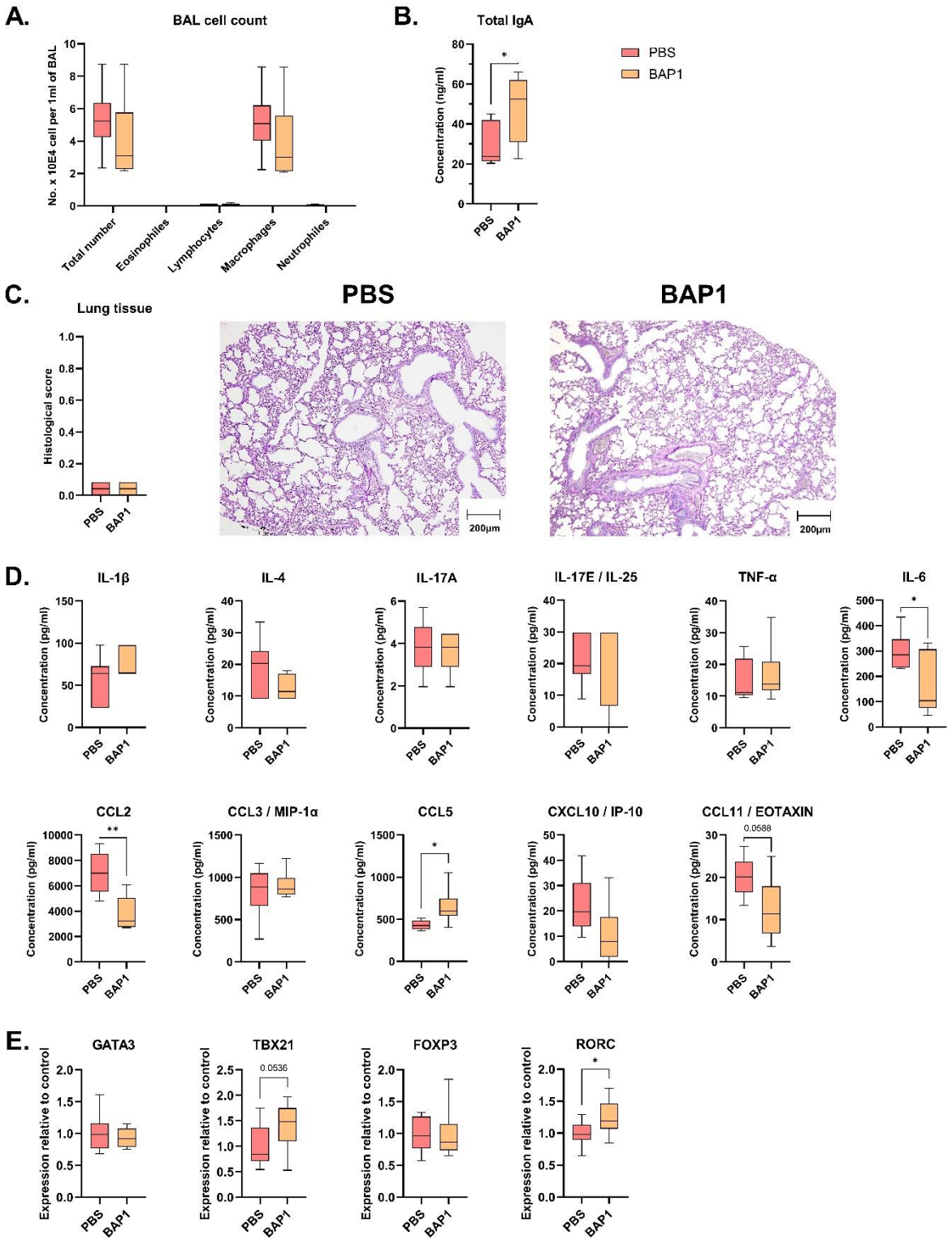

Figure 2. Lung-related response of GF mice to BAP1 treatment. **A.** Cell count in BAL. **B.** Total IgA BALF antibodies tested by ELISA. **C.** Histopathological analysis and representative histopathological section of lungs from mice treated with PBS or BAP1 stained with Periodic Acid-Schiff (magnification 100x, scale 200 um). **D.** Spontaneous cytokines and chemokines production in PBS- and BAP1-treated mice measured in lung cell cultures by Luminex. **E.** Gene expression detected in lungs of GF mice treated